Robert Koch-Institute Berlin

Ljungan virus – prevalence in rodents and virus pathogenesis

Inaugural-Dissertation

to obtain the academical degree

Doctor rerum naturalium (Dr. rer. nat.)

submitted at the Department of Biology, Chemistry and Pharmacy

Freie Universität Berlin

by

René Kallies

from Görlitz

September 2010

1st Reviewer: Prof. Dr. Matthias Niedrig, Robert Koch-Institute Berlin

2nd Reviewer: Prof. Dr. Rupert Mutzel, Freie Universität Berlin

Date of submission: September 30th, 2010

Date of disputation: November 4th, 2011

to my family

„They are ill discoverers that think there is no land, when they can see nothing but sea.”

Sir Francis Bacon

Index

Summary

Ljungan virus (LV) is a member of the *Picornaviridae* that was isolated from various species of voles and mice in Scandinavia, North America, and Italy, suggesting a wide host range and a world wide distribution of this virus. LV causes severe disease in its rodent reservoirs, such as diabetes and myocarditis. In addition, laboratory mice infected with LV suffer from encephalitis and fetal deaths indicating that LV might also induce this diseases in the wild. In addition, LV has been associated with human disease during pregnancy and of neonates, respectively.

A real-time RT-PCR assay was established to identify and quantify LV in different types of sample. The method was evaluated using *in vitro* transcribed RNA and RNA extracted from cell culture supernatant and LV infected laboratory mice, respectively. The assay was specific to all known LV strains, but not to closely related picornaviruses. A linear detection range with high sensitivity (10^6 - 10^1 *in vitro* transcribed RNA molecules) was demonstrated. Furthermore, a melting curve analysis, pyrosequencing and a RT-PCR assay targeting the LV VP1 region were established for characterisation and genotyping of LV positive samples.

A panel of 22 monoclonal antibodies (mAbs) against LV genotypes 1 and 2 were produced by immunization of BALB/c mice with whole virus. Thirteen mAbs were class IgG antibodies and nine were class IgM antibodies, all contained kappa light chains. All mAbs were reactive by capture enzyme-linked immunosorbent assay and indirect immunofluorescent assay. In addition, 5 mAbs showed a positive staining in immunohistochemistry. No mAb bound to denatured capsid proteins as detected by immunoblotting. In contrast, the target capsid protein(s) of 20 mAbs were identified by immunoprecipitation, revealing the conformational nature of epitopes required for mAb binding. Furthermore, 7 mAbs were identified that inhibited LV infection to cell culture.

Assays developed in this thesis should provide usefool tools for the development of diagnostic assays and the investigation of LV properties and its pathogenesis.

Three different strains of laboratory rats were investigated for the presence of LV. LV specific RNA was found in brain and heart by RT-PCR. In addition, LV proteins were visualised in the pancreas by immunohistochemistry and specific antibodies were detected by indirect immunofluorescence test, suggesting that the laboratory rat is one of several rodent reservoirs of this new picornavirus.

Wild rodents from Germany and Thailand were investigated for LV presence by RT-PCR. In total, 454 (Germany) and 87 samples (Thailand), respectively, were analysed. A total of 44 (9.7 %) (Germany) and 14 (16.1 %) (Thailand) samples were positive for LV, belonging to the following species: Germany: *Microtus agrestis, Microtus arvalis, Myodes glareolus, Apodemus agrarius, Apodemus flavicollis, Apodemus sylvaticus, Micromys minutus, Mus musculus, Rattus norvegicus*; Thailand: *Bandicota indica, Bandicota savilei, Mus caroli, Rattus rattus, Tupaia glis*. LV positive animals were found in the German areas of Baden-Württemberg, Saxony-Anhalt, Brandenburg, Mecklenburg-Western Pomerania, the city of Cologne, and Thai provinces Bangkok, Buri Nam, and Prachuap Khiri Khan. A putative new LV genotype was found in a bank vole sample from Germany.

The data present a so far unknown picture of LV prevalence in wild rodents also in Central Europe and Asia.

In this thesis, organs of laboratory mice infected with LV were investigated for the presence of LV genome by real-time RT-PCR through time. The animals had clinical signs of encephalitis a few days post infection and developed diabetes later in life. All organs were found positive for LV over the whole period of 174 days. This work shows that LV causes a systemic persistent infection in laboratory mice that might support the onset of diabetes in adult individuals. Bank voles trapped in the wild were investigated for the presence of LV by real-time RT-PCR. Several organs were found positive with copy numbers close to those found in laboratory mice during persistent infection, indicating a systemic persistent LV infection also in wild bank voles.

LV production was analysed in two cell lines. Both Vero-B4 and BHK-21 cells were susceptible for LV infection. An increase of LV RNA and LV protein was detected in both cell lines. In contrast, only Vero-B4 cell supernatant had an increasing titer of LV particles, indicating LV infection of BHK-21 cells is restricted. Furthermore, only Vero-B4 cells showed a clear cytopathic effect post LV infection that was associated with induction of apoptosis.

Apoptosis might play a role in LV induced onset of encephalitis, myocarditis, and diabetes, respectively.

Zusammenfassung (German summary)

Ljunganvirus (LV) gehört zur Familie der *Picornaviridae* und wurde in verschiedenen Wühlmaus- und Mausspezies in Skandinavien, Nordamerika und Italien nachgewiesen, was ein breites Wirtsspektrum sowie eine weltweite Verbreitung dieses Virus vermuten lässt. LV verursacht ernsthafte Erkrankungen, wie Diabetes und Myokarditis, in seinen Nagerreservoiren. LV infizierte Labormäuse entwickeln zudem neurologische Symptome und reproduktive Störungen. Diese Erkrankungen könnten ebenfalls bei Wildtieren durch LV induziert werden. Der Nachweis von LV im Menschen wurde mit Erkrankungen während der Schwangerschaft und von Neugeborenen assoziiert.

In dieser Arbeit wurde eine *real-time* RT-PCR Methode etabliert, um LV in verschiedenem Probenmaterial nachzuweisen und zu quantifizieren. Die Methode wurde mittels *in vitro* transkribierter RNA, RNA aus Zellkulturüberständen und RNA aus LV infizierten Labormäusen evaluiert. Die RT-PCR war spezifisch für alle bekannten LV-Stämme, nicht jedoch für eng verwandte Picornaviren. Ein linearer Nachweisbereich mit hoher Sensitivität (10^6 - 10^1 *in vitro* transkribierte RNA Moleküle) konnte gezeigt werden. Für eine weitere Charakterisierung LV positiver Proben wurden eine Schmelzpunktanalyse, *Pyrosequencing* sowie eine RT-PCR Methode zum Nachweis der LV VP1-Region etabliert.

Ein Panel von 22 monoklonalen Antikörpern (mAk) wurde durch Immunisierung von BALB/c Mäusen mit Vollvirus produziert. Dreizehn mAk gehörten zur IgG Subklasse und neun mAk zur IgM Subklasse. Alle mAk waren positiv in einem *capture enzyme-linked immunosorbent assay* und im Immunfluoreszenztest. Fünf der mAk detektierten ebenfalls LV-Antigen in der Immunhistochemie. Keiner der mAk konnte denaturierte LV Kapsidproteine nachweisen, wohingegen die Interaktionspartner von 20 mAk durch Immunpräzipitation identifiziert werden konnten, was darauf schließen lässt, dass die mAk an Konformationsepitope der LV Kapsidproteine binden. Zusätzlich wurden sieben neutralisierende mAk identifiziert.

Die in dieser Arbeit etablierten Methoden bieten die Grundlage für die Entwicklung diagnostischer Methoden zum LV Nachweis. Die Erforschung der biochemischen und physikalischen Eigenschaften des LV und der LV-Pathogenese sollte mit Hilfe dieser Methoden gezielt durchgeführt werden können.

Drei verschiedene Laborratten-Stämme wurden auf eine LV-Infektion untersucht. LV spezifische RNA wurde mittels RT-PCR in Hirnen und Herzen der Tiere nachgewiesen. LV-Proteine wurden zudem im Pankreas infizierter Tiere mit Hilfe der Immunhistochemie gezeigt und spezifische anti-LV Antikörper wurden durch einen Immunfluoreszenztest nachgewiesen. Diese Daten legen nahe, dass Laborratten eines von mehreren Nagerreservoiren für LV sind.

In einem weiteren Projekt wurde die LV-Prävalenz in Wildnagern aus Deutschland und Thailand untersucht. Insgesamt wurden 454 Tiere aus Deutschland und 87 Tiere aus Thailand mittels RT-PCR getestet. Aus Deutschland waren 44 (9,7 %) Proben und aus Thailand 14 (16,1 %) Proben LV positiv. Folgende Spezies wurden LV positiv getestet: Deutschland: *Microtus agrestis, Microtus arvalis, Myodes glareolus, Apodemus agrarius, Apodemus flavicollis, Apodemus sylvaticus, Micromys minutus, Mus musculus, Rattus norvegicus*; Thailand: *Bandicota indica, Bandicota savilei, Mus caroli, Rattus rattus, Tupaia glis*. LV positive Tiere wurden in folgenden Regionen gefunden: Baden-Württemberg, Sachsen-Anhalt, Brandenburg, Mecklenburg-Vorpommern, Köln (Deutschland), Bangkok, Buri Nam und Prachuap Khiri Khan (Thailand). Ein vermutlich neuer LV Genotyp wurde in einer Rötelmausprobe aus Deutschland detektiert.

Diese Daten repräsentieren eine bisher unbekannte Verbreitung von LV auch in Zentraleuropa und Asien.

Organe von LV infizierten Labormäusen wurden im Zeitverlauf mittels *real-time* RT-PCR auf LV-Präsenz untersucht. Die Tiere erkrankten wenige Tage nach der Infektion an einer Enzephalitis und entwickelten im späteren Verlauf klinische Symptome eines Diabetes. Alle Organe waren über den gesamten Zeitverlauf von 174 Tagen LV positiv. Es konnte somit gezeigt werden, dass LV eine systemische

persistierende Infektion verursacht, die zum Ausbruch von Diabetes in erwachsenen Tieren beitragen dürfte. Organe von in der Wildnis gefangenen Rötelmäusen wurden ebenfalls getestet. Verschiedene Organe waren LV positiv. Die Anzahl der LV Kopien war dabei vergleichbar mit denen aus Labormäusen während der persistierenden Infektion, was darauf hinweist, dass LV auch in Wildnagern persistiert.

Die LV-Produktion wurde in zwei verschiedenen Zellinien untersucht. Sowohl Vero-B4 als auch BHK-21 Zellen waren für eine LV-Infektion empfänglich. In beiden Zellinien wurde eine Zunahme von LV RNA und LV Protein im Zeitverlauf beobachtet. Ein ansteigender Virustiter konnte allerdings nur im Überstand von Vero-B4 Zellen detektiert werden. Weiterhin wurde lediglich in Vero-B4 Zellen ein virusinduzierter cytopathischer Effekt beobachtet, welcher durch Apoptose induzierende Effekte ausgelöst scheint.

LV induzierte Apoptose könnte eine Rolle in der Entstehung von Enzephalitis, Myokarditis und Diabetes spielen.

1 Introduction

Viruses are small infectious replicating units that can only replicate inside a living host cell. Viruses are present in all domains of life (archaea, bacteria, eukarya) with several millions of types known. The virus particle constists of a nucleic acid that encodes the genetic information, a protein structure for protection of the nucleic acid and in some virus families an envelope of lipids. After attachment to a specific receptor and entry into the host cell, viruses start their life cycle using the cellular machinery and cell metabolism for reproduction. The influence(s) of a virus-induced cytopathology and/or immunopathology on the organism can sometimes result in disease.

Zoonoses are defined as infectious diseases that are transmitted from animals to humans and/or humans to animals, respectively. A reservoir host is an animal that carries the pathogen and serves as a source of infection. Important viral zoonoses are, for instance, tick-borne encephalitis (TBE) (TBE virus is transmitted by ticks) and the severe acute respiratory syndrome (SARS) (caused by the SARS coronavirus that originates from bats). An example of a zoonotic agent associated with rodents is Hanta virus. Hanta virus infections cause severe disease in humans, i.e. hemorrhagic fever with renal syndrome and hanta virus pulmonary syndrome. Rodents can carry additional viruses, some of them possibly also zoonotic. The understanding of the biological characteristics, the ecology and the pathogenesis of such viruses can help assess the risk of human infection, and these viruses can also serve as model systems to understand human disease.

This thesis is about Ljungan virus that was isolated from voles close to the Ljungan river in Sweden in the late 1990s.

1.1 *Picornaviridae*

1.1.1 Characteristics and taxonomy

Members of the *picornaviridae* family are non-enveloped viruses with a single-strand RNA genome in positive orientation. The spherical virus particle has a size of 27-30 nm in diameter and is composed of the RNA genome and 60 protomers, each consisting of four structural proteins that form an icosaedral capsid. The capsid proteins VP1, VP2 and VP3 are at the external side of the particle while VP4 is at the internal side (Figure 1.1) (Rossmann *et al.*, 1985; Stanway, 1990; Racaniello, 2007).

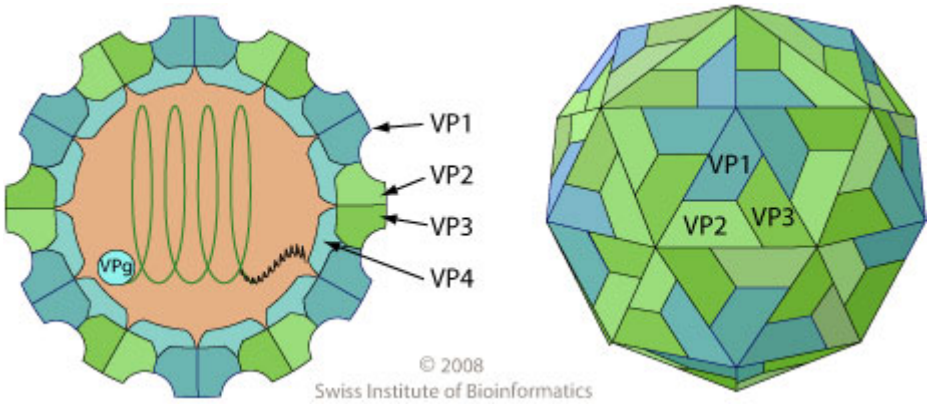

Figure 1.1 Picornavirus virion. The RNA genome is surrounded by a protein shell consisting of 60 protomers forming the icosaedral capsid. Each protomer consists of the four capsid proteins VP1, VP2, VP3 (all external) and VP4 (internal). Source: http://br.expasy.org (modified).

The original classification of Picornaviruses is based on their physical properties and serological aspects. During the past years, a re-classification was necessary when more genetic information became available together with newly identified picornaviruses. Today, the following species definition is used: "A picornavirus species is a polythetic class of phylogenetically related serotypes or strains which would normally be expected to share (i) a limited range of hosts and cellular receptors, (ii) a significant degree of compatibility in proteolytic processing, replication, encapsidation and

genetic recombination, and (iii) essentially identical genome maps" (Stanway *et al.*, 2000; International Committee on Taxonomy of Viruses).

Currently, picornaviruses are separated into 12 genera including important vertebrate and human pathogens (table 1.1, figure 1.2). In addition, a number of unassigned picornaviruses and picorna-like viruses are not yet completely characterised (Stanway *et al.*, 2005). Many picornavirus-like agents also found in plants and invertebrates share similarities with picornaviruses. As a result, they are all classified into the order *picornavirales* (Le Gall *et al.*, 2008).

Table 1.1. Picornavirus genera with representative species and the respective diseases.

Genus	Representative species	Disease
Enterovirus	Poliovirus	Poliomyelitis
Cardiovirus	Encephalomyocarditis virus	Encephalomyocarditis
Aphtovirus	Foot-and-mouth disease virus	Foot-and-mouth disease
Hepatovirus	Hepatitis A virus	Hepatitis
Parechovirus	Human Parechovirus, Ljungan virus	Respiratory and gastrointestinal disease, neonatal sepsis, encephalitis, diabetes
Erbovirus	Equine rhinitis B virus	Upper respiratory infections
Kobuvirus	Aichi virus	Gastroenteritis
Teschovirus	Porcine teschovirus	Encephalomyelitis
Sapelovirus	Porcine sapelovirus	Reproductive disorders
Senecavirus	Seneca Valley virus	Oncolytic virus
Tremovirus	Avian encephalomyelitis virus	Encephalomyelitis
Avihepatovirus	Duck hepatitis virus	Hepatitis

Picornaviruses are either transmitted by the faecal-oral route or enter the host by aerogen or smear infection, respectively. The latter group of viruses is acid-labile and can therefore not survive the acidic environment in the gastric area. As a consequence, these viruses infect the nasal, mouth and throat area, as for instance Rhinovirus (genus enterovirus, the major cause of common cold in humans and responsible for exacerbation of asthma) and the Foot-and-mouth disease virus (FMDV) that is an important pathogen of cattle, swine, sheep and goat (Bachrach, 1968; Racaniello,

2007; Peltola *et al.*, 2008; Gern, 2010). Viruses transmitted by the faecal-oral route are acid-stable. That is why they can not be inactivated in the acidic gastric area. These viruses often infect the intestinal tract from where they can reach other organs as for instance, the central nervous system (CNS) (Racaniello, 2007).

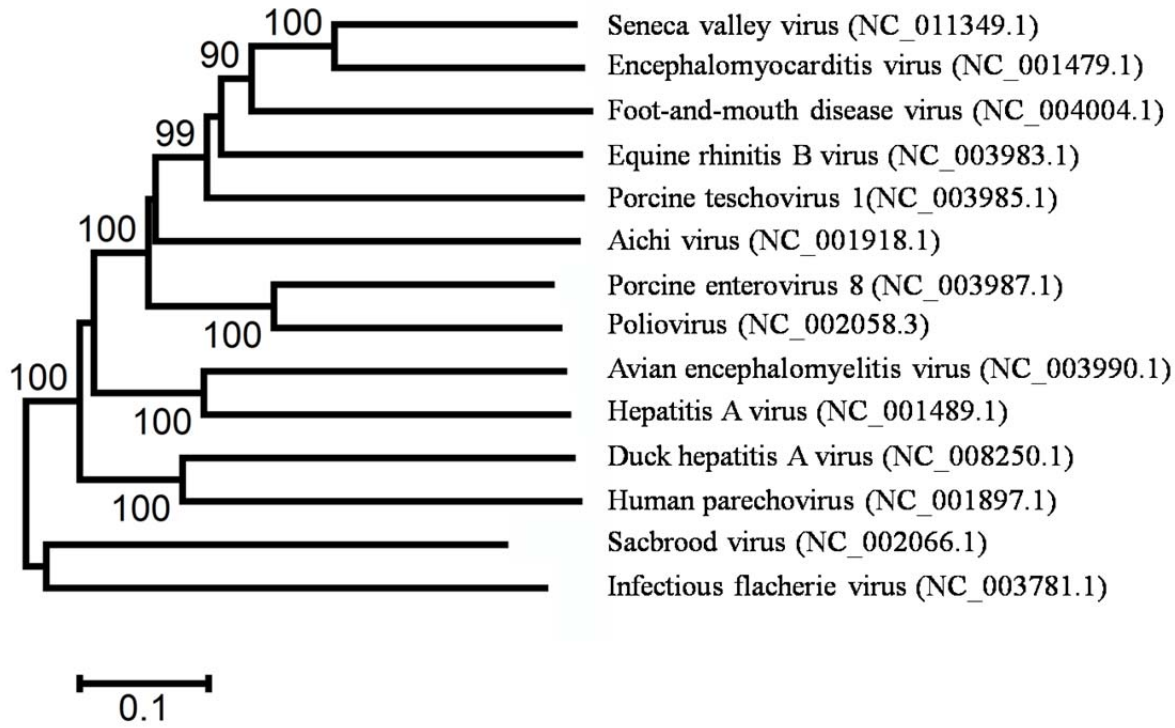

Figure 1.2 Phylogenetic tree of representative species of all 12 picornavirus genera. Reference 3D RNA-polymerase sequences were obtained from NCBI GenBank. Two insect picorna-like viruses were used as outgroup. The evolutionary history was inferred using the Neighbor-Joining method (Saitou and Nei, 1987). The optimal tree with the sum of branch length = 4.40230389 is shown. The percentage of replicate trees in which the associated taxa clustered together in the bootstrap test (1000 replicates) are shown next to the branches (Felsenstein, 1985). The tree is drawn to scale, with branch lengths in the same units as those of the evolutionary distances used to infer the phylogenetic tree. All positions containing gaps and missing data were eliminated from the dataset (Complete deletion option). There were a total of 392 positions in the final dataset. Phylogenetic analyses were conducted in MEGA4 (Tamura *et al.*, 2007).

1.1.2 Genome structure and viral proteins

The picornavirus RNA genome is approx. 7000 to 9500 bases in length (Hughes and Stanway, 2000) and it is *per se* infectious due to its positive polarity. A small viral protein that is necessary for viral replication (chapter 1.1.3) is covalently linked with the 5'-end of the genome (VPg = virus protein genome linked). The first 335 to 1199 bases of the genome consist of an untranslated region (5'UTR) with many secondary structures (Doherty *et al.*, 1999; Racaniello, 2007). The internal ribosomal entry site (IRES) is part of the 5'UTR responsible for binding to ribosomes and initiation of viral protein translation (chapter 1.1.3). Different types of IRES structures among picornaviruses are known. Type I IRES are found in the 5'UTRs of enteroviruses, type II IRES in aphthovirus and cardiovirus and type III IRES in hepatitis A virus genome. The three IRES types differ in location of the initiation codon, secondary structures and the mechanism of binding to the ribosomal subunit 40S (Racaniello, 2007).

A second untranslated region is located at the 3'-end of the genome (3'UTR). This region is 47 to 125 bases in length and is polyadenylated. The poly(A)-tail has 35 to 100 bases. The 3'UTR also contains secondary structures and possibly serves as priming site for the viral replicase complex (Racaniello, 2007; Zoll *et al.*, 2009a).

A single open reading frame (ORF) coding for all viral proteins is located between both UTRs. This ORF is divided into three main parts: P1, P2 and P3. P1 encodes for the structural proteins VP4, VP2, VP3 and VP1. In addition, some picornavirus genera (Aphthovirus, Cardiovirus, Erbovirus, Kobuvirus, Teschovirus and Sapelovirus) encode for a leader protein that is located at the N-terminus of the polyprotein. Both, the P2 and the P3 region encode for non-structural proteins including enzymes responsible for virus replication (figure 1.3) (Whitton *et al.*, 2005).

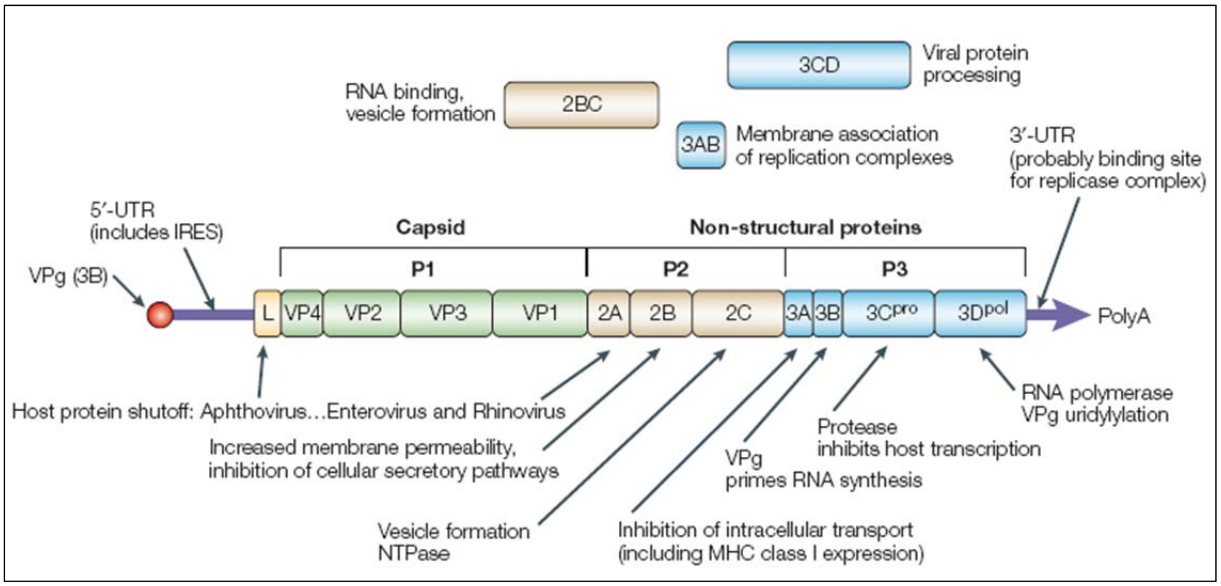

Figure 1.3 Schematic of the picornavirus genome, the polyprotein products and their main functions. A diagrammatic representation of the picornavirus genome is shown, combining features from all of the genera. The 12 mature polypeptides are shown, together with the three main cleavage intermediates. The main biological functions are included for each polypeptide. IRES, internal ribosome entry site; UTR, untranslated region; VPg, viral protein genome-linked. Source: Whitton *et al.*, 2005

The picornavirus genome encodes for up to 12 proteins with different cleavage intermediates. The viral RNA is directly translated via binding to ribosomes by IRES. The nascent polyprotein is automatically cleaved by viral proteases during translation. The main functions and characteristics of picornavirus proteins are described as follows:

Structural proteins

Picornaviruses have four structural proteins, i.e. VP4, VP2, VP3 and VP1 (figures 1.1 and 1.3) that constitute the virus capsid. The C-termini of proteins VP2, VP3 and VP1 form the particle surface and virus serotype is thus determined by these structures and connecting loops. These three proteins have all the same topology of an eight-stranded, antiparallel β-sheet. The VP4 protein is located within the particle and connected with the N-termini of the three other capsid proteins by myristyl groups that are attached to the VP4 N-terminus. The precursor protein for VP4 and VP2 is VP0 that is cleaved

during virus assembly. The C-terminal part of VP0 has protease activity. A close interaction with the virus genome in the immature virus particle is necessary for cleavage. A successful cleavage leads to formation of the mature particle. However, in the case of the Parechovirus and Avihepatovirus genera and Aichivirus, respectively, this precursor is not cleaved. As a result, in these viruses VP0 is part of the virus capsid that consequentially consists of only three proteins (Hyypiä *et al.*, 1992; Stanway *et al.*, 1994; Yamashita *et al.*, 1998; Kim *et al.*, 2006; Racaniello, 2007).

2A protein

Viral 2A protein is a proteinase in enteroviruses and rhinoviruses. In the early stages of infection, it cleaves the C-terminus of the protomer from its N-terminus cotranslationally (cleavage between P1 and P2) (Ryan and Flint, 1997). The 2A protein of enteroviruses also cleaves several cellular proteins. Most important is the cleavage of proteins that belong to the eukaryotic initiation factor-4A (eIF4) family. The eIF4 complex is involved in the initiation of translation of cellular mRNAs by binding to the 5'Cap structure of mRNAs and in mediation of binding to the ribosome. The activity of picornavirus 2A inhibits the functionality of eIF4 and leads to virus-host shutoff because cellular mRNAs can not be translated (Bernstein *et al.*, 1985). The protease activity of the 2A protein of aphthoviruses and cardioviruses is different from that of enteroviruses and rhinoviruses. The mechanisms of 2A-mediated cleavage in these viruses is unclear (Donnelly *et al.*, 1997). The 2A protein of hepatoviruses, parechoviruses and kobuviruses does not have proteinase activity (Jia *et al.*, 1993; Schultheiss *et al.*, 1995; Yamashita *et al.*, 1998). 2A protein of these viruses contains motifs with characteristics of cellular proteins involved in the control of cell growth, suggesting an important role in virus life cycle (Hughes and Stanway, 2000).

2BC precursor

The 2BC precursor of proteins 2B and 2C remains uncleaved to a high extent and is essential in virus replication (Paul *et al.*, 1998b). The functions of 2BC are similar to those of 2B. However, the degree of influence is higher when both proteins are present rather than one protein alone (Aldabe *et al.*, 1996).

2B protein

The picornavirus 2B protein is little understood and most of the knowledge comes from enterovirus research. Based on these data, 2B is probably involved in the modification of intracellular membrane structures and functions. It is a hydrophobic membrane protein localised at the endoplasmic reticulum (ER) and the Golgi complex membranes, respectively (Bienz *et al.*, 1987; Sandoval and Carrasco, 1997; De Jong *et al.*, 2003). It has been shown that 2B generates pores in membranes of ER and Golgi complex (Agirre *et al.*, 2002; De Jong *et al.*, 2004) and thereby reducing the levels of calcium and hydrogen ions, respectively, in the ER and Golgi complex lumens (Van Kuppeveld *et al.*, 1997; Campanella *et al.*, 2004; De Jong *et al.*, 2006). The 2B protein also inhibits protein trafficking through Golgi complex (Doedens and Kirkegaard, 1995; De Jong *et al.*, 2006). In contrast, recent studies on 2B proteins of Hepatitis-A virus (HAV) (genus hepatovirus), FMDV (genus aphthovirus) and Encephalo-myocarditis virus (EMCV) (genus cardiovirus) revealed no sequence or structural relationship to enterovirus 2B and among themselves. Moreover, 2B of these three genera lacks any effect on ER and Golgi complex calcium ion homeostasis and does not inhibit protein trafficking through Golgi complex (De Jong *et al.*, 2008).

2C protein

The 2C protein is highly conserved among picornaviruses (Gorbalenya *et al.*, 1989) and is involved in viral RNA synthesis. 2C has many functions, such as ATPase and GTPase activity (Rodriguez and Carrasco, 1993; Mirzayan and Wimmer, 1994), membrane-binding and RNA-binding activities (Aldabe and Carrasco, 1995; Echeverri and Dasgupta, 1995; Rodriguez and Carrasco, 1995; Kusov *et al.*, 1998). It has further been shown that 2C binds to the viral negative-strand RNA and is involved in anchoring this RNA in intra-cellular membrane structures (part of the replication complex) and in this way aids positive-strand synthesis (Banerjee *et al.*, 1997; Banerjee *et al.*, 2001; Banerjee and Dasgupta, 2001).

3AB precursor

The 3AB precursor is multifunctional. The hydrophobic domain in the 3A fraction of the protein interacts with membrane vesicles, probably to anchor the replication complex to the virus-induced vesicles (Towner *et al.*, 1996; Fujita *et al.*, 2007). Recombinant 3AB interacts with poliovirus 3D and 3CD and, when membrane associated, stimulates 3CD proteinase activity and possibly serves as anchor for 3D in membrane associated replicase complex (Xiang *et al.*, 1995a; Hope *et al.*, 1997). Furthermore, 3AB functions as substrate for 3D in VPg uridylylation (Richards *et al.*, 2006).

3A protein

The 3A protein is a small hydrophobic membrane protein that is necessary for viral replication (Bernstein *et al.*, 1986; Giachetti *et al.*, 1992; Xiang *et al.*, 1995b; Teterina *et al.*, 2003). 3A is also involved in host range and tropism by an unknown mechanism (Lama *et al.*, 1998; Beard and Mason, 2000; Nunez *et al.*, 2001; Harris and Racaniello, 2005). In addition 3A inhibits cellular protein transport from ER to Golgi complex (Doedens and Kirkegaard, 1995; Wessels *et al.*, 2005). This inhibition has been suggested to be a picornaviral immune evasion strategy (Deitz *et al.*, 2000; Dodd *et al.*, 2001; Neznanov *et al.*, 2001).

3B protein

3B protein (also VPg) is a small peptide covalently linked to the 5'-end of the picornavirus genome. 3B interacts with the viral RNA-dependent RNA polymerase (3D) that incorporates uridyl monophosphate into 3B (Paul *et al.*, 1998a). The uridylyated 3B serves as primer in both, RNA positive-strand and RNA negative-strand synthesis (Pettersson *et al.*, 1978).

3CD precursor

The 3CD protein is the precursor of picornavirus 3C protease and 3D polymerase. It has protease activity but no polymerase activity (Harris *et al*., 1992). Poliovirus 3CD is capable of fully processing P1 into VP0, VP3 and VP1 whereas 3C or 3D alone have

minor or no effect, respectively (Jore *et al.*, 1988). Furthermore, poliovirus 3CD interacts with both the 5'-end and the 3'-end of the viral RNA, resulting in circularisation of the viral genome which initiates poliovirus RNA synthesis (Harris *et al.*, 1994). Poliovirus 3CD also interacts with several cellular proteins and the viral 3AB protein, that, together with binding to stem-loop I of 5'UTR, form important complexes in viral replication (Gamarnik and Andino, 2000).

3C protein

Picornavirus 3C protein exhibits proteinase activity. Primary cleavage between 2C and 3A is mediated by 3C. Unlike the other picornavirus proteinases, 3C is also responsible for secondary cleavages of the P1 and P2 precursors. Furthermore, 3C cleaves a number of cellular proteins, e.g. transcription factor IIIC. As a result, the function of cellular RNA polymerase III is inhibited (reviewed by Ryan and Flint, 1997; Racaniello, 2007).

3D protein

The picornavirus 3D protein is the RNA-dependent RNA polymerase (Van Dyke and Flanegan, 1980). It is most highly conserved among *picornaviridae*. 3D also uridylates the 3B protein that is then used as primer for viral RNA synthesis (Paul *et al.*, 1998a; Paul *et al.*, 2003). Furthermore, 3D interacts with the cellular protein Sam68 that mediates alternative splicing of cellular RNA (McBride *et al.*, 1996). As other RNA polymerases, 3D has a high error frequency of 10^{-3} to 10^{-4}, resulting in 1 to 2 misincorporated nucleotides per genome copy event (Ward *et al.*, 1988). As a consequence, picornaviruses undergo rapid mutation and evolution in the host.

1.1.3 Virus entry, replication and viral egress

After entering the host (chapter 1.1.1), picornaviruses attach to a specific receptor on the cell membrane. For some picornaviruses a single receptor is sufficient for cell attachment (e.g. poliovirus, CD155), whereas other viruses also require a co-receptor (e.g. coxsackievirus A21, CD55 and ICAM-1). Some picornavirus capsids

(enteroviruses) have a canyon with a hydrophobic pocket beneath, that often contains a lipid. This canyon is the receptor binding site for e.g. poliovirus and major group rhinoviruses. However, minor group rhinoviruses also have a canyon but it is not the binding site. Rather a structure surrounding the canyon is responsible for attachment to the receptor. In contrast, some picornaviruses lack the canyon (e.g. aphthoviruses, cardioviruses). Receptor binding with these viruses is mediated through surface loops (Racaniello, 2007).

The site for picornavirus replication is the cell cytoplasm. Once the virus is attached to its receptor, RNA must be released into the cell. Two mechanisms for cell entry are discussed, first, formation of a pore in the cell membrane through which the viral RNA enters the cell and second, entry by endocytosis (Racaniello, 2007). Interaction of poliovirus with the receptor leads to conformational changes in the capsid, i.e. the externalisation of the lipophilic N-terminus of VP1 (Fricks and Hogle, 1990). Release of viral RNA into the cell is thought to happen by inducing the formation of a pore through which RNA can enter the cell (Tosteson and Chow, 1997; Belnap *et al.*, 2000). Virus entry by receptor-mediated endocytosis has been shown for FMDV and rhinovirus. Uncoating of the virus particle in the cell cytoplasm may be triggered by acidification of the endosome (Carrillo *et al.*, 1984; Mason *et al.*, 1994).

Once the viral RNA is released into the cell, viral proteins have to be translated. Viral IRES binds to the 40S subunit of cellular ribosomes. The picornavirus polyprotein is then translated and cleaved by viral proteinases during processing (described in 1.1.2). A requirement for viral replication is the formation of a nucleoprotein complex. A cloverleaf structure at the 5'UTR of virus RNA interacts with viral 3CD and cellular poly r(C)-binding proteins. Viral 3D polymerase is primer dependent. An oligo(U) primer linked to viral VPg (3A) is used for initiation of viral negative strand generation. The template for VPg uridylylation is a viral RNA hairpin within the cis-acting replication element (cre) of the virus genome. The viral replication takes place in replication complexes. The primer associates with the poly-A sequence at the 3' part of the virus genome and initiates binding of 3D polymerase that synthesises the RNA negative strand. The originated intermediate of positive and negative RNA

serves as template for the generation of more positive RNA strands that in turn serve as templates for replication and also for viral protein translation. Virus assembly occurs by self-assembly of protomers that self-assemble into pentamers, pentamers assemble into empty particles. The synthesised viral positive-stranded RNA is inserted into the particles and form the provirion. The final step is mediated through cleavage of VP0 into VP4 and VP2. Viral egress is effected by changes in cellular membrane permeability (Racaniello, 2007). Figure 1.4 shows a summary of the picornavirus life cycle.

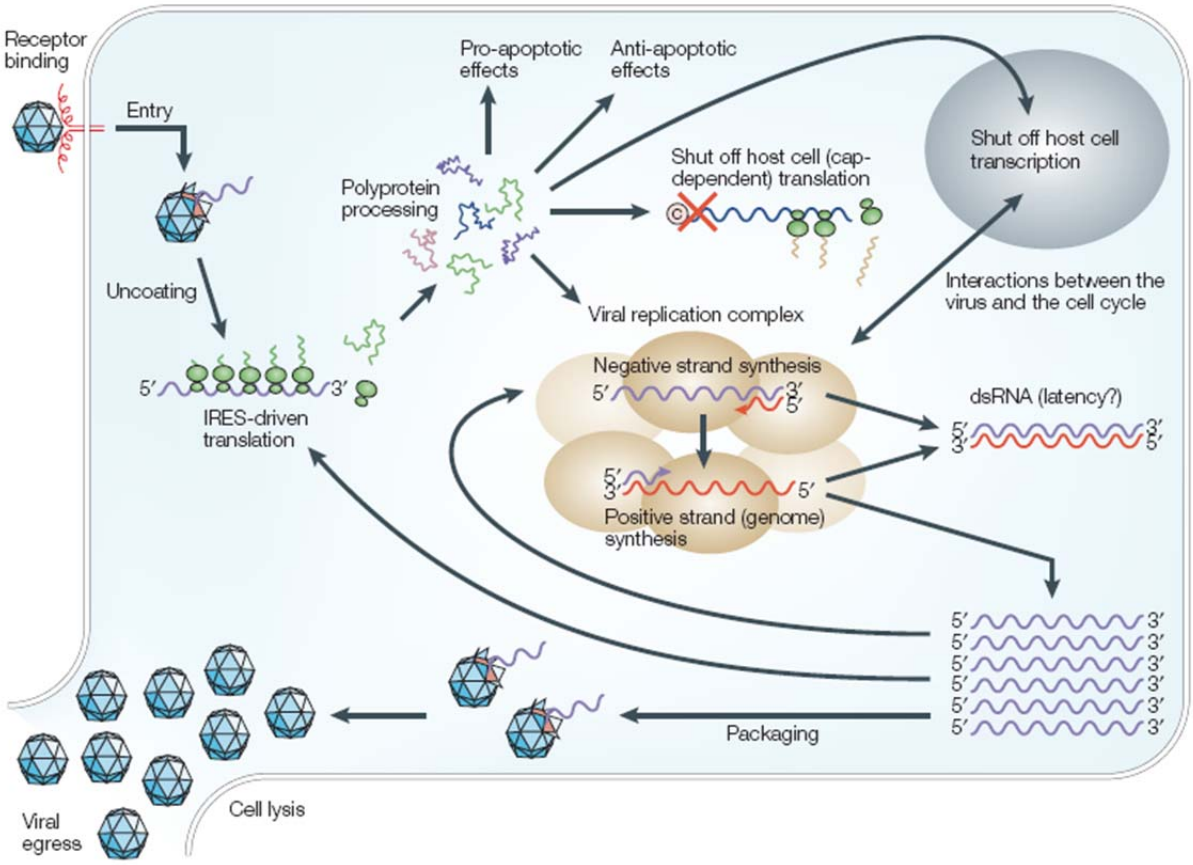

Figure 1.4 Picornavirus life cycle. Positive-sense RNA is shown in purple and negative-sense RNA is shown in red. ©: m^7G cap, dsRNA: double-stranded RNA, IRES: internal ribosome entry site. Source: Whitton *et al.*, 2005 (modified).

1.1.4 Viral pathogenesis

Many factors are involved in determining viral pathogenesis. This includes cell tropism, virus cell entry, the ability of infection to cause cytopathology, the host response to infection and immunopathology. The nature and severity of virus-caused disease depends on additional factors, such as (among others) the site of infection, virus ability to enter target tissue, susceptibility of target cells, virus ability to cause cell death, host immunity, host genotype and age of host (Flint *et al.*, 2004).

The first step of the picornavirus life cycle is attachment to a specific receptor that facilitates cell entry. It is therefore self-evident that the binding of picornavirus capsid proteins to receptors play a major role in virus tropism and pathogenesis. However, receptor usage is not the sole determinant of tissue tropism. It has been shown for several picornaviruses (e.g. poliovirus, rhinoviruses, and FMDV) that their receptor molecules have broader tissue distribution than tissue tropism of the viruses (Evans and Almond, 1998). Other factors must be involved reflecting events post virus entry. Data from enteroviruses indicate that IRES is another determinant of tissue tropism. For instance, the poliovirus Sabin strain, that is used for vaccination, contains attenuating mutations in the IRES (Evans *et al.*, 1985) and host range phenotype of poliovirus is induced by mutations in the IRES (Shiroki *et al.*, 1997).

Acute virus infections are characterised by rapid production of infectious particles, followed by virus clearance from the host. In contrast, persistent infections are not cleared efficiently by the adaptive immune system (Flint *et al.*, 2004). Most picornavirus infections used to be considered to be acute cytolytic infections (Whitton *et al.*, 2005). However, in recent years it became evident that picornaviruses also might persist. Human enteroviruses establish long-term persistence, possibly through emergence of new virus variants (Reagan *et al.*, 1984; Colbere-Garapin *et al.*, 1998; Tam and Messner, 1999). In addition, Coxsackievirus B (CVB) RNA persists over months and years *in vivo* (Klingel *et al.*, 1992; Adachi *et al.*, 1996; Tam and Messner, 1999). Furthermore, CVB infection is affected by the cell cycle of infected cells. Quiescent cells infected with CVB do not produce infectious virus nor viral proteins,

but still contain infectious RNA. Once the cell is stimulated to cell division, e.g. by wounding, CVB starts replication. This observation suggests latent CVB infection that can be reactivated by an appropriate stimulation (Feuer *et al.*, 2002). The presence of persistent CVB infection is discussed to contribute directly or indirectly to disease. As an example, CVB gene products are cytopathic in tissue culture (Wessely *et al.*, 1998a) and restricted replication of CVB genome in the heart can induce dilated cardiomyopathy in transgenic mice (Wessely *et al.*, 1998b). It has also been proposed that persistent CVB RNA could lead to sporadic production of CVB particles resulting in disease (Feuer *et al.*, 2002).

Apoptosis (also called programmed cell death) is a conglomeration of biochemical alterations in the cell. The controlled, regulated cell death is a response to a variety of stimuli. Viruses regulate the apoptotic pathway either as a defence or as an offense tactic, sometimes one following the other. Viruses may enter the host cell and inhibit apoptosis to gain time to proliferate. Conversely, viruses may induce the apoptotic pathway to cell death allowing the spread to neighbouring cells (Hay and Kannourakis, 2002). Data from picornaviruses support this idea. Poliovirus switches from apoptosis inhibition to induction of apoptosis in the middle of the life cycle (Agol *et al.*, 2000). Picornavirus-caused disease is sometimes associated with apoptosis: poliovirus induces apoptosis in the CNS of mice (Girard *et al.*, 1999) and apoptotic cells are present in coxsackievirus-infected heart and CNS tissue, respectively (Gebhard *et al.*, 1998; Feuer *et al.*, 2003).

1.1.5 Parechoviruses

The genus *Parechovirus* consists of two species, i.e. Human Parechovirus (HPeV) and Ljungan virus (LV). HPeV types 1 and 2 were isolated in 1956 from rectal swabs of infants during a summer diarrhoea outbreak in Ohio, USA. By means of cross-neutralisation tests, these viruses were identified as new ECHO (entero cytopathogenic human orphan) viruses and designated as echoviruses 22 and 23, respectively (Wigand and Sabin, 1961). After isolation it became evident that compared to enteroviruses

these two viruses had different growth properties and cytopathology in cell culture (Shaver *et al.*, 1961; Wigand and Sabin, 1961; Jamison, 1974). Sequence analysis demonstrated that echovirus 22 is distinct from other picornavirus genera (Hyypiä *et al.*, 1992; Stanway *et al.*, 1994) and it was hence classified as prototype member HPeV1 into the new genus *Parechovirus* (Mayo and Pringle, 1998). The sequence of echovirus 23 was shown to be closely related to HPeV1. As a consequence, this virus was renamed HPeV2 and classified as second *Parechovirus* member (Stanway *et al.*, 1994; Ghazi *et al.*, 1998). In recent years, 12 new parechovirus types were identified, designated as HPeV types 3-14 (Oberste *et al.*, 1998; Ito *et al.*, 2004; Benschop *et al.*, 2006; Al-Sunaidi *et al.*, 2007; Watanabe *et al.*, 2007; Baumgarte *et al.*, 2008; Drexler *et al.*, 2009; Li *et al.*, 2009).

HPeV types 1 and 2 primarily cause disease of the respiratory and gastrointestinal tract, e.g. bronchiolitis, pneumonitis and enteritis (Berkovich and Pangan, 1968; Abed and Boivin, 2006; Baumgarte *et al.*, 2008; van der Sanden *et al.*, 2008; Chen *et al.*, 2009; Harvala *et al.*, 2009) but also *Otitis media* (Abed and Boivin, 2006; Tauriainen *et al.*, 2008) and in rare cases disease of the CNS (Figueroa *et al.*, 1989; Koskiniemi *et al.*, 1989; Legay *et al.*, 2002). In contrast, HPeV3 infections are clearly associated with CNS disease and neonatal sepsis (Ito *et al.*, 2004; Boivin *et al.*, 2005; Abed and Boivin, 2006; van der Sanden *et al.*, 2008; Verboon-Maciolek *et al.*, 2008a; Verboon-Maciolek *et al.*, 2008b; Wolthers *et al.*, 2008; Harvala *et al.*, 2009; Levorson et al., 2009). Rare cases of HPeV3 infections also cause respiratory disease (Chen *et al.*, 2009). However, the association of HPeV3 with CNS infection and HPeV1 and 2 with respiratory and gastrointestinal disease, is significant (van der Sanden *et al.*, 2008). Infections of HPeV types other than 1 to 3 were reported in connection with bronchopneumonia, TORCH-syndrome, lymphadenitis (type 4) (Wakatsuki *et al.*, 2008; Chen *et al.*, 2009), gastrointestinal symptoms, fever, arthralgia, rash (type 5) (van der Sanden *et al.*, 2008), Reye-syndrome (type 6) (Watanabe *et al.*, 2007), enteritis (types 6 and 8) (Baumgarte *et al.*, 2008; Drexler *et al.*, 2009), non-polio acute flaccid paralysis (type 7) (Li *et al.*, 2009).

Most diseases caused by HPeV infection occur among young children (< 5 years), the majority of whom is younger than two years. The seroprevalence to HPeV1 increases with age and reaches ≤95 % in adults (Joki-Korpela and Hyypiä, 1998; Tauriainen *et al.*, 2007). Children infected with HPeV3 are frequently younger than children infected with HPeV1 or 2, respectively (Abed and Boivin, 2006; Benschop *et al.*, 2008; van der Sanden *et al.*, 2008; Harvala *et al.*, 2009). Among HPeV infections, HPeV1 and 3 are found most frequently. HPeV1 is found to circulate continuously whereas HPeV3 seems to emerge biannually (Benschop *et al.*, 2008, van der Sanden *et al.*, 2008). An epidemiological study on HPeV infections associated with respiratory symptoms revealed a more frequent infection of males than females (ratio 2.4:1). The same study found a significant number of HPeV and adenovirus (AdV) co-infections, raising the question whether HPeV could reactivate AdV (Harvala *et al.*, 2009).

Parechoviruses have no close relatives among picornaviruses and constitute a distinctive genetic lineage (Stanway and Hyypiä, 1999). It has been estimated that currently circulating HPeV types shared a common ancestor around 1600 and that HPeV types evolved in different genetic lineages since then (Faria *et al.*, 2009). Recombination events occur frequently in RNA viruses (Simmonds, 2006). Parechoviruses recombine as frequently as other picornaviruses emphasising the importance of recombination in the generation of genetic diversity among parechoviruses. One exception is HPeV3 that is thought to evolve into a new genetic lineage among parechoviruses in the future (Williams *et al.*, 2009; Zoll *et al.*, 2009b; Benschop *et al.*, 2010; Calvert *et al.*, 2010). Three main recombination breakpoints in parechoviruses were identified, similar to those of other picornaviruses, i.e. between 5'UTR/VP0, P1/P2 (including 5' part of 2A), and within P3 upstream 3B (Simmonds and Welch, 2006; Zoll *et al.*, 2009b).

HPeVs have molecular features that are distinct from other picornaviruses (Hyypiä *et al.*, 1992; Stanway *et al.*, 1994; Ghazi *et al.*, 1998; Oberste *et al.*, 1998). During capsid protein processing no cleavage of the precursor VP0 into VP4 and VP2 occurs (Stanway *et al.*, 1994). The major capsid proteins share similarities in primary structures with other picornaviruses suggesting a similar architecture with the

exception of a 30 aa long N-terminal extension at the VP3 protein (Stanway and Hyypiä, 1999). As described in section 1.1.2, unlike most other picornaviruses, HPeV 2A protein has no proteolytic activity (Schultheiss *et al.*, 1995). Proteolytic processing is rather mediated entirely by 3C protein (Stanway and Hyypiä, 1999). The functions of HPeV 2A are unclear. However, some data suggest a function in viral replication through binding to the viral 3'UTR (Samuilova *et al.*, 2004). The HPeV1 2C was shown to have ATP hydrolysis and AMP Kinase enzymatic activities, properties that have not been described for other picornaviruses (Samuilova *et al.*, 2006) (compare 1.1.2). In addition, the HPeV1 replication complex is different from enteroviruses. HPeV1 replication takes place in several small discrete foci in the cytoplasm, not in accumulations of membrane vesicles (Krogerus *et al.*, 2003). Also different from enteroviruses, HPeVs lack host cell protein synthesis shut-off (Coller *et al.*, 1990; Stanway *et al.*, 1994).

Identification of structural and sequence elements of HPeV1 5'UTR showed similarities in several functions to 5'UTR of aphtho- and cardioviruses (Nateri *et al.*, 2000). The C-terminus of HPeV1 VP1 protein contains an arginine-glycine-aspartatic acid (RGD) motif (Hyypiä *et al.*, 1992; Stanway *et al.*, 1994). Such motifs are known to participate in cell-cell and cell-matrix interactions (Ruoslahti and Pierschbacher, 1987). Other picornaviruses, such as FMDV and coxsackievirus A9 also contain an RGD motif that interacts with cell surface integrins during virus attachment to the cell (Fox *et al.*, 1989; Chang *et al.*, 1992). Site-directed mutagenesis studies identified the RGD motif essential for HPeV1 cell entry (Boonyakiat *et al.*, 2001). Further studies demonstrated that HPeV1 utilises both integrins αvβ1 and αvβ3 as receptors, probably with higher affinity to integrin αvβ3 (Triantafilou *et al.*, 2000) and uses the clathrin-dependent endocytic pathway for entry into the host cell (Joki-Korpela *et al.*, 2001). However, recently discovered HPeV types 3, 7, and 8 lack RGD motifs (Ito *et al.*, 2004; Drexler *et al.*, 2009; Li *et al.*, 2009) and receptor binding of these viruses has still to be elucidated.

1.1.6 Ljungan virus

LV is one of two species of the Parechovirus genus within the *Picornaviridae* family (Niklasson *et al.*, 1999; Lindberg and Johansson, 2002). LV was originally isolated from bank voles (*Myodes glareolus*) close to the Ljungan river in Sweden (Niklasson *et al.*, 1999) and has later been identified in several other species of voles and lemmings, i.e. gray red-backed vole (*Myodes rufocanus*), field vole (*Microtus agrestis*), Norway lemming (*Lemmus lemmus*) and wood lemming (*Myopus schisticolor*) (Niklasson *et al.*, 2003a; Niklasson *et al.*, 2006b). Species of voles in North America, i.e. Montane vole (*Microtus montanus*) and southern red-backed vole (*Myodes gapperi*), have also been found to be carriers of LV (Johnson 1965; Whitney *et al.*, 1970; Main *et al.*, 1976; Johansson *et al.*, 2003; Tolf *et al.*, 2009a). Recently, LV was detected in both, bank voles and yellow-necked mice (*Apodemus flavicollis*) from Northern Italy (Hauffe *et al.*, 2010). These data suggest a wide geographical distribution of LV and also a wide host range of this virus among rodents.

Five LV strains were analysed. The strains 87-012, the prototype strain, 174F and 145SL were isolated from bank voles in Sweden (Niklasson *et al.*, 1999). The genomes of LV 87-012 and LV 174F are closely related and represent the first genotype, while LV 145SL is distinct and constitutes the second genotype (Johansson *et al.*, 2002). Two further LV strains (M1146 and 64-7855) were isolated from American voles (Montane vole and southern red-backed vole, respectively) representing the third and the fourth genotype, respectively (Johansson *et al.*, 2003; Tolf *et al.*, 2009a) (figure 1.5).

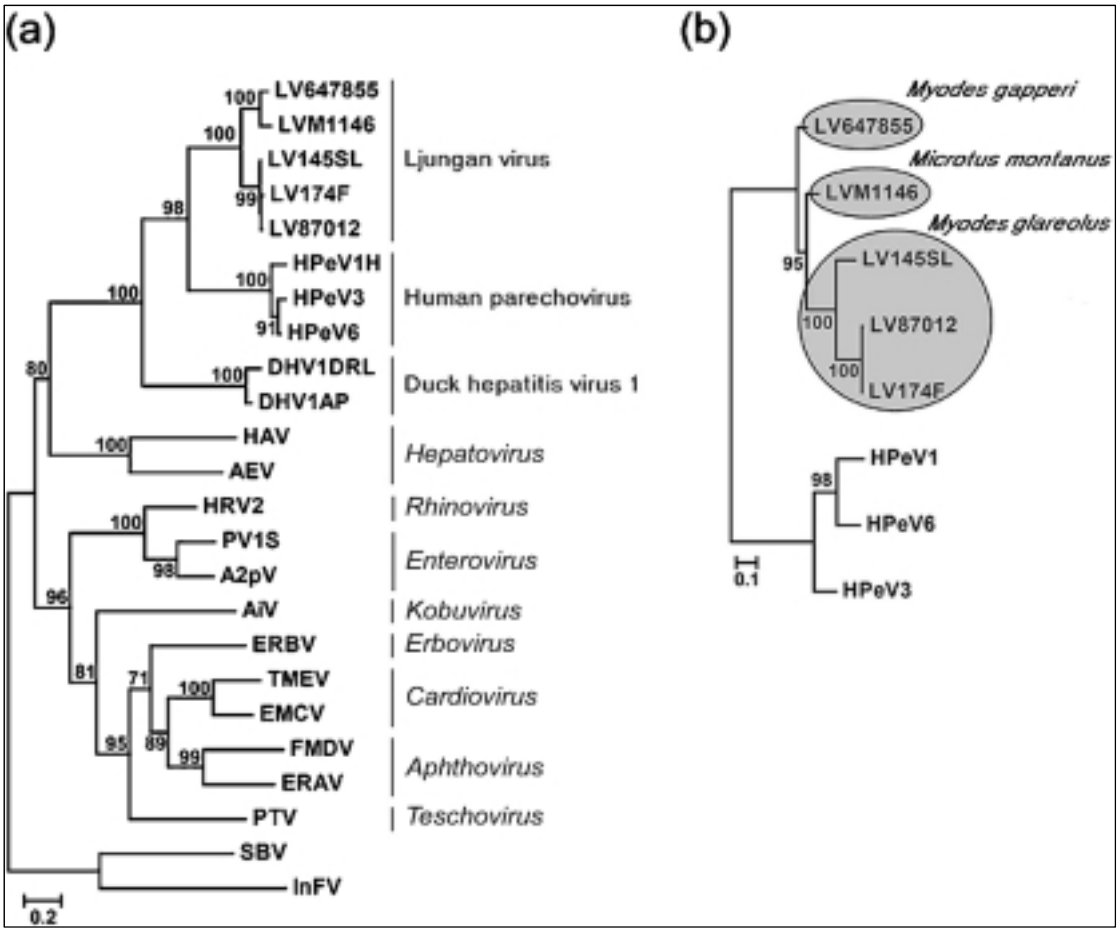

Figure 1.5. Phylogenetic relationships of the 64-7855 LV strain with representative members of the nine genera of the *Picornaviridae* and duck hepatitis virus type 1. (a) Phylogenetic tree based on $3D^{pol}$ protein sequences rooted with two picorna-like insect viruses: sacbrood virus and infectious flacherie virus. (b) Midpoint rooted tree based on VP1 protein sequence of members of the parechovirus. Grey spheres denote the vole species (indicated in italics) from which the LV strains were isolated. Numbers at nodes indicate the percentage of 500 bootstrap replicates supporting that node. Bootstrap values of 70 % or more are indicated. Bars, substitutions per site. Source: Tolf *et al.*, 2009a.

The LV particle is 27 nm in diameter and in electron microscopy, it appears spherical with an almost featureless surface (Niklasson *et al.*, 1999). The virion can be inactivated by heat, but is resistant to acidic pH, detergents and to oxidising environments suggesting a high resistance to chemical and non-physiological environments, respectively (Ekström *et al.*, 2007b).

The LV genome comprises approx. 7600 nucleotides (nt) and has a GC content of 42 % to 45 %. The genome encodes a polyprotein of approx. 2250 amino acids (aa). The 5'UTR varies in length among LV isolates, i.e. from approx. 580 nt (LV 64-7855) to approx. 730 nt (LV 87-012, 174F and 145SL) but has been analysed to have a type II IRES structure as shown for aphtho- and cardioviruses respectively. LV 3'UTR is approx. 110 nt in length and is predicted to fold into two hairpins (Johansson *et al.*, 2002; Johansson *et al.*, 2003; Ekström *et al.*, 2007a; Tolf *et al.*, 2009a). Like for HPeVs, it has been proposed that the LV capsid consists of only three structural proteins (VP0, VP1 and VP3) (Johansson *et al.*, 2002). These data were confirmed by experimental analyses of the LV capsid (Johansson *et al.*, 2004) and the generation of polyclonal antibodies directed against each of the three capsid proteins (Tolf *et al.*, 2008). Unlike HPeVs, the LV polyprotein possesses two 2A proteins (2A1 and 2A2), an uncommon feature among picornaviruses. The N-terminal 2A1 protein belongs to the NPGP 2A protein family that also appears in cardio-, erbo-, tescho-, and aphthoviruses. The C-terminal 2A2 protein is related to the H-NC 2A protein family that is encoded by kobu-, parecho-, and tremoviruses. The cluster of two unrelated 2A proteins suggests an unique regulation of the LV life cycle (Johansson *et al.*, 2002).

Wildtype LV replicates poorly in cell culture with only minor cytopathic effect (CPE) (Niklasson *et al.*, 1999). However, LV could be adapted to growth in green monkey kidney (GMK) cells showing CPE three to four days post infection (dpi). Analysis of the genome of adapted LV showed mutations over the whole genome in both, structural and non-structural proteins (Johansson *et al.*, 2004). Analysis of LV replication in GMK cells using an infectious cDNA clone suggested a different regulatory mechanism for synthesis of positive and negative RNA, respectively. Similar to HPeV infection, LV infection does not result in cellular mRNA host shut-off. It was further shown that LV spreads by both, virus release into the cell culture supernatant and by cell-to-cell transmission (Ekström *et al.*, 2007a).

Wild bank voles develop clinical signs of myocarditis and type-1 diabetes (T1D), the latter characterised by high blood glucose levels, diabetic auto antibodies and a full destruction of pancreas beta cells. An addition, antibodies to LV were detected in sera

of diabetic voles and LV antigen was visualised by immunohistochemistry (IHC) in islet cells of these animals (Niklasson *et al.*, 2003a; 2003b). It has also been demonstrated that bank voles develop characteristics of both type 1 and type 2 diabetes (Blixt *et al.*, 2007). A high proportion of wild caught bank voles and their laboratory offspring develop polydipsia, polyuria and glucosuria after a few months in captivity (Schoenecker *et al.*, 2000). The number of animals developing symptoms of diabetes in captivity is increased through exposure to stress (Freimanis *et al.*, 2003). These observations led to the hypothesis that the outcome of diabetes in wild bank voles is determined by natural stress, i.e. a higher stress level in cyclic versus noncyclic populations (Niklasson *et al.*, 2003b). Vole populations in Northern Scandinavian latitudes have a cyclic fluctuation, reaching a peak of abundance every three to four years (Hansson and Henttonen, 1985; Hörnfeldt *et al.*, 1986; Hörnfeldt, 1994; Stenseth, 1999; Hörnfeldt, 2004). The reason(s) for these fluctuations remain unclear (Stenseth, 1999). However, predation might be one explanation (Hanski and Henttonen, 1996; Hanski *et al.*, 2001; Gilg *et al.*, 2003). But also the possible role of disease has been discussed (Cavanagh *et al.*, 2004). It has been suggested that LV can cause or contribute to predispose voles to other direct factors, such as predation, resulting in a rapid population decline (Niklasson *et al.*, 2006b).

Immune competent CD-1 laboratory mice have been used to study LV infection under controlled conditions in the laboratory (Niklasson *et al.*, 2006a). These animals (mostly males) develop clinical signs of encephalitis a few dpi. Most individuals recover from this acute disease, but develop type 2 diabetes later in life. Behavioural stress of adult mice infected in utero has been shown to be essential for the onset of diabetes (Niklasson *et al.*, 2006a). In addition, LV infection in utero combined with stress leads to intra uterine fetal death (IUFD), fetal malformation and delayed pregnancy in LV infected CD-1 laboratory mice (Samsioe *et al.*, 2006), and fetal deaths persist through recurrent pregnancies in mice, suggesting that LV persists a long time post initial infection (Samsioe *et al.*, 2008).

A temporal correlation of bank vole population density with incidence of death from myocarditis, incidence of Guillain-Barré Syndrome and insulin-dependent diabetes

mellitus incidence (Niklasson *et al.*, 1998) led to an outbreak investigation linked to cases of lethal myocarditis (Wesslen *et al.*, 1992; Niklasson *et al.*, 1999). Antibodies to LV were detected in sera of myocarditis patients (Niklasson *et al.*, 1999) and also in sera of children with recent onset of type 1 diabetes (Niklasson *et al.*, 2003a). In addition, LV was linked to human cases of IUFD, sudden infant death syndrome and central nervous system malformations in termed pregnancy (Niklasson *et al.*, 2007a; 2009a; 2009b; Samsioe *et al.*, 2009).

1.2 Aim of this thesis

The aim of this thesis is three-fold:

(i) to establish assays available for LV detection and characterisation, such as the development of RT-PCR assays and of monoclonal antibodies specific to LV,

(ii) to extend the information about LV hosts and genetic diversity of LV, and

(iii) to obtain first insights in LV pathogenesis, i.e. mechanisms of persistence and apoptosis.

2 Material and Methods

2.1 Viruses, cells, animals and chemicals

LV strains were kindly provided by Prof. Bo Niklasson, Stockholm, Sweden. All LV strains were isolated using BHK-21 cells. Cell culture supernatants were inoculated to 1-day-old suckling mice and virus was passaged in suckling mouse brains (SMB) as described by Niklasson *et al.* (1999). Ten percent SMB in PBS were inoculated to Vero-B4 cells. The cells were passaged blindly until signs of CPE occurred. The supernatants were harvested and used for further propagation in Vero-B4 cells.

Further viruses were provided as either supernatant from infected A549 cells (HPeV) or supernatant from infected Vero cells (TMEV and EMCV) (table 2.1).

Table 2.1 Viruses

Designation	Strain	Accession no.	Source
Ljungan virus	87-012	AF327920	Prof. B. Niklasson[a]
	174F	AF327921	Prof. B. Niklasson
	145SL	AF327922	Prof. B. Niklasson
	M1146	AF538689	Prof. B. Niklasson
	64-7855	EU854568	Prof. B. Niklasson
Human Parechovirus type 1	Harris	L02971	ATCC
Human Parechovirus type 2	Williamson	AJ005695	Prof. E. Schreier[b]
TMEV	BeAn 8386	M16020	ATCC
	GD 7	M20562	ATCC
EMCV	M	L22089	Prof. B. Niklasson
	76/5167	n.a.	Prof. B. Niklasson
	ATCC VR-129B	AJ617356	ATCC

[a] Apodemus AB, Stockholm, Sweden, [b] Robert Koch-Institute, Berlin, Germany
Abbreviations: *TMEV*: *Theiler's Murine Encephalomyelitis virus*,
EMCV: *Encephalomyocarditis virus*, n.a.: not available

Cells were obtained from the Robert Koch-Institute (RKI) reference stock collection or the European collection of cell cultures and cultured as described in 2.2.

Table 2.2 Cell lines

Designation	Tissue	Organism	Source
BHK-21	Kidney	Hamster	RKI[a]
Vero-B4	Kidney	Green monkey	RKI
Sp2/0-Ag 14	Myeloma	Mouse	ECACC[b] No. 85072401

[a] Robert Koch-Institute

[b] European collection of cell cultures

Laboratory animals were used for *in vivo* infection studies (CD-1 mice), generation of mAbs (BALB/C mice) and prevalence analyses among laboratory rat strains. The animal facilities were located at the Karolinska Institute, Stockholm, Sweden and the Robert Koch-Institute, Berlin, Germany. All animal experiments complied with Swedish and German law, respectively, and were approved of by the institutes' ethical committees.

Table 2.3 Laboratory animals

Species	Strain
Mouse	CD-1 (Outbred)
	BALB/C
Rat	BioBreeding (BB)
	Wistar Albino Glaxo (WAG)
	Sprague Dawley® (SD)
	Lewis

All laboratory animals were purchased from Charles River Laboratories, Sulzfeld, Germany.

All chemicals used in this thesis were purchased at either Roth, Karlsruhe, Germany or Sigma-Aldrich, St. Louis, MO unless otherwise noted.

2.2 Cell culture

Both, BHK-21 and Vero-B4 cells were grown and maintained in Dulbecco's Modified Eagles Medium (DMEM) (Gibco, Karlsruhe, Germany) supplemented with 10 % fetal calf serum (FCS), 1 % L-glutamine (L-Gln) and 25 units of penicillin (P) as well as

25 units of streptomycin (S) (all PAA Laboratories, Linz, Austria) in a humid 37 °C incubator with 5 % CO_2.

For cell passaging, DMEM was removed and the cell monolayer was washed once with versen solution (table 2.4) and the cells were subsequently treated with trypsin (PAA Laboratories). After incubation at 37 °C for 10 min, the cells were resuspended in DMEM and cell suspension was split 1:10. For infection experiments the cells were counted using a Neubauer chamber (Roth) and cells were seeded at a density of 5 x 10^5 per ml to reach 80 % confluency on the following day.

Table 2.4 Chemical composition of versen solution

Versen solution	8 g/l sodium chloride
	0.4 g/l potassium chloride
	0.06 g/l sodium hydrogenphosphate
	0.06 g/l potassium hydrogenphosphate
	1 g/l glucose
	0.37 g/l sodium hydrogencarbonate
	adjust to pH 7.0
	add 0.2 % EDTA

When cells had been frozen for long-time storage, the cells were washed with versen solution and treated with trypsin as described above. The cells were pelleted by centrifugation at 800 x g for 5 min. The cell pellet was resuspended in 90 % FCS and 10 % DMSO and the cells were stored at -80 °C for one week and were then transferred to liquid nitrogen.

The cells were tested for mycoplasma contamination at regular intervals using a PCR assay as described by van Kuppeveld *et al.* (1993).

2.3 Virus infection

2.3.1 Cell culture

For cell culture infection, the cells were counted using a Neubauer chamber and the appropriate volume of virus supernatant was determined (according to the desired MOI). The medium of 80 % confluent cell monolayers was removed and the cells were overlaid with virus supernatant (diluted in DMEM without supplements). Virus was allowed to adsorb at 37 °C and 5 % CO_2 for 1 h. After virus adsorption the supernatant was removed and cells were washed twice with PBS and incubated with DMEM at 37 °C and 5 % CO_2 for the indicated time periods.

2.3.2 Laboratory mice

For *in vivo* infection studies, one-day-old Outbred CD-1® laboratory mice were infected with LV 145SL diluted in PBS. Approx. 1000 cell culture infectious dose 50 ($CCID_{50}$) was administered to each animal intraperitoneally (i.p.). For negative controls the same volume of PBS and inactivated LV 145SL, respectively, were used. LV was inactivated by gamma-irradiation at a dosis of 25 kGray.

2.4 Virus titration

Virus titres of LV-containing cell culture supernatants and of organs from LV-infected laboratory mice were determined by $CCID_{50}$ calculation. For the latter, approx. 5-10 mg of organ were homogenised in 100 µl PBS either with a FastPrep system or by using a pipette. Vero-B4 cells were seeded in 96-well plates and Log-10 dilutions of LV supernatants and homogenised organs, respectively, were added. The cells were observed for CPE for 14 dpi. The $CCID_{50}$ was calculated by means of octuple samples by the Spearman-Kärber method (Finney, 1978).

2.5 Study design and sampling of rodent material

LV infection study in CD-1® laboratory mice.

One-day-old CD-1® laboratory mice were infected with 1000 $CCID_{50}$ of LV 145SL as described in 2.3.2. LV-infected animals were kept at the Astrid Fagraeus laboratory, Swedish Institute for Infectious Disease Control, Stockholm, Sweden. From day 25 on, the animals were exposed to stress by keeping three to five male mice in one individual cage (behavioural stress). Mice were sacrificed on days 13, 17, 27, 56, 98, 130 and 174 pi, respectively, and brain, heart, pancreas, lung, kidney, liver, spleen and large intestine were removed. Samples from thymus (13, 17, 27 and 56 dpi) and bladder (98 and 130 dpi) were collected when possible. Control animals were injected with the same volume of normal saline at the same time (six mice sacrificed on day 13 pi and six mice sacrificed on day 174 pi, respectively). All organs were placed in RNA later buffer (Ambion, Cambridgeshire, UK) immediately after sampling and stored at 4 °C for 2-3 days. The tissues in RNA later were shipped over-night at room temperature to the RKI for RNA extraction (2.8.2) and subsequent RT-PCR analysis (2.15.1).

To gain more information about the acute phase of LV infection in laboratory mice, a follow-up study was performed. Mice were infected as described above and were sacrificed on days 1, 2, 3, 5, 7 and 10 pi, respectively. Brain, heart, pancreas, lung, kidney, liver, spleen, large intestine and bladder (when possible) were taken and stored at -80 °C until analysis. Organs were used for virus titration (2.4) and for RNA extraction (2.8.2) and subsequent RT-PCR analysis (2.15.1).

Sampling of Laboratory rat organs.

Brain, heart and pancreas from 8 SD, 8 WAG and 8 Lewis rats were taken and stored at -70 °C until RNA extraction (2.8.2). A piece of pancreas tissue from each animal was fixed in formalin and analysed for LV protein by IHC (2.22). In addition, approx. 2 ml blood were collected from each animal, buffy coat (2.7) and plasma were separated and used for RNA extraction (2.8.1) and IIFT (2.21), respectively.

Sampling of wild rodent organs.

Wild bank voles from Sweden were trapped in the region of Umeå in 2004 and stored at -70 °C. Thirteen animals were blindly chosen from the sample bank, and brain, heart, pancreas, lung, liver and kidney were taken and immediately placed in RNA later buffer. This work was done in collaboration with Prof. Birger Hörnfeldt, Department of Ecology and Environmental Science, Umeå University, Umeå, Sweden.

Wild rodent brain samples from Germany were investigated for presence of LV in collaboration with Dr. Rainer Ulrich, Friedrich Löffler-Institute, Riems, Germany and the network of "rodent carrying pathogens" (Ulrich *et al.*, 2009). Rodents were trapped using snap traps at 28 different locations in Germany as described by Ulrich *et al.* (2008). In total, brains from 454 animals consisting of 15 different species were sent to RKI for RNA extraction (2.8.2) and subsequent RT-PCR analysis (2.15.1). LV-positive samples were further subjected to VP1 RT-PCR (2.15.3) for phylogenetic analysis.

2.6 Generation of monoclonal antibodies against LV

Immunisation of laboratory mice and generation of monoclonal antibodies (mAbs) were performed by Apodemus AB, Stockholm, Sweden.

2.6.1 Immunisation of mice

Female BALB/C mice (Charles River laboratories, Sulzfeld, Germany) were used for immunisation and preparation of immune lymphocytes for hybridoma fusion. Approximately 10^8 CCID50 of LV strain 145SL passaged 6 times in SMB was given to each mouse i.p. (Niklasson *et al.*, 1999). Mice were immunised 4 weeks later with 10^8 CCID50 of LV strain 145SL passaged 6 times in SMB mixed with an equal amount of Freund complete adjuvans subcutaneously. A booster immunization of 10^9 CCID50 of LV strain 87-012 passaged 4 times in SMB mixed with equal amount of

Freund incomplete adjuvans subcutaneously were given 2-4 months following the first infection and always one week prior to the hybridoma fusion.

2.6.2 Generation of mAbs

The Sp2/0-Ag 14 mouse myeloma cell line was thawed one week prior to hybridoma fusion, grown and maintained in DMEM supplemented with 10 % FCS, 1 % L-Gln, 0.1 % gentamycine and 1 % non essential amino acids (NEAA) at 37 °C with 5 % CO_2. Mice were euthanized by CO_2 overdose and cervical dislocation. The spleens were removed aseptically and splenocytes were collected in DMEM by homogenisation of the spleen using a sterile syringe with a gauge sterile needle.

Hybridoma fusion was basically performed as described by Kohler and Milstein (1975). Briefly, splenocytes were fused with log-growth Sp2/0-Ag 14 cells at a ratio of 2:1. The cell mixture was washed once with DMEM, and 1 ml of polyethylene glycole 4000 (50 % solution in Dulbecco's phosphate buffered saline) (Gibco, Carlsbad, CA) was added dropwise to the myeloma-splenocytes pellet over 90 sec at 37 °C with gentle tapping of the tube. Ten ml DMEM were added dropwise over 1 min and the cells were resuspended in additional 35 ml DMEM. After 10 min incubation at room temperature and centrifugation at 800 x g for 5 min the cell pellet was resuspended in 40 ml hypoxanthine aminopterin thymidine medium containing 20 % FCS, 1 % NEAA, 2 % L-Gln, 0.1 % gentamycin and 1x OPI media supplement (Sigma). The cells were plated into 96-well cell culture plates (Sarstedt, Landskrona, Sweden) and the plates were incubated at 37 °C with 7.5 % CO_2 in a humidified chamber. After 3-4 days supernatants were screened by capture ELISA as described in 2.23.1 and positive single colonies were picked from the plates, placed in 96-well plates containing thymus-conditioned medium (DMEM containing 30 % FCS, 1 % 2-mercaptoethanol, 1 % NEAA, 2 % L-Gln, 0.1 % gentamycin) and incubated as described above.

All mAbs were isotyped using a mouse monoclonal antibody isotyping test kit (Serotec, Kidlington, UK).

2.7 Separation of buffy coat from whole blood

After centrifugation of whole blood three layers are formed. The erythrocytes-containing red bottom layer and the plasma-containing yellow top layer are separated by a third layer consisting of leukocytes and thrombocytes, the buffy coat. Buffy coat was used for RNA extraction (2.8.1) and subsequent RT-PCR analysis (2.15.1).

Whole blood was centrifuged at 800 x g for 10 min. The plasma was taken and stored at -20 °C. The grey buffy coat layer was collected and mixed with 10 ml of red cell lysis buffer (10 mM Tris pH 7.6, 10 mM magnesium chloride, 5 mM sodium chloride) to remove remaining erythrocytes. After incubation at 4 °C for 5 min the cells were pelleted by centrifugation at 800 x g for 10 min. The cell pellet was resuspended in 500 µl PBS* (PBS*: without sodium bicarbonate, calcium and magnesium ions) and pelleted again by centrifugation at 800 x g for 5 min. After another resuspension in 500 µl PBS* and centrifugation as described above, the cells were lysed in 350 µl RLT buffer (Qiagen, Hilden, Germany) and stored at -20 °C until RNA extraction.

2.8 Nucleic acid extraction

2.8.1 RNA extraction from cells and viral RNA extraction from fluids

RNA from cultured cells and white blood cells was extracted by use of an RNeasy Mini Kit (Qiagen) and viral RNA from cell culture supernatants, serum and plasma samples, respectively, was isolated with a QIAamp Viral RNA Mini Kit (Qiagen), both as recommended by the manufacturer.

2.8.2 Extraction of total RNA from tissues

Total RNA from tissue was extracted as described by Chomczynski and Sacchi (1987). Approx. 20-50 mg tissue were homogenised in 500 µl denaturation solution (4 M GTC, 25 mM sodium citrate pH 7.0, 0.5% N-Lauryl sarcosine) using a FastPrep FP 120 system (Eubio, Vienna, Austria). After adding 0.1 volumes 2 M sodium acetate, 1

volume phenol and 0.2 volumes chloroform / isoamyl alcohol, the samples were mixed and then incubated on ice for 15 min. After a centrifugation for 15 min at 115000 x g and 4 °C, the aqueous RNA-containing supernatant was transferred into a fresh tube and 1 volume isopropanol was added. The samples were incubated on ice for 30 min and were then centrifuged for 20 min at 4 °C and full speed. The supernatant was discarded and the pellet was washed twice with 70 % ethanol. The air-dried RNA pellet was dissolved in 100 µl molecular grade water, RNA concentration was determined photometrically (2.12) and the samples were stored at -70 °C until use.

2.8.3 DNA extraction from mouse liver

DNA extraction from mouse liver was performed as described by Lambert *et al.* (2000). Approx. 1 mg of tissue was homogenised in 100 µl of TKM buffer (10 mM Tris pH 7.6, 10 mM KCl, 2 mM EDTA, 4 mM $MgCl_2$) with a pipette using a filter-tip, and 400 µl TKM buffer and 37.5 µl 10 % SDS were subsequently added. The tube was then vortexed and incubated at 55 °C for 5 min. The denatured proteins were precipitated by adding 200 µl of 6 M NaCl. After vortexing and centrifugation for 5 min at 12000 x g, a 500 µl aliquot was transferred into a fresh tube and 900 µl of 100 % ethanol were added to precipitate the DNA. The DNA was pelleted by centrifugation for 10 min at full speed. The pellet was washed once with 70 % ethanol. The air-dried DNA pellet was dissolved in 100 µl molecular grade water and the samples were stored at -20 °C until PCR analysis.

2.8.4 DNA extraction from agarose gel

DNA from agarose gel slices was extracted by use of a QIAquick Gel Extraction Kit (Qiagen) according to the manufacturer's instructions.

2.8.5 Extraction of low-molecular-weight DNA

DNA fragmentation is a hallmark of apoptosis and was analysed by isolating low-molecular-weight DNA using the SDS-high-salt method as described by Zhirnov *et al.*, 2002. Cultured cells (approx. 10^6) were scraped off the surface of the cell culture flask using a cell scraper and cells were separated by centrifugation for 15 min at 1500 x g. The cell pellet was resuspended in 80 µl PBS, and 300 µl TES-buffer (10 mM Tris-HCl pH 7.6, 10 mM EDTA, 0.6 % SDS) were added. The samples were gently mixed and 500 µl of 5 M NaCl were added. The mixtures were gently mixed and incubated overnight at 4 °C. The samples were centrifuged for 20 min at 15000 x g and 4 °C. The low-molecular-weight-containing supernatants were treated with RNase A (final concentration 1 mg/ml) for 20 min at 37 °C and subsequently with Proteinase K (final concentration 0.2 mg/ml) for 20 min at 37 °C. Two volumes of 100 % ethanol were added and the samples were incubated overnight at -20 °C. The precipitated low-molecular-weight DNA was pelleted by centrifugation for 20 min at 15000 x g and 4 °C. The air-dried pellets were dissolved in 20 µl molecular-grade water and DNA fragmentation was analysed by agarose gel electrophoresis (2.16).

2.9 Molecular cloning and bacterial transformation

Purified PCR amplicons were cloned into the TA-based pDrive cloning vector using a Qiagen PCR Cloning Kit (Qiagen). The ligation-reaction mixture contained 0.5 µl pDrive Cloning Vector, 2 µl PCR product and 2.5 µl Ligation Master Mix. The reaction was performed in a thermo cycler using a touch-up protocol. The mixtures were incubated at 4 °C and temperature was increased stepwise by 1 °C until 25 °C were reached. Duration time for each temperature step was 5 min.

One Shot® TOP10 Chemically Competent *E. coli* cells (Invitrogen, Karlsruhe, Germany) were thawed on ice and 2.5 µl of the ligation mixture were added. The reaction was gently mixed and incubated on ice for 30 min. The cells were heat-shocked for 30 sec at 42 °C and immediately placed on ice. After incubation on ice for 2 min, 250 µl of SOC medium (Invitrogen) were added. The vials were shaken

horizontally at 37 °C for 1 h at 200 rpm. Transformed cultures were plated on LB (lysogeny broth) plates (table 2.5) containing 100 µg/ml ampicillin (+ amp), 40 µg/ml X-gal (bromo-chloro-indolyl-galactopyranoside) and 0.2 mM IPTG (isopropyl β-D-1 thiogalactopyranoside) and the plates were incubated overnight at 37 °C. Colonies containing a plasmid with insert were identified by blue-white-screening and were further subjected to a colony-screen PCR to determine the correct insert size and the direction of the insert (2.15.6).

Table 2.5 Chemical composition of LB medium

LB medium	10 g/l Bacto-Tryptone
	5 g/l Bacto-Yeast extract
	10 g/l sodium chloride
	adjust to pH 7.0 with 10 M sodium hydroxide

For production of LB agar plates 15 g/l Bacto-Agar were added.
Abbreviation: LB: lysogeny broth

2.10 Production of chemically competent *E. coli* cells

One single colony of One Shot® Top10 *E. coli* was inoculated in 5 ml LB medium + amp and grown overnight at 37 °C. Two ml of the overnight culture were inoculated in 250 ml LB medium + amp and grown until an optical density of 0.4-0.6 was reached. Cells were harvested by centrifugation at 2500 x g and 4 °C for 5 min. The cell pellet was resuspended in 40 ml ice-cold TFB1 buffer (table 2.6) and was incubated on ice for 10 min. After centrifugation as described above, the cell pellet was resuspended in 8 ml TFB2 buffer (table 2.6) and the solution was aliquoted at 80 µl each. Aliquots were immediately transferred to liquid nitrogen and stored at -70 °C until use.

Table 2.6 Chemical composition of buffers used for production of chemically competent *E. coli*

TFB1	30 mM potassium acetate
	50 mM manganese chloride
	100 mM rubidium chloride
	10 mM calcium chloride
	15 % glycerin
	adjust to pH 5.8 with acetic acid
TFB2	10 mM MOPS
	75 mM calcium chloride
	10 mM rubidium chloride
	15 % glycerin
	Adjust to pH 7.0 with potassium hydroxide

Buffers were sterile filtrated before use.

2.11 Plasmid preparation

E. coli clones that were identified as positive by colony-screen PCR (2.15.6) were inoculated in 3 ml LB medium + amp and were incubated overnight at 37 °C and rotation at 200 rpm. Plasmid preparation was performed using an Invisorb® Spin Plasmid Mini Kit (Invitek, Berlin, Germany) according to the manufacturer's instructions. The plasmid concentration was determined photometrically (2.12) and correct cloning was confirmed by sequence analysis (2.17).

2.12 Photometrical determination of nucleic acid yield and purity

Extracted nucleic acids were analysed for their yield and purity with a Biophotometer (Eppendorf, Hamburg, Germany). A minimum of 50 µl solution was applied to a disposable plastic cuvette with a diameter of 1 cm (Eppendorf). As reference the corresponding solving liquid was used. Nucleic acids were quantitated at a wave length of 260 nm. A DNA solution in a 1 cm cuvette with an optical density has a concentration of 50 µg/ml (or 40 µg/ml in case of RNA). A wave length of 320 nm was also applied for background correction. Concentration was determined as

absorption (260 nm) - absorption (320 nm) x factor (50 µg/ml [DNA], 40 µg/ml [RNA] with a pathlength of 1 cm).

2.13 *In vitro* transcription

In vitro transcribed RNA was produced to create RT-PCR standards and to evaluate a quantitative real-time RT-PCR specific for the detection of LV RNA (2.15.1).

Viral RNA was reverse transcribed (2.14) and a 187-bp fragment from the LV 5'NTR was amplified by PCR (2.15.1). The PCR amplicon was gel purified (2.8.4) and cloned into the T7-promotor-sequence containing pDrive cloning vector (2.9). Successful cloning was confirmed by colony-screen PCR, and the direction of the PCR product was determined by sequencing (2.17). The plasmid was isolated (2.11) and concentration was determined photometrically (2.12). The isolated plasmid was linearised by incubation with the restriction enzyme SalI (Fermentas, St. Leon-Roth, Germany). For this purpose approx. 3 µg plasmid were digested with 3 U SalI at 37 °C overnight and digestion enzyme was inactivated at 65 °C for 20 min. Prior to restriction enzyme digestion, the insert-containing plasmid was scanned for possible further restriction sites of SalI to ensure a single digestion behind the insert. No further restriction sites were found. Plasmid DNA was *in vitro* transcribed using the Riboprobe® System-T7 (Promega, Madison, WI). A 20 µl reaction was applied containing 100 ng plasmid DNA, 4 µl 5x transcription buffer, 200 nmol dithiothreitol (DTT), 20 U RNaseOUT™ RNase inhibitor, 10 nmol dNUTPs (with dUTP instead of dTTP) and 20 U T7-polymerase. The reaction was allowed to proceed at 37 °C for 1 h. To remove remaining plasmid DNA, the reaction mixture was incubated twice with 6 U Turbo™ DNase (Ambion) at 37 °C for 2 h. *In vitro* transcribed RNA was purified by phenol-chloroform extraction, amount of RNA was determined and samples were stored in aliquots at -80 °C.

2.14 Reverse transcription reaction

RNA was reverse transcribed to obtain stable complementary DNA (cDNA) by use of a reverse transcriptase. The cDNA served as template in subsequent PCR assays using a DNA-dependent DNA polymerase. Reverse transcription (RT) was performed by use of gene-specific primers.

RNA samples were denatured prior to RT-reaction to reduce secondary RNA structures. Therefore, 5 µl RNA were mixed with 5 nmol dNTPs (Fermentas) and 5 pmol reverse primer (20 pmol for primer LjR1). For detection of LV negative-strand RNA by 5'NTR-RT-PCR assay 5 pmol forward primer were used instead. The mixtures were incubated at 80 °C for 2 min, 75 °C for 2 min, 70 °C for 2 min and 65 °C for 6 min and immediately put on ice.

RT reaction using MMLV (Moloney murine leukemia virus) reverse transcriptase.

The RNA-dNTPs-primer mix was added to a reaction containing 2 µl of 5 x RT reaction buffer, 50 nmol DTT, 10 U RNaseOUT™ RNase inhibitor and 50 U MMLV (all Invitrogen). RT reaction was performed at the respective primer annealing temperature for 5 min, 37 °C for 50 min and 70 °C for 15 min. The cDNA samples were stored at 4 °C until PCR analysis.

RT reaction using Superscript® III reverse transcriptase

Superscript® III reverse transcriptase works with full activity at 50 °C. The higher working temperature of this enzyme leads to an increased specificity with gene-specific primers compared to MMLV reverse transcriptase.

RNA, dNTPs and primer were incubated as described above and a reaction mix consisting of 4 µl 5x RT reaction buffer, 100 nmol magnesium chloride, 200 nmol DTT, 10 U RNaseOUT™ RNase inhibitor and 200 U Superscript® III reverse transcriptase (all Invitrogen) was added to a final volume of 20 µl. Reaction proceeded at 50 °C for 50 min and 85 °C for 5 min.

2.15 Polymerase chain reaction

2.15.1 Ljungan virus-specific real-time TaqMan® PCR assay

An LV-specific real-time RT-PCR assay targeting the 5'UTR of the LV genome and using the TaqMan® format was performed to quantitate the amount of LV RNA. The RT-PCR was performed either as one-step assay or as two-step assay. The two-step assay was used when a specific detection of either positive-strand RNA or negative-strand RNA was necessary.

The one-step assay was performed by use of the QuantiTect Probe RT-PCR Kit (Qiagen) as recommended by the manufacturer in a 25 µl reaction containing 20 pmol of both forward and reverse primer, and 2.5 pmol of each probe LjMGBc and LjMGBg. Reaction was performed at 50 °C for 30 min and 95 °C for 15 min followed by 40 cycles: 95 °C for 15 sec and 60 °C for 30 sec.

The two-step assay was performed as follows: 5 µl cDNA was applied to a 25 µl reaction containing 2.5 µl 10 x buffer (with ROX reference dye), 100 nmol magnesium chloride, 20 nmol dNUTPs, 5 pmol forward and reverse primer, respectively, 2.5 pmol of both probes, LjMGBc and LjMGBg, 1.25 U Platinum® *Taq*-polymerase and 0.25 U of uracil-DNA glycosylase. Reaction conditions were: 50 °C for 2 min and 95 °C for 10 min followed by 40 cycles: 95 °C for 15 sec and 60 °C for 30 sec.

Degenerate primers LjF1 and LjR1 were designed during the RT-PCR evaluation to increase the specificity of the assay, in particular for detection of LV RNA whit sequences that are distinct from those of the known LV strains. Probes LjMGBc and LjMGBg differ at the 5th position of the probe sequence. This was made due to a sequence variation between LV strains 87-012, 174F, and 145SL and the strain M1146 at this position. Both probes were conjugated with the reporter dye 6-FAM-phosphoramidite (6-FAM) at the 5'-end. A minor groove binder with quencher was conjugated to the 3'-end of the probes to form stable duplexes with single-stranded DNA targets resulting in a higher specificity.

Sequences of primers and probes used in this assay are shown in table 2.7.

Table 2.7 Sequences of primers and probes used for LV-specific real-time RT-PCR assay

Designation	Sequence (5'→3')	Direction	Position†
Primers			
LjF	GCG GTC CCA CTC TTC ACA G	forward	256-274
LjR	GCC CAG AGG CTA GTG TTA CCA	reverse	442-422
LjF1	GGG CGG TCC YAC TCT YYA CAG	forward	254-274
LjR1	GCC CAG AGG CTR GTG TTA CCA	reverse	442-422
Probes			
LjMGBc	6-FAM-TGT CCA GAG GTG AAA GC-MGB	reverse	306-290
LjMGBg	6-FAM-TGT CGA GAG GTG AAA GC-MGB	reverse	205-189

† Primer and probe positions refer to the LV strain 87-012 genome sequence (Accession no. AF327920). Probe LjMGBg positions correspond to LV M1146 sequence (Accession no. AF538689).

2.15.2 RT-PCR assay targeting a sequence of the 2A/2B region of the LV genome

An RT-PCR assay with primers located at the 2A/2B region of the LV genome was established with the aim to confirm RT-PCR results obtained from the 5'NTR region.

A 25 µl reaction contained 5 µl cDNA, 2.5 µl 10 x PCR-buffer, 37.5 nmol magnesium chloride, 1 U Platinum *Taq*-polymerase (all Invitrogen), 5 nmol dNTPs (Fermentas), 12.5 pmol of forward primer 5'-GGC TTY TAT AAR CAT TAT GG-3' (LV 87-012 genome position 3208-3227) and 12.5 pmol of reverse primer 5'-ATC ATT ATT AAA RGT TTC ACA CAT-3' (LV 87-012 genome position 3675-3652). The assay was performed at 95 °C for 2 min followed by 40 cycles at 95 °C for 30 sec, 50 °C for 30 sec, 72 °C for 45 sec and a final amplification step at 72 °C for 3 min.

2.15.3 Semi-nested RT-PCR assay for LV VP1 sequences

Most genetic divergence among picornavirus genomes is found in the VP1 region allowing sequence analyses for phylogenetic studies (Oberste *et al.*, 1999a; Oberste *et al.*, 1999b). For this reason, a semi-nested RT-PCR assay was established to amplify a

530 bp fragment from the LV VP1 region. Reverse primers LV-VP1-R3341a and LV-VP1-R3341b were mixed to equal concentrations and used as one primer (LV-VP1-R3341a/b). RT and first PCR were performed using a Qiagen OneStep RT-PCR Kit (Qiagen) with 10 pmol forward primer LV-VP1-F2659 and 10 pmol reverse primer LV-VP1-R3341a/b according to the manufacturer's instructions. Reaction conditions were 50 °C for 25 min and 95 °C for 15 min followed by 10 touchdown cycles: 95 °C for 15 sec, 60-50 °C for 30 sec (-1 °C for each cycle) and 72 °C for 75 sec. Reaction was completed by 40 further cycles: 95 °C for 15 sec, 54 °C for 30 sec and 72 °C for 75 sec. A second PCR was performed with 1 µl of the 683 bp long first PCR product in a 50 µl-reaction containing 10 nmol dNTPs (Fermentas), 5 µl 10x reaction buffer, 125 nmol magnesium chloride, 2 U Platinum *Taq*-polymerase (all Invitrogen), 20 pmol forward primer LV-VP1-F2659 and 20 pmol reverse primer LV-VP1-R3188. Reaction was performed at 95 °C for 3 min followed by 10 touchdown cycles: 95 °C for 15 sec, 62-52 °C for 30 sec (-1 °C for each cycle) and 72 °C for 60 sec. Reaction was completed by 40 cycles: 95 °C for 15 sec, 54 °C for 30 sec and 72 °C for 60 sec. PCR products were separated by agarose gel electrophoresis and visualised under UV light (2.16). Primer sequences are shown in table 2.8.

Table 2.8. Sequences of primers used in LV VP1 RT-PCR

Designation	Sequence (5'→3')	Direction	Position[†]
LV-VP1-F2659	AAA GTT GCW CAY ACM TGG TTT GG	forward	2659-2681
LV-VP1-R3341a	GCA TGT GTC CAA TTT CCA TCA TC	reverse	3341-3319
LV-VP1-R3341b	GCA TGA ACC CAT TTG CCA TCA TC	reverse	3341-3319
LV-VP1-R3188	TCR ATR TCR GGG CCW GGG TT	reverse	3188-3169

[†] Primer positions refer to the LV strain 87-012 genome sequence (Accession no. AF327920).

2.15.4 Sex determination of suckling CD-1® laboratory mice by PCR

CD-1® laboratory mice younger than 10 days at time of sacrifice were analysed for their sex by PCR. DNA extracted from mouse liver (2.8.3) was investigated by a duplex PCR assay as described by Lambert *et al.* (2000).

2.15.5 Hypoxanthine-guanine Phosphoribosyl Transferase mRNA detection by real-time RT-PCR

Hypoxanthine-guanine Phosphoribosyl Transferase (HPRT) has been described as constitutively expressed housekeeping gene especially in the brain. Detection of HPRT mRNA by RT-PCR can be used as internal control for successful preparation of RNA from samples (Pernas-Alonso *et al.*, 1999). A real-time RT-PCR assay was performed to detect murine HPRT mRNA extracted from tissue of LV-infected laboratory mice and wild rodents analysed for presence of LV. Primers and probe were purchased from Tibmolbiol, Berlin, Germany with the following order numbers: forward primer (HPRT ex7.8): 746750, reverse primer (mu HPRT R): 746751 and probe (mu HPRT TM): 746752. RNA was reverse transcribed (2.14) and 2.5 µl cDNA was applied to a 25 µl reaction containing 2.5 µl 10 x buffer (with ROX reference dye), 100 nmol magnesium chloride, 20 nmol dNUTPs, 5 pmol of forward and reverse primer, respectively, 2.5 pmol of the probe, 1.25 U Platinum® *Taq*-polymerase and 0.25 U of uracil-DNA glycosylase. Reaction conditions were: 50 °C for 2 min and 95 °C for 10 min followed by 35 cycles: 95 °C for 15 sec and 65 °C for 30 sec.

2.15.6 Colony-screen PCR

Successful cloning of PCR products into the pDrive cloning vector was confirmed by colony-screen PCR.

Single colonies were picked from LB agar plates after incubation (2.9). Each colony was resuspended in 50 µl water and 5 µl were transferred into a reaction tube containing 50 µl LB medium (containing 100 µg/ml ampicillin). The latter was stored

at 4 °C. The water-containing tubes were vortexed and incubated at -80 °C for 5 min. The tubes were again vortexed followed by incubation at 100 °C for 5 min. After centrifugation at full speed for 1 min, 2.5 µl of the supernatant were transferred into a 25 µl PCR reaction mix containing 2.5 µl 10 x buffer, 37.5 nmol magnesium chloride, 5 nmol dNTPs, 12.5 pmol of forward and reverse primer, respectively, and 1 U Platinum® *Taq*-polymerase. The following primer set was used which is available at pDrive cloning vector manual (Qiagen): M13 forward (-20) primer 5'-GTA AAA CGA CGG CCA GT-3' and M13 reverse primer 5'-AAC AGC TAT GAC CAT G-3'. PCR reaction comprised of initial denaturation at 94 °C for 2 min followed by 35 cycles: 94 °C for 30 sec, 64 °C for 30 sec, 72 °C for 1 min and a final elongation at 72 °C for 3 min. PCR products were visualised with an agarose gel under UV light (2.16).

Positive colonies were inoculated into 3 ml LB medium + amp for plasmid preparation (2.11).

2.16 Agarose gel electrophoresis

Agarose gel electrophoresis was performed to separate and visualise PCR products and fragmented DNA (after apoptosis induction), respectively. Samples were mixed with 6 x loading dye (Fermentas) to a final concentration of 1 x and were applied to an 1-2 % agarose (Biozym, Oldendorf, Germany) gel in Tris-borate-EDTA (TBE) buffer (Eppendorf) containing 0.5 µg / ml ethidium bromide. Gels were run in TBE buffer at 80-100 V and DNA was visualised under UV light.

2.17 Sequencing reaction

Sequencing was performed with a Big Dye Terminator Cycle 69 Sequencing Kit on a 377 DNA automated sequencer (Applied Biosystems). Concentration of purified PCR products (2.8.4) was determined photometrically (2.12), and 1-3 ng DNA (for PCR products with a length of 100-200 bp) or 3-10 ng DNA (for PCR products with a

length of 200-500 bp) were applied to a reaction containing 5 pmol of either forward or reverse primer. Cycling conditions were 96 °C for 2 min followed by 25 cycles at 96 °C for 10 sec, primer annealing temperature for 5 sec, 60 °C for 4 min. Samples were stored at -20 °C until gel filtration.

2.18 Melting curve analysis

A melting curve analysis (MCA) was established to further analyse samples that were detected positive for LV by real-time RT-PCR (2.15.1). The reaction was performed using a LightCycler 1.5 instrument (Roche Applied Science, Basel, Switzerland). A LightCycler capillary was applied containing 2 µl of real-time RT-PCR product, 1 µl 10x PCR buffer, 400 nmol magnesium chloride (both Invitrogen), 5 pmol of donor probe Lj Fl: 5'-GTG TGT AGG CGT AGC GGC TAC TTG A-fluorescein-3' (LV 87-012 genome positions 376-400) and 5 pmol of acceptor probe Lj LC: 5'-LightCycler Red 640-TGC CAG CGG ATT ACC CCT A-phosphate-3' (LV 87-012 genome positions 402-420) in a total volume of 10 µl. Samples were denatured at 95 °C for 30 sec and cooled to 40 °C with 20 °C per sec. Reheating was performed with a ramping rate of 0.4 °C per sec. Samples were finally cooled to 35 °C with a slope of 20 °C per sec. The data were analysed using the LightCycler software 3.5.

2.19 Pyrosequencing

Pyrosequencing of LV-specific real-time RT-PCR products was established as an alternative to MCA, in particular to obtain sequences that do not belong to one of the known LV strains.

Pyrosequencing was performed using a PyroMark ID System (Biotage, Uppsala, Sweden). Real-Time PCR was performed with a biotinylated primer LjF1 (2.15.1) to allow single-strand DNA preparation by binding to streptavidin-coated sepharose beads. The single-stranded real-time PCR amplicon was annealed to the LV-specific sequencing primer LjPS: 5'-CCC AGA GGC TRG TGT-3'. Pyrosequencing reaction

was completed using Pyrogold SQA reagents (Biotage) with the complete real-time PCR product according to the manufacturer's instructions.

2.20 Plaque reduction neutralisation assay

LV-specific mAb-containing hybridoma cell culture supernatants were assayed for their ability to neutralise LV. Mixtures of LV supernatant (1 ml, 1000 $CCID_{50}$) and hybridoma cell culture supernatant (1 ml) were incubated at 37 °C for 1 h. The mixtures were applied to monolayers of Vero-B4 cells, grown on 6-well plates in DMEM (2.2). After incubation at 37 °C for 1 h, the samples were removed and cells were washed once with DMEM. Since the assay was performed in presence of mAb, 500 µl hybridoma cell culture supernatant mixed with 1 ml DMEM was added and cells were overlaid with 1.5 ml carboxy methyl cellulose (1.4 % in DMEM). For positive control, 1000 $CCID_{50}$ in 1.5 ml DMEM were used. After incubation for 10 days the samples were removed and cells were fixed with 4 % paraformaldehyde for 30 min. The cells were stained with naphthol black solution (1 g naphthol blue black, 13.g sodium acetate, 60 ml glacial acetic acid, ad 1 l $Aqua_{dest}$) for 1 h. The naphthol black solution was removed, cells were washed with water and air dried. Plaques were counted and the neutralisation effect was determined as percentage of preventing the virus to enter Vero-B4 cells compared to the positive control.

2.21 Indirect Immunofluorescent assay

Cells were grown on 12 mm-glass slides (Roth) in 24-well cell culture plates (Nunc) as described in 2.2. The medium was removed and cells were fixed with acetone for 20 min. After two washes with PBS, the slides were treated with blocking buffer (3 % FCS and 0.1 % TWEEN® 20 in PBS) for 1 h to reduce the background. The slides were washed twice with PBS and primary antibody was applied:

Characterisation of LV-specific mAbs: hybridoma supernatants were added undiluted; while mouse immune and preimmune sera, respectively, were diluted 1:100 in IFA sample buffer (Euroimmun, Lübeck, Germany).

LV prevalence in laboratory rats: rat sera were diluted 1:2, 1:4, 1:8 and 1:16 in IFA sample buffer.

LV cell culture studies: 200 ng / slide of a rabbit anti-LV-VP1 polyclonal antiserum (Tolf *et al.*, 2008); 100 ng / slide of the mouse anti-LV monoclonal antibody LV-05sA4-H; rabbit anti-active-Caspase-3 monoclonal antibody (Sigma-Aldrich), diluted 1:500. All antibodies were diluted in IFA sample buffer.

Primary antibody was incubated in a wet chamber at 37 °C for 1 h. The slides were washed twice with PBS and cells were stained with either a fluorescein isothiocyanate conjugated goat anti-rabbit polyclonal antibody (1:200; Dianova, Hamburg, Germany) or a rhodamine conjugated goat anti-mouse polyclonal antibody (1:200; Dianova) at 37 °C for 45 min in a wet chamber. After two washes with PBS and one wash with distilled water, the cells were mounted with either Shandon-Mount^{TM} medium (Thermo, Runcorn, UK)) or DAPI-containing ProLong Gold antifade reagent (Invitrogen). The slides were stored at 4 °C until examination.

2.22 Immunohistochemistry

Immunohistochemistry (IHC) was performed by Apodemus AB, Stockholm, Sweden.

LV-infected GMK cells (LV strain 87-012) were fixed in formalin and embedded in paraffin and used to screen for mAbs that could be used in immunohistochemistry. Uninfected GMK cells treated the same way were used as controls. Four µm sections were cut and mounted onto SuperFrost® Plus Slides (Menzel-Gläser, Braunschweig, Germany). Immunohistochemistry was performed as described previously (Lee *et al.*, 1999; Shi *et al.*, 1991; Shi *et al.*, 1997) with minor modifications. Antigen retrieval was performed using the 2100 Retriever (Histolab Products AB, Gothenburg, Sweden) and Novacastra epitope retrieval solutions pH 9 (Leica, Wetzlar, Germany). MAb

supernatants were tested at different dilutions ranging from 1:5-1:200 diluted in PBS. A biotinylated goat anti-mouse antibody, Vectastain ABC reagent and a VECTOR Red Substrate Kit (Vector Laboratories, Burlingame, CA, USA) were used for staining.

2.23 Enzyme linked immunosorbent assay

2.23.1 LV-specific capture Enzyme linked immunosorbent assay

Hybridoma culture supernatants were assayed for binding to LV using a capture enzyme linked immunosorbent assay (cELISA) assay. The Maxisorp^{TM} flat-bottom 96-well plates (Nunc) were coated with 2 µg of a protein A purified rabbit anti-LV-VP1 antiserum (Tolf *et al.*, 2008) diluted in 0.05 M sodium carbonate overnight at 4 °C. The plates were blocked with 1 mg/ml bovine serum albumin (BSA) in 0.05 M sodium carbonate, for 1 h at room temperature or overnight at 4 °C, and then washed three times with 0.05 % TWEEN 20 in 0.15 M sodium chloride and tapped dry on a paper towel. LV cell culture supernatant (approx. 10^6 $CCID_{50}$) was diluted 1:1 in dilution buffer (0.1 % BSA and 0.05 % TWEEN 20 in PBS), added to the plates and incubated for 2 h at room temperature. Cell culture supernatant of Mock-infected cells was used as negative control. The plates were washed three times as described above and hybridoma cell culture supernatants were added (25 µl/well) and the plates were incubated for 3 h at room temperature. Both mouse immune and preimmune sera, diluted 1:500 in dilution buffer, were used as controls. After three washes as described above, a polyclonal rabbit anti-mouse horse-radish peroxidase (HRP) conjugated antibody (Dako, Stockholm, Sweden) was diluted 1:1000 in dilution buffer and applied to the ELISA plates for 2 h at room temperature. The plates were washed four times as described above and positive binding was detected with a TMB Peroxidase EIA Substrate Kit (Bio-Rad Laboratories, Hercules, CA). After 30 min the reaction was stopped with 0.18 M sulphuric acid and optical density was read at 450 nm. All samples were analysed in triplicate. Cut-off was determined with means of negative controls plus three standard deviations.

2.23.2 HPeV type 1 Enzyme linked immunosorbent assay

Hybridoma supernatants were also assayed for their binding to HPeV type 1 using an ELISA assay. In principle, ELISA was performed as described in 2.23.1, with the difference that 50 µl of HPeV type 1 (approx. 10^6 $CCID_{50}$ per ml) were directly coated to the wells. A polyclonal monkey anti-HPeV type 1 antiserum (Niklasson *et al.*, 1999) was used as positive control. For detection of monkey antisera, a polyclonal goat anti-human HRP conjugated antibody (Dianova) was applied (diluted 1:5000).

2.24 Terminal deoxynucleotidyl transferase dUTP nick end labelleling (Tunel) assay

For detection of DNA strand breaks in LV-infected cells at the single-cell level, the *In Situ* Cell Death Detection Kit, Fluorescein (Roche) based on terminal transferase dUTP nick end labelling (TUNEL) was used. Briefly, cells were fixed with 4 % paraformaldehyde for 1 h. After two washes with PBS the cells were permeabilised with 0.1 % Triton-X 100 in PBS for 10 min followed by two washes with PBS. TUNEL label solution was then added and the cells were incubated at 37 °C in a wet chamber for 1 h. The cells were washed twice with PBS, once with water and subsequently mounted (Shandon-Mount™ medium). The cells were analysed for fluorescence on an Axioskop 20 microscope (Zeiss, Jena, Germany).

2.25 Protein extraction

Cell medium of cultured cells was removed and the cells were washed once with ice-cold PBS. The cells were scraped off the surface using a cell scraper and were resuspended in ice-cold PBS. After centrifugation at 800 x g for 5 min at 4 °C the cell pellet was lysed in 750 µl M-PER® Mammalian Protein Extraction Reagent (Pierce, Rockford, IL) and 12.5 U of Benzonase® (Novagen, Madison, WI), and 0.75 µl Proteinase-Inhibitor Cocktail Set III (Calbiochem, San Diego, CA) were added. After incubation on ice for 20 min, the cell debris was removed by centrifugation at

20,000 x g for 30 min at 4 °C. The protein-containing supernatant was transferred into a fresh tube and protein concentration was determined (2.26). Proteins were stored at -80 °C until use.

2.26 Determination of protein concentration

Concentration of extracted proteins was determined using the Coomassie Plus™ Protein Assay Reagent (Pierce) according to the manufacturer's instructions. Standard dilutions were prepared with BSA ranging from 1 mg/ml to 31.25 µg/ml. Samples (6.25 µl) were mixed with 187.5 µl Coomassie Plus™ Protein Assay Reagent and incubated for 10 min at room temperature. The corresponding solving liquid was used as reference. Protein concentration was measured at an optical density of 595 nm using a Biophotometer (Eppendorf).

2.27 Concentration of proteins and hybridoma supernatants

If necessary, protein and hybridoma supernatants, respectivelly, were concentrated using Microcon® Centrifugal Filter Devices (Millipore, Billerica, MA) with cut-off 10,000 kDa according to the manufacturer's instructions.

2.28 Immune precipitation of LV proteins

The target capsid protein(s) of LV-specific mAbs were determined by immune precipitation of LV proteins. Vero-B4 cells growing in a T-75 cell culture flask were infected with the LV strain 87-012 (MOI 1) (2.3.1) and protein was extracted 7 dpi (2.25). The concentration of mAbs in hybridoma cell culture supernatants was determined with an Easy-Titer® Mouse IgG Assay Kit (Pierce) according to the manufacturer's instructions. Immune precipitation was performed using Dynabeads® Protein G (Invitrogen) as recommended by the manufacturer. Briefly, 10 µg mAb diluted in 200 µl PBS were bound to Dynabeads®. The bead-mAb complex was

incubated with 20 µg of total protein extracted from LV-infected Vero-B4 cells. The mAb-antigen complex was eluted in 30 µl SDS gel loading buffer at 95 °C for 10 min. Samples were stored at -80 °C until SDS-PAGE (2.29).

2.29 SDS-PAGE

Proteins were separated by SDS-PAGE according to their molecular weight. A discontinuous SDS-PAGE was applied with a stacking and a separating gel. In all experiments a 5 % stacking gel and a 15 % separating gel were prepared. The chemical gel composition is shown in 2.9. The protein samples were mixed with SDS loading buffer and incubated at 70 °C for 10 min before they were applied to the SDS gel. The PageRuler™ Prestained Protein Ladder (Fermentas) was used as reference. The gel was run at 14 V/cm and analysed by western blotting (2.30).

Components of buffers used in SDS-PAGE are shown in table 2.10.

Table 2.9 Components of a 15 % SDS gel

Stacking gel		Separating gel	
H2O bidest	1.75 ml	H2O bidest	1.38 ml
2 M Tris (pH 8.8)	0.5 ml	0.5 M Tris (pH 6.8)	1.05 ml
20 % SDS	18.75 µl	20 % SDS	25 µl
PAA†	0.625 ml	PAA†	2.475 ml
60 % sucrose	0.875 ml		
10 % APS	87.5 µl	10 % APS	60 µl
TEMED	8.75 µl	TEMED	7.5 µl

† polyacrylamide (Roth)

Table 2.10 Chemical composition of buffers used in SDS-PAGE

Running buffer (5 x)	15 g/l Tris
	72 g/l glycine
	5 g/l SDS
SDS loading buffer (4 x)	50 mM pH 6.8
	40 % glycerine
	8 % β-mercaptoethanol
	4 g/l bromphenolblue
	80 g/l SDS

2.30 Western Blot Analysis

After SDS-PAGE (2.29), the SDS gel, a 0.45 µm nitro cellulose membrane and Whatman blocking paper were equilibrated in transfer buffer (25 mM Tris, 150 mM glycine, 10 % methanol) for 5 min. Proteins were then transferred onto the nitro cellulose membrane by semi-dry electroblotting using the Fastblot B 34 system (Biometra, Göttingen, Germany). An amperage of approx. 150 mM was applied with a maximum of 25 V. After 1 h, the membrane was rinsed in PBS containing 0.1 % TWEEN® 20 (PBS-T) and then blocked with 10 % non-fat milk in PBS-T at 4 °C overnight. After three washes with PBS-T for 10 min each, the membranes were incubated with the primary antibody (diluted in 1 % non-fat milk in PBS-T) with rotating at 4 °C overnight. Primary antibodies are shown in table 2.11. For characterisation of mAbs specific for LV, 10-fold concentrated (2.27) hybridoma cell culture supernatants were assayed undiluted. For this purpose, approx. 150 µg total protein extracted from LV 87-012 infected and Mock-infected Vero-B4 cells, respectively, (2.25) was separated on an SDS gel by use of a one-pocket comb. The membrane was cut into stripes after western blotting and one stripe was used for one mAb hybridoma supernatant. The membrane was washed three times with PBS-T for 10 min each and subsequently incubated with an HRP-conjugated secondary antibody (diluted in 1 % non-fat milk in PBS-T) (table 2.12) with rotating at room temperature for 1 h. After three washes with PBS-T for 10 min each, the proteins were visualised

using the SuperSignal® West Femto Chemiluminescent substrate (Pierce) with an X-ray film (Pierce) and a Curix 60 developer (Agfa-Gevaert Group, Mortsel, Belgium).

Table 2.11 Primary antibodies used in Western Blot analysis

Designation	clonality	Target antigen	Species (origin)	Applied dilution	source
anti-VP0	p	LV-VP0	rabbit	1:1000	Prof. Niklasson[a]
anti-VP1	p	LV-VP1	rabbit	1:1000	Prof. Niklasson
anti-VP3	p	LV-VP3	rabbit	1:1000	Prof. Niklasson
anti-Caspase-3	m	Caspase-3	rabbit	1:1000	Sigma-Aldrich[b]
anti-caspase-3 (active)	m	Caspase-3 (active)	rabbit	1:1000	Sigma-Aldrich
anti-β-actin	m	β-actin	mouse	1:10,000	Sigma-Aldrich

[a] Apodemus AB, Stockholm, Sweden, [b] Munich, Germany
Abbreviations: p: polyclonal, m: monoclonal

Table 2.12 Secondary HRP conjugated antibodies used in Western blot analysis

Specificity	clonality	Species (origin)	Applied dilution	Source
anti-rabbit	p	goat	1:10,000	Pierce[a]
anti-mouse	p	rabbit	1:10,000	Dako[b]

[a] Rockford, IL, [b] Stockholm, Sweden
Abbreviations: p: polyclonal

2.31 Propagation and purification of mAbs

Large scale production of mAbs was performed with a tumbling chamber as described by Jaspert *et al.* (1995). Briefly, hybridoma cells were grown to a density of 10^6/ml,

and approx. 50 ml were applied to a dialysis tube that was placed in a rotating chamber. The apparatus allows high yields of monoclonal antibodies and avoids impurities by nutrients and metabolic waste products. The hybridoma cells were grown for 3 weeks and the mAb-containing supernatant was harvested by centrifugation.

MAbs were purified using either an ImmunoPure® (A/G) IgG Purification Kit (Pierce) in the case of class IgG antibodies or a HighTrap-IgM column (Pharmacia, Uppsala, Sweden) in the case of class IgM antibodies, both as recommended by the manufacturer.

2.32 Software and statistical analyses

For sequence analyses the following software was used: DNASTAR® Lasergene 7, BioEdit Sequence Alignment Editor (Hall, 1999), NCBI BLAST 2.2.9 (www.ncbi.nlm.nih.gov/BLAST/) and Molecular Evolutionary Genetics Analysis software version 4.0 (MEGA4) (Tamura *et al.*, 2007).

Fluorescence images were analysed with Axio VSLE V 4.4.0.0 and with cLSM 510 META Software, Version 3.0, SP3, respectively (Zeiss, Jena, Germany).

Statistical analyses were performed with SPSS 17.0 (SPSS Inc, Chicago, IL) and SigmaPlot 11.0 (Systat Software Inc., San Jose, CA).

3 Results

I

3.1 Development and evaluation of RT-PCR assays for detection and characterisation of Ljungan virus

3.1.1 A quantitative real-time RT-PCR assay for detection of Ljungan virus strains

In this thesis, a contribution was made to establish and evaluate a real-time RT-PCR assay for detection of LV strains. Therefore only results achieved in association with this thesis are presented. Further results are described elsewhere (Donoso Mantke *et al.*, 2007).

3.1.1.1 Specificity of the assay

Cross reactivity of the assay to other picornaviruses was tested. RNA was extracted from cell culture supernatants of cells infected with HPeV type 1, HPeV type 2, TMEV BeAn 8386, TMEV GD 7, EMCV M, EMCV 76/5167 and EMCV ATCC VR-129B, respectively. RNA was reverse transcribed and analysed by real-time RT-PCR. All samples were negative by real-time PCR (data not shown).

3.1.1.2 Characteristics of the assay

Log10 dilutions of RNA (10^6-10^1 molecules) transcribed *in vitro* (iv) were tested by both one-step and two-step RT-PCR. Both assays showed a linear detection range from 10^6 to 10^1 ivRNA molecules with a correlation of r^2=0.9791 (one-step) and r^2=0.9784 (two-step), respectively (figure 3.1).

Assay sensitivity was further evaluated using RNA extracted from LV 87-012 cell culture stocks whose titre was determined (range: 250 to 2.5x10^{-5} $CCID_{50}$). Sextuple samples were run with a linear detection range (r^2=0.99797) from 250 to 2.5x10^{-2}

$CCID_{50}$ (resulting in approx. $4x10^7$ to 50 genome copies). Sensitivity of the real-time RT-PCR is higher than that of cell culture by 3 to 5 log scales.

Reproducibility of the assay was determined by intra- and intervariability, respectively. Different amounts of ivRNA (10^6, 10^4, 10^2) were tested in triplicate with cycle threshold (C_T) value variations <1 for each dilution and both assays. Mean C_T values of the two-step assay were lower compared to those of the one-step assay, indicating a higher sensitivity for the two-step assay (table 3.1).

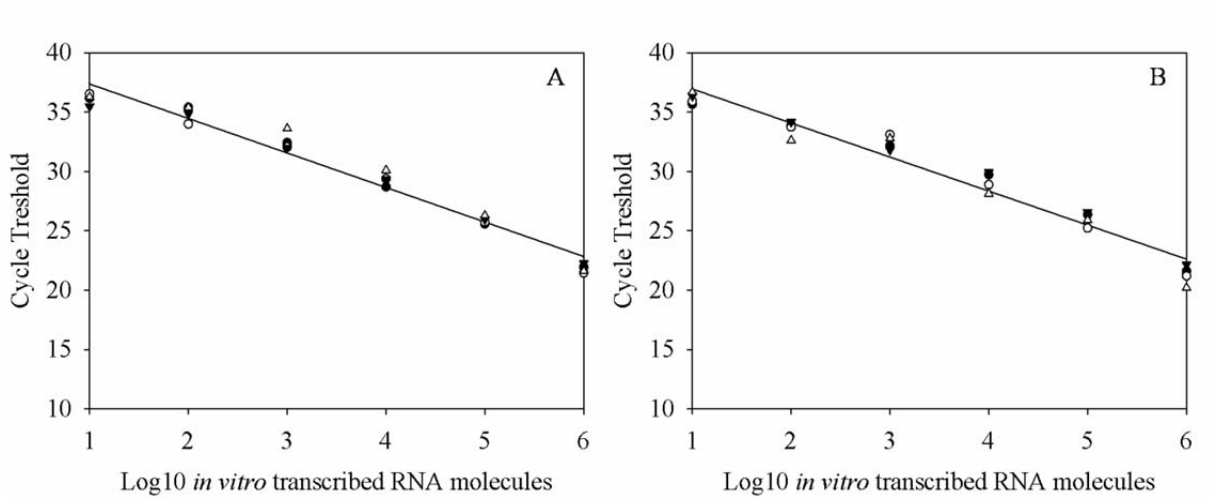

Figure 3.1. Standard curves of log10 dilutions of ivRNA assayed by one-step (A) and two-step (B) LV real-time RT-PCR. Samples were run in quadruplicate for each dilution and both assays.

Table 3.1. Intra- and inter-assay for LV-specific real-time RT-PCR.

	One-step assay			Two-step assay		
Amount ivRNA	10^6	10^4	10^2	10^6	10^4	10^2
Intra-assay[a]						
Mean C_T	21.77	29.59	34.74	21.19	28.98	33.50
SD	0.43	0.43	0.70	0.98	0.91	0.80
Inter-assay[b]						
Mean C_T	22.01	29.92	34.58	20.93	28.88	33.10
SD	0.42	0.69	0.77	0.36	0.47	0.53

[a] Intra-assay was performed three times for each ivRNA quantity by one operator.
[b] Inter-assay was performed by three operators, each three times for each ivRNA quantity.
Abbreviations: ivRNA*: in vitro* transcribed RNA, C_T: cycle threshold, SD: standard deviation.

3.1.1.3 Evaluation of the assay

One-day-old CD-1® laboratory mice were infected with LV strains 87-012, 174F and 145SL, respectively (2 animals each). Mice were sacrificed 6 dpi when clinical signs of encephalitis occurred. Brain, heart, pancreas, liver, lung and kidney were taken, and extracted RNA was analysed by real-time RT-PCR. All organs from each of the six mice were found to be LV positive, with the highest LV genome copy numbers in the brain (>10^{10} per gram of tissue) (figure 3.2). As a negative control, four one-day-old mice were injected with PBS and also sacrificed at 7 days of age. The same types of organ were taken and analysed by real-time RT-PCR. All of these samples were negative for LV (data not shown).

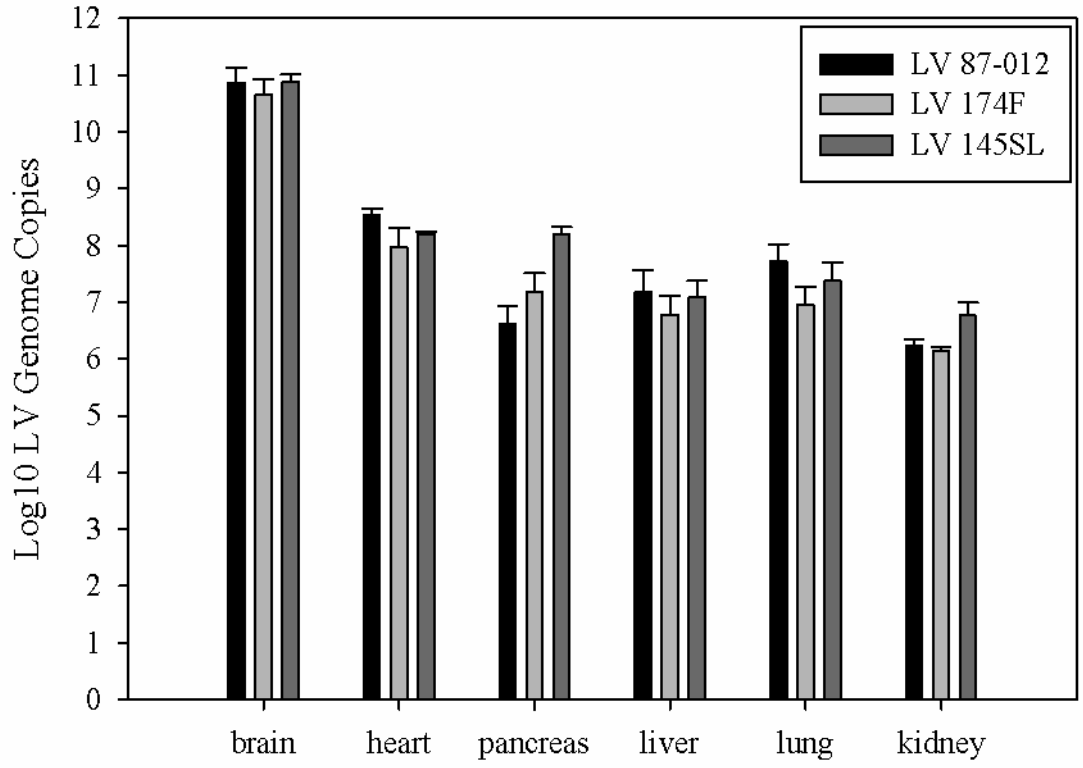

Figure 3.2. LV genome copies detected in organs of LV-infected CD-1® laboratory mice. One-day-old mice were infected with LV 87-012, 174F and 145SL, respectively (2 animals for each LV strain), organs were taken 6 dpi and analysed by real-time RT-PCR. Means of duplicate samples are shown. LV load was normalised to 1 gram of tissue. (http://dx.doi.org/10.1016/j.jviromet.2006.11.029)

LV genome copies in wild rodents are often found in small amounts (own observations). For a possible improvement of the assay degenerate primers were designed. RNA was extracted from heart tissue of CD-1® laboratory mice infected with LV strains 87-012, 174F and 145SL, respectively. The difference in mean C_T value of sextuples between non-degenerate primers and degenerate primers was >1 for each strain (table 3.2), suggesting that the use of degenerate primers results in a higher sensitivity in detecting LV by 5'UTR RT-PCR.

Table 3.2 Comparison of non-degenerate primers and degenerate primers in real-time RT-PCR with heart tissue of laboratory mice infected with different LV strains.

LV strain	mean C_T LjF/LjR[a]	mean C_T LjF1/LjR1[b]	C_T difference (LjF/LjR-LjF1/LjR1)
87-012	23.74	22.55	1.24
174F	25.04	23.42	1.62
145SL	24.59	22.90	1.69

[a] non-degenerate primers
[b] degenerate primers

3.1.2 Melting curve analysis for typing of Ljungan virus strains

The LV-specific real-time RT-PCR assay detects all (known) LV strains but does not allow discrimination between LV strains. Melting curve analysis (MCA) was established for further characterisation of real-time RT-PCR amplicons. Because of high sequence variation between strains 87-012, 174F and 145SL on the one hand, and strains M1146 and 64-7855 on the other hand, MCA was established for strains 87-012, 174F and 145SL only.

Two hybridisation probes were designed with target sequences within the real-time RT-PCR amplicon. The 3'-fluorescein-conjungated donor probe has no mismatch with the target sequence of all three strains. The acceptor probe was conjugated with LightCycler® Red 640 at its 5'-end and has three mismatches with LV 145SL (genome positions 412-414), one mismatch with LV 174F (genome position 412), and no mismatch with LV 87-012 (data not shown). As a result, LV 87-012 RT-PCR amplicons had the highest melting point at approx. 67.5 °C, followed by LV 174F at

approx. 62.5 °C and LV 145SL at approx. 56.5 °C (figure 3.3). RT-PCR products obtained from LV-containing cell culture supernatants were sequenced before evaluation of MCA to exclude sequence variation between laboratory LV strains and sequences available at GenBank that were used for probe design. No sequence variation was found (data not shown).

MCA was further evaluated with RT-PCR products obtained from heart tissue of laboratory mice infected with LV-87-012, LV 174F and LV 145SL, respectively (figure 3.2). Melting points of all samples could be detected to correspond to the strain of infection (figure 3.3).

RT-PCR products of LV strains M1146 and 64-7855 showed no signal in MCA (data not shown). Real-time RT-PCR-positive but MCA-negative samples should therefore be further characterised by e.g. pyrosequencing (3.1.3) or direct sequencing of the PCR product.

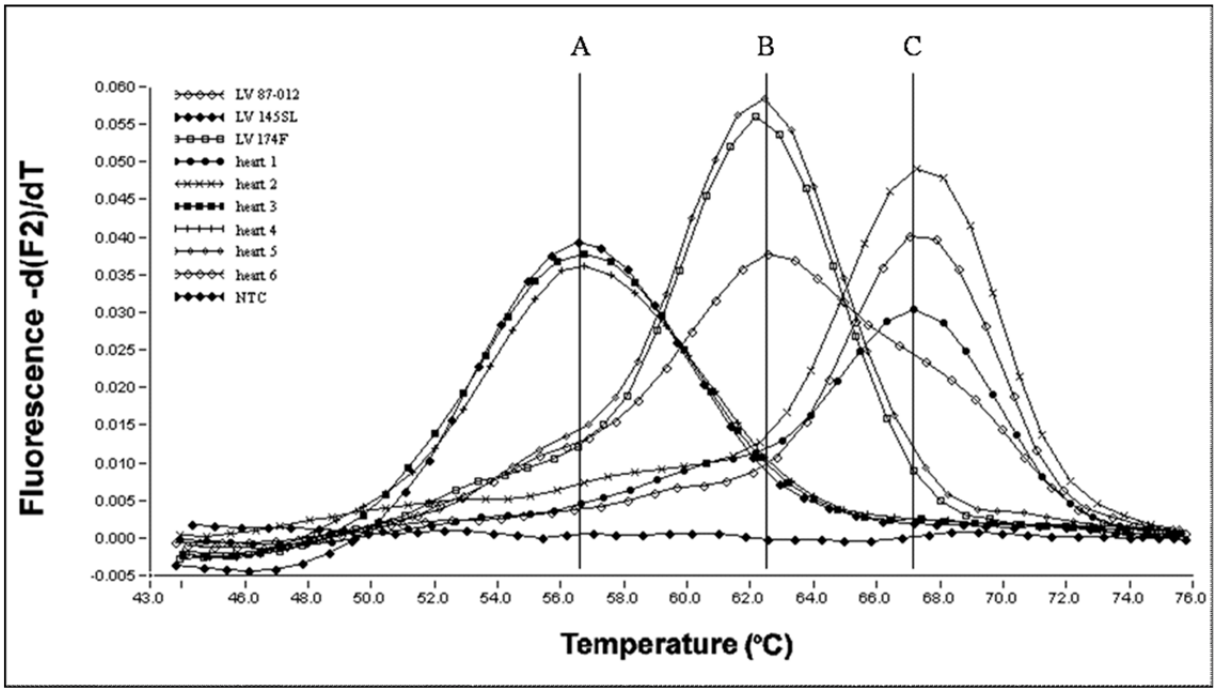

Figure 3.3. Melting curve analysis for LV strains 87-012, 174F and 145SL. Laboratory mice were infected with LV strains 87-012 (1 and 2), 174F (5 and 6) and 145SL (3 and 4), respectively, and RNA was extracted from heart tissue. RNA was analysed for LV by real-time RT-PCR and LV strains were determined by MCA: A: 87-012, B: 174F, C: 145SL. (http://dx.doi.org/10.1016/j.jviromet.2006.11.029)

3.1.3 Pyrosequencing

Pyrosequencing is a method used for sequencing of short DNA strands. The complementary DNA strand is synthesised enzymatically by adding different nucleotides separately. Each incorporated nucleotide results in a light signal that can be detected. All light signals are presented as peaks in a pyrogram. Since MCA comprises no more than three LV strains, pyrosequencing for typing of LV strains was established. This method is intended to offer an alternative to MCA, in particular to detect unknown LV sequences.

Real-time RT-PCR was performed using pyrosequencing primers (2.19), and 50 to 58 nucleotide long sequences corresponding to the respective LV strain could be obtained. Sequence analysis showed a clear differentiation between LV strains 87-012, 174F, 145SL and M1146 after amplification by real-time RT-PCR. A representative pyrogram for LV M1146 is shown in figure 3.4. Assay detection limit was determined using 10-fold dilutions of *in vitro* transcribed LV RNA. Sequences could be generated when ≥1000 RNA molecules were applied to the assay. In contrast, no sequences were obtained when less than 1000 molecules were used.

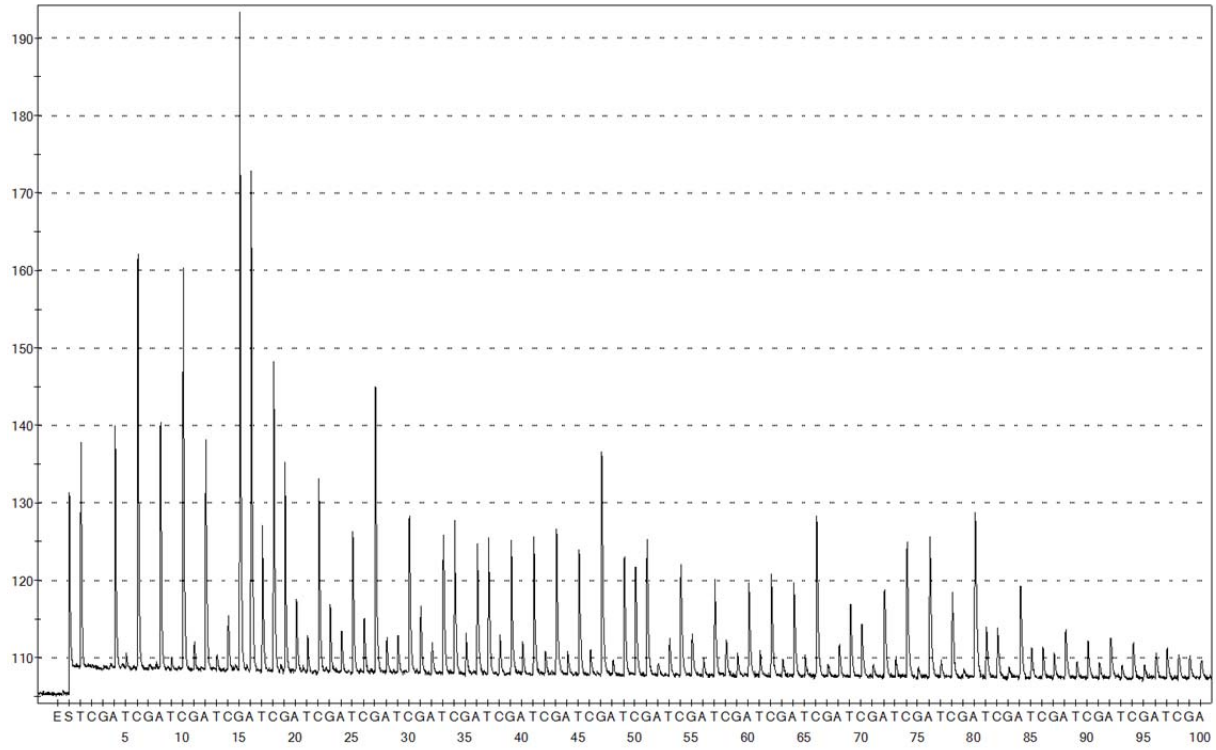

Figure 3.4. Representative pyrosequencing result of LV real-time RT-PCR assay. RNA was extracted from M1146-positive cell culture supernatant and analysed by real-time RT-PCR, and cDNA was applied to pyrosequencing. A pyrogram is shown for LV M1146 with the obtained sequence indicated under the pyrogram.

3.1.4 RT-PCR assays for characterisation and genotyping of Ljungan virus

The only available LV-specific RT-PCR targets the 5'UTR (Donoso Mantke *et al.*, 2007) and is therefore not type specific (Oberste *et al.*, 1999b). Two further RT-PCR assays for characterisation and genotyping of LV samples tested positive were established. To extend the range of available LV-specific RT-PCR assays, primers were designed for amplification of a 467 bp fragment from the LV 2A/2B region. The picornavirus serotype correlates with the VP1 sequence (Oberste *et al.*, 1999a) and accordingly, the HPeV VP1 gene has been established for typing of HPeV (Al-Sunaidi *et al.*, 2007). Therefore, consensus primers for amplification of partial LV VP1 gene were developed, resulting in a 530 bp PCR product. Both assays successfully detected all four LV strains included (87-012, 174F, 145SL and M1146) (figure 3.5) and results

were confirmed by sequencing (data not shown). The LV strain 64-7855 was recently characterised by use of an original isolate (Tolf *et al.*, 2009a). This strain was not available for analysis. However, sequences of 64-7855 were included in designing primers for VP1 RT-PCR assay. Primer sequences are shown in table 2.8.

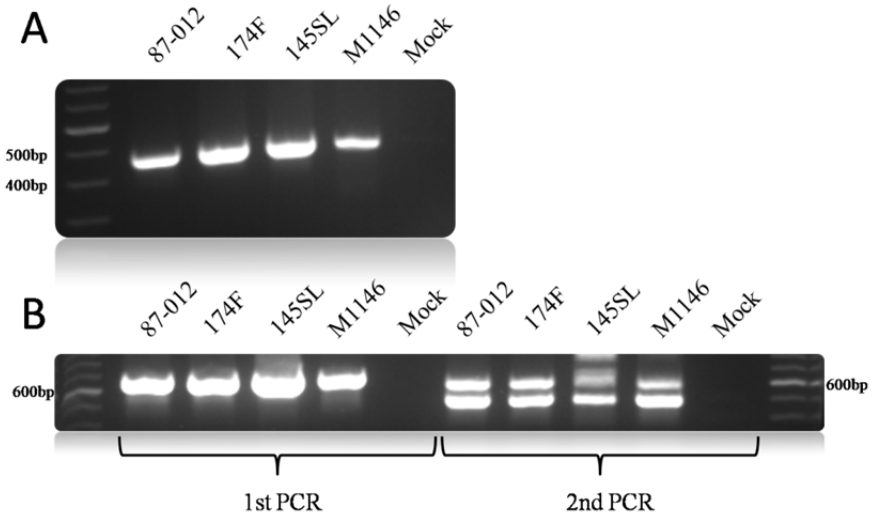

Figure 3.5. RT-PCR assays developed for characterisation and genotyping of LV-positive samples. RNA was extracted from supernatants of Vero-B4 cells infected with the LV strains indicated, 100 ng RNA were reverse transcribed and amplified. A: RT-PCR with primers located in the 2A/2B region of the LV genome for amplification of a 467 bp fragment. B: Semi-nested RT-PCR targeting the LV VP1 gene. Left side: First round RT-PCR giving a 683 bp amplicon. Right side: Second-round PCR amplifying a 530 bp fragment.

3.2 Development and characterisation of murine monoclonal antibodies to Ljungan virus

Antibodies directed against viruses are used in a wide range of applications, such as diagnostics, study of virus pathogenesis and the treatment of virus caused disease (e.g. immunotherapy and vaccination) (Dorn-Beineke *et al.*, 2007). The production and characterisation of polyclonal antibodies against the capsid proteins of LV has recently been described (Tolf *et al.*, 2008). However, for some purposes the use of monoclonal antibodies (mAb) is recommended because of their homogeneity and consistency. The

possibility to regenerate mAbs from a constant renewable source (the hybridoma cells) is another advantage (Lipman *et al.*, 2005).

BALB/C laboratory mice were infected with LV 145SL and LV 87-012, respectively. The spleens of seropositive mice were collected and splenocytes were fused with the mouse myeloma cell line Sp2/0-Ag 14. Hybridoma clones that produced mAbs against LV were identified by cELISA, selected and grown in cell culture medium. This work was performed in collaboration with Apodemus AB (Stockholm, Sweden).

3.2.1 Characteristics of mAbs binding to LV

A number of successful fusions were achieved using splenocytes from BALB/c mice immunized with LV. After two to three weeks, hybridoma cell supernatants were screened for LV-specific antibodies by cELISA. Positive binding was determined as absorbance that was at least four-fold higher than the negative control. A total number of 60 clones were identified that produce mAbs reactive with LV. Twenty-two of these mAbs with the highest reactivity in immuno assays were subcloned by limiting dilutions and expanded for further analyses. All mAbs were isotyped, showing that nine mAbs belong to the subclass IgG2a, three were subclass IgG2b, one was subclass IgG3 and nine mAbs were subclass IgM. All mAbs contained kappa light chains (table 3.3).

3.2.2 Immunostaining

MAbs were screened by IIFT using Vero-B4 cells infected with LV strains 87-012, 174F, 145SL and M1146, respectively. All mAbs showed reactivity in indirect immunofluorescence to Vero-B4 cells infected with LV 87-012 and LV 174F, respectively, with staining in the cell's cytoplasm. Three mAbs (LV-05sA1-D, LV-05sA4-G, LV-05sA4-H) were positive also for LV 145SL while no fluorescence was observed in Mock-infected cells. Clone LV-05sA4-H showed the broadest reactivity with strong signals to all strains (except for M1146) with staining in the cell

cytoplasm. No fluorescence was observed in Mock-infected cells. A representative staining is displayed in figure 3.6. Data are summarised in table 3.3.

All mAbs were further characterised for a potential cross reactivity to LV M1146 (representing the third LV genotype) and the related HPeV types 1 and 2, respectively. Infected cells did not show any fluorescence after incubation with mAbs. In contrast, positive staining of cells could be observed using antisera against M1146, HPeV1 and 2, respectively (data not shown).

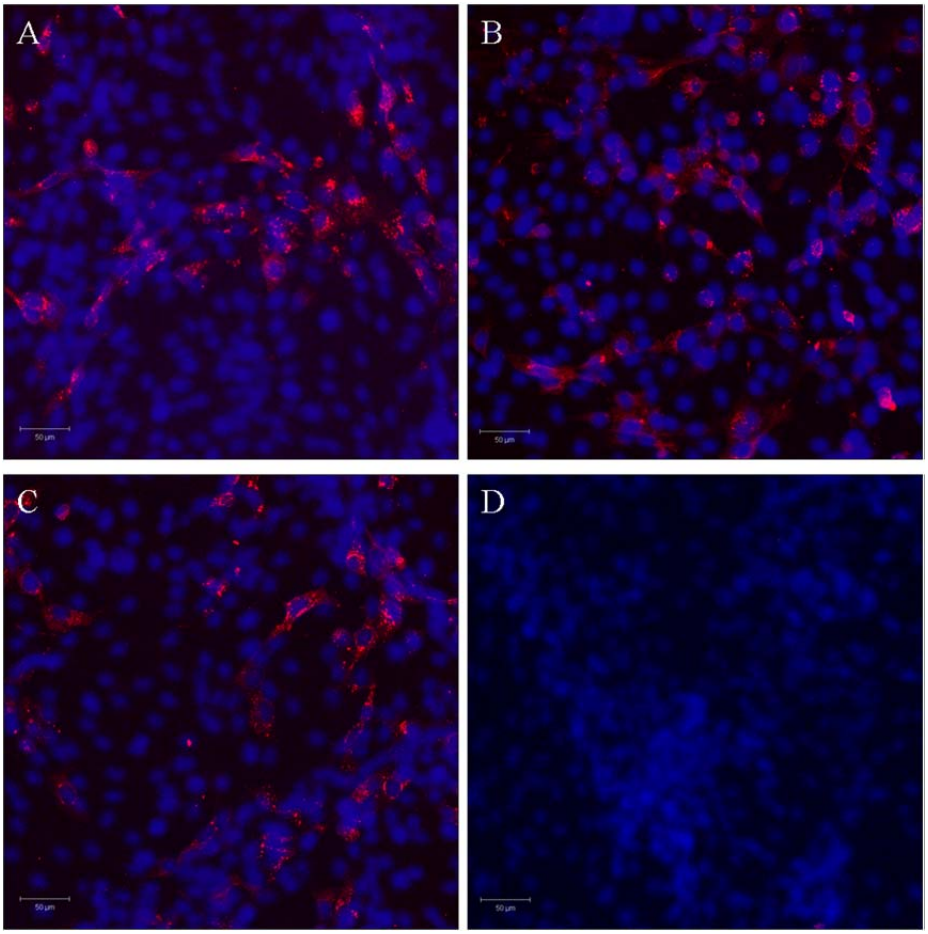

Figure 3.6. Representative example of indirect Immunofluorescence staining of Vero-B4 cells infected with LV 87012 (A), LV 174F (B) and LV 145SL (C), Mock-infected (D). MAb LV-05sA4-H was applied to the cells and a rhodamine-conjugated goat anti-mouse polyclonal antibody was used for staining (red). Cell nucleus DNA was stained with 4′,6-Diamidino-2-phenylindol (DAPI) (blue). (http://dx.doi.org/10.1016/j.jviromet.2012.05.001)

Table 3.3 Summary of mAbs to LV.

Clone	Isotype	NT[a]	Protein target	IIFT[b]			IHC[c]
				87-012	174F	145SL	
LV-05sA1-D	G2b/κ	-	VP1	++	++	+	-
LV-05sA4-G	G2a/κ	-	VP0/VP3	+++	+	+++	-
LV-05sA4-H	G2a/κ	-	VP0	+++	+++	+++	-
LV-05fB2-Q	M/κ	-	unknown	++	+	-	+
LV-06s08a-T	G2a/κ	-	VP1	+++	+++	-	-
LV-06s08a-U	M/κ	-	VP0/VP1	+	+	-	+
LV-06s08a-V	G2a/κ	-	VP1	+++	++	-	-
LV-06s06b-X	M/κ	-	VP0/VP1	+	+	-	+
LV-06s08a-AE	G2a/κ	-	VP0/VP3	++	+++	-	-
LV-06s22a-OE	G2a/κ	-	VP1	+++	+++	-	-
LV-06sV12b-9	M/κ	-	VP0/VP3	++	++	-	+
LV-06sV12b-10	M/κ	-	VP0/VP3/VP1	++	++	-	+
LV-06sV12b-12	G2a/κ	+	VP1	++	+++	-	-
LV-06sV12b-13	G3/κ	+	VP1	++	++	-	-
LV-06sV12b-19	G2b/κ	-	VP0/VP3/VP1	+	++	-	-
LV-06sV12b-20	M/κ	+	VP0	+	++	-	-
LV-06sV12b-21	M/κ	+	VP1	+	++	-	-
LV-06sV12b-22	M/κ	+	VP0/VP3	+	++	-	-
LV-06sV12b-28	G2a/κ	-	VP0/VP3/VP1	+++	+++	-	-
LV-06sV12b-29	G2b/κ	+	VP1	+++	++	-	-
LV-06s05b-33	M/κ	+	unknown	+	++	-	-
LV-06sV12b-35	G2a/κ	-	VP0/VP3/VP1	++	++	-	-

[a] Neutralisation test. Neutralisation effect of ≥80 % was considered as positive neutralisation.

[b] Indirect Immunofluorescence test.

[c] Immunohistochemistry.

3.2.3 Immunohistochemistry

IHC is used to demonstrate antigen(s) in tissue sections by means of specific antibodies. After binding of the antibody to the antigen, the antigen-antibody complex can be visualised with a coloured histochemical reaction (Ramos-Vara, 2005). The standard fixative for tissue processing in IHC is formaldehyde. Formaldehyde causes major chemical changes of the antigen. Although numerous improvements in antigen retrieval techniques have been developed, many antibodies are limited in their use in IHC (Shi *et al.*, 1997).

Using IHC all 22 mAbs were analysed for binding to formalin-fixed paraffin-embedded GMK cells infected with both, LV 87-012 and LV 145SL. Five mAbs (LV-05fB2-Q, LV-06s08a-U, LV-06s06b-X, LV-06sV12b-9 and LV-06sV12b-10) had positive binding with LV-infected cells (for both strains used) and staining in the cell cytoplasm. No staining was observed in Mock-infected cells (figure 3.7 A-B). Controls were included using mouse immune serum and a polyclonal rabbit anti-VP1 antiserum (Tolf *et al.*, 2008). Positive staining was observed in 145SL-infected GMK cells (figure 3.7 C and E). In contrast, no staining could be seen in 145SL-infected cells when incubated with negative control mouse serum and negative control rabbit serum, respectively (figure 3.7 D and F).

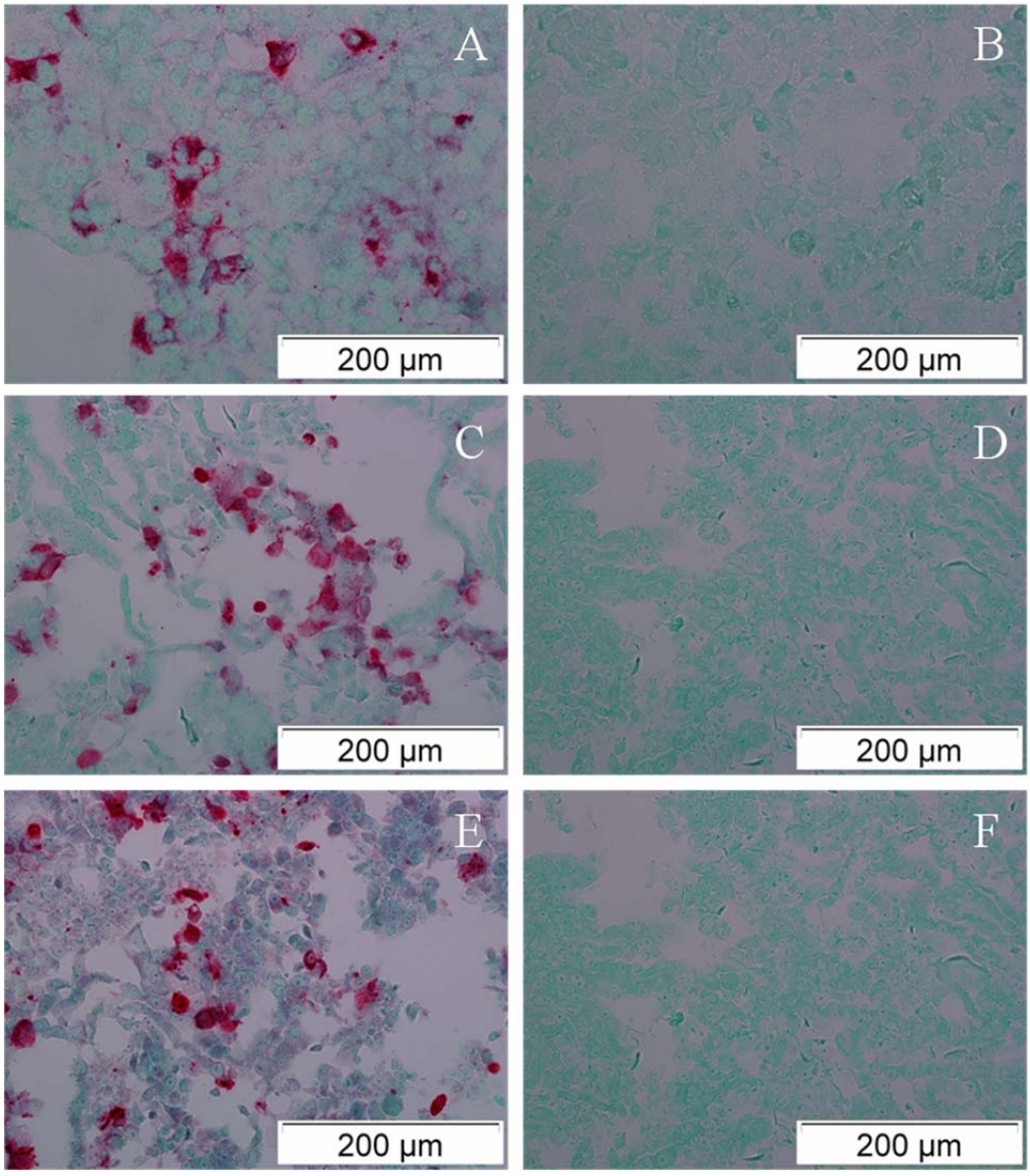

Figure 3.7. Immunohistological staining of GMK cells infected with LV 145SL (A, C, E) and Mock-infected cells (B, D, F). Cells were formalin fixed and paraffin embedded. LV is stained red and background is stained green. A, B: LV-06sV12b-10; C, D: mouse immune serum diluted 1:800; E, F: polyclonal rabbit anti-VP1 antiserum diluted 1:3000. Pictures were taken and kindly provided by Prof. Bo Niklasson.
(http://dx.doi.org/10.1016/j.jviromet.2012.05.001)

3.2.4 Immunoblotting

To determine the binding of mAbs to linear epitopes, all mAbs were analysed by immunoblotting. For this purpose, Vero-B4 cells were infected with LV 87-012, total protein was extracted, separated by SDS-PAGE and transferred to nitrocellulose

membranes by electroblotting. The membranes were incubated with diluted hybridoma supernatants ranging from 1:20 to 1:200. No proteins corresponding to the molecular masses of LV capsid proteins could be detected. However, positive binding was observed using mouse immune sera and protein A purified rabbit anti-LV capsid protein antibodies, respectively (data not shown), indicating the conformational nature of epitopes for mAb binding.

3.2.5 Immune precipitation

A direct immune precipitation assay was used to identify specific binding of mAbs to conformational epitopes of LV capsid proteins. MAbs were bound to magnetic beads and capsid proteins were precipitated from total protein. The specific binding of each mAb was determined by western immunoblotting after SDS-PAGE of the protein-mAb complex eluted from the beads. For this purpose, each of the three anti-capsid protein polyclonal antisera (anti VP0, anti VP3 and anti VP1) was separately used as primary antibody. A signal corresponding to the molecular masses of LV capsid proteins (i.e. 27 kDa for VP0, 26 kDa for VP3 and 37 kDa for VP1 [Johansson *et al.*, 2004]) could be detected for 20 of the 22 mAbs. The mAbs LV-05sA4-H and LV-06sV12b-20 showed binding to VP0 only. Eight mAbs (LV-05sA1-D, LV-06s08a-T, LV-06s08a-V, LV-06s22a-OE, LV-06sV12b-12, LV-06sV12b-13, LV-06sV12b-21, LV-06sV12b-29) showed reactivity with anti-VP1 antisera and no signal when incubated with anti VP0 and anti VP3 antisera, respectively. No mAb bound to VP3 only. Ten mAbs had positive binding to more than one capsid protein. The mAbs LV-05sA4-G, LV-06s08a-AE, LV-06sV12b-9 and LV-06sV12b-22 interacted with both VP0 and VP3, the mAbs LV-06s08a-U and LV-06s06b-X with VP0 as well as VP1. Binding to all three capsid proteins was detected for mAbs LV-06sV12b-10, LV-06sV12b-19, LV-06sV12b-28 and LV-06sV12b-35. The target capsid proteins for mAbs LV-05fB2-Q and LV-06s05b-33 remained unknown since no reactivity could be detected for these mAbs. Results are shown in figure 3.8 and are summarised in table 3.3.

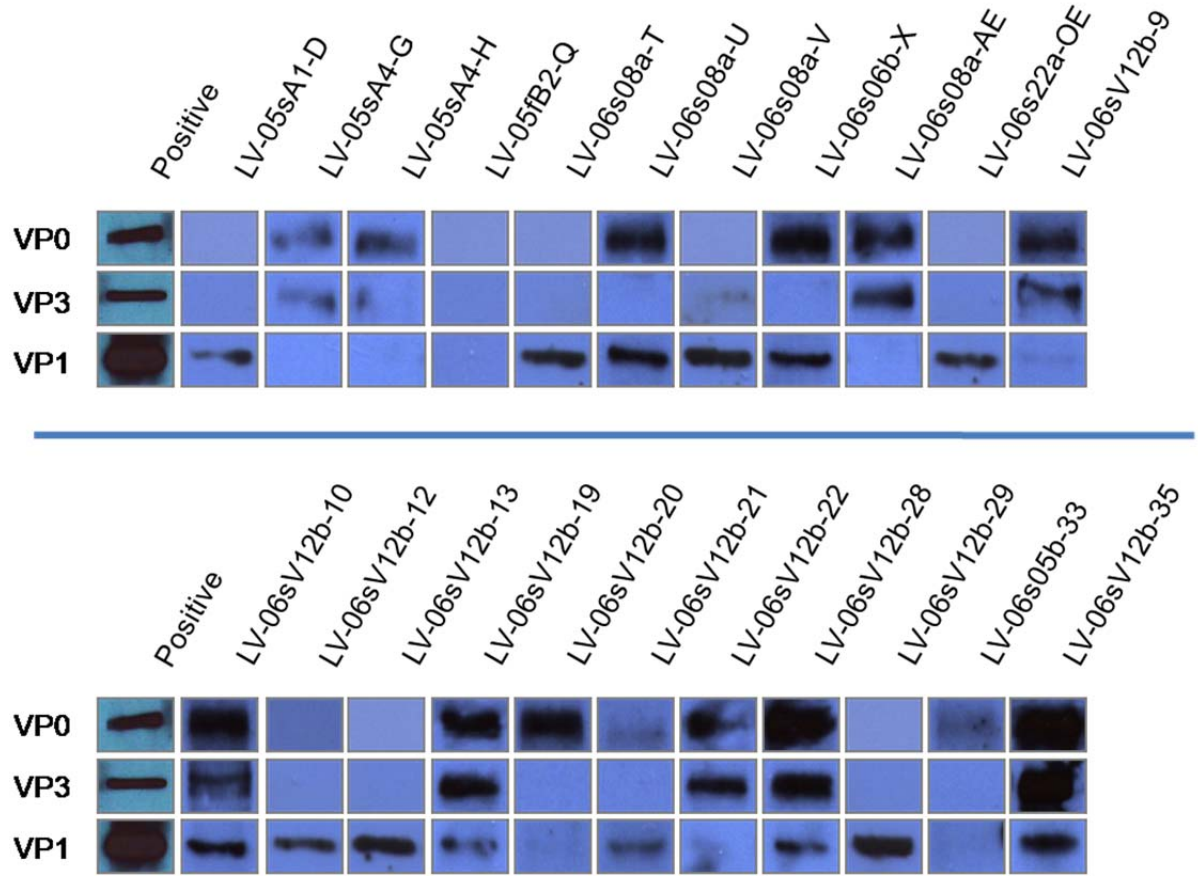

Figure 3.8. Immune precipitation of LV capsid proteins with mAbs. Vero-B4 cells were infected with LV 87-012 and total protein was extracted. LV capsid proteins were precipitated with mAbs that were bound to magnetic beads. The proteins were separated by SDS-PAGE and blotted onto nitrocellulose membranes. Capsid proteins were detected independently for each mAb using polyclonal rabbit antisera specific to VP0, VP3 and VP0, respectively. For positive control, total protein from LV 87-012 infected Vero-B4 cells was separated by SDS-PAGE and detected with the specific antisera after western immunoblotting. The molecular masses of the capsid proteins are as follows: VP0: 27 kDa; VP3: 26 kDa; VP1: 37 kDa. (http://dx.doi.org/10.1016/j.jviromet.2012.05.001)

3.2.6 Virus neutralisation

All 22 mAbs were further characterised to determine the LV neutralising activity by plaque reduction assay. Seven mAbs (LV-06sV12b-12, LV-06sV12b-13, LV-06sV12b-20, LV-06sV12b-21, LV-06sV12b-22, LV-06sV12b-29, LV-06s05b-33) showed a neutralisation effect of ≥80 % in LV (87-012) infection to Vero-B4 cells when hybridoma supernatants were applied to the cells.

II

3.3 Laboratory rats are infected with Ljungan virus

The BB rat is one of the most frequently used animal models to study type-1 diabetes. As shown by IHC and RT-PCR analysis, respectively, this animal model is infected with LV (Niklasson *et al.*, 2007b). The interpretation of results based on a disease model is dependent on a full understanding of the biological characteristics of this animal model. That includes its possible carriage of infectious agents. Three additional strains of commonly used laboratory rats were investigated for the presence of LV.

Brain, heart and pancreas from 8 Sprague Dawley® (SD), 8 Wistar Albino Glaxo (WAG) and 8 Lewis rats were analysed for the presence of LV-specific RNA using RT-PCR (5'UTR). Twelve of the 24 rats tested positive for LV by RT-PCR with positive individuals in all three strains of rats included in the study (table 3.4). LV RNA was found in brain and heart while all pancreas specimens were negative. RNA was also extracted from plasma of each animal. None of the plasma samples was tested positive for LV-specific RNA by RT-PCR.

A selected number of the 24 rats were also tested for presence of LV by IHC. Four of 15 pancreas specimens tested by IHC were LV positive. The IHC positives represented two of three rat strains (representative result in figure 3.9).

All animals were tested by serology. Plasma was investigated for the presence of LV-specific antibodies using an IIFT. A low titre (1:4) of LV-specific antibodies was found in 3 animals (animals 3, 7 and 9) representing 2 of the 3 rat strains investigated. Immunofluorescence was observed only in LV 87-012-infected Vero cells. In contrast, none of the sera showed reactivity with LV 145SL infected cells. Thus, potential cross reactivities can be excluded.

RT-PCR (5'UTR) positive samples were further analysed by VP1 RT-PCR. Four samples were positive by VP1 RT-PCR (2-WAG, 3-WAG, 10-SD and 13-SD). Three sequences share similarity of 98 % to 99 % with LV M1146 on aa level (2-WAG,

10-SD, 13-SD). A short sequence of 126 nt was obtained from 3-WAG with 71 % aa identity to LV M1146.

Table 3.4 Summary of laboratory rat strains tested for the presence of LV by RT-PCR, IHC, serology and virus isolation.

Animal designation	RT-PCR[a]	IHC[b]	Serology[c]	Virus isolation[d]
1-WAG	-	negative	negative	n.d.
2-WAG	heart	negative	negative	unsuccessful
3-WAG	heart	negative	positive	unsuccessful
4-WAG	-	negative	negative	n.d.
5-WAG	brain	negative	negative	n.d.
6-WAG	heart	positive	negative	unsuccessful
7-WAG	-	positive	positive	n.d.
8-WAG	brain	negative	negative	unsuccessful
9-SD	-	negative	positive	n.d.
10-SD	heart	n.d.	negative	unsuccessful
11-SD	-	negative	negative	n.d.
12-SD	brain	negative	negative	n.d.
13-SD	brain	negative	negative	unsuccessful
14-SD	-	negative	negative	n.d.
15-SD	heart	positive	negative	unsuccessful
16-SD	brain	positive	negative	n.d.
17-Lewis	brain	n.d.	negative	unsuccessful
18-Lewis	heart	n.d.	negative	unsuccessful
19-Lewis	-	n.d.	negative	n.d.
20-Lewis	-	n.d.	negative	n.d.
21-Lewis	-	n.d.	negative	n.d.
22-Lewis	-	n.d.	negative	n.d.
23-Lewis	-	n.d.	negative	n.d.
24-Lewis	-	n.d.	negative	n.d.

[a] RNA was extracted from brain, heart and pancreas of each animal. Shown are organs that were positive by LV specific RT-PCR.
[b] Immunohistochemistry with formalin-fixed paraffin-embedded pancreas tissue.
[c] Plasma of each animal was tested by IIFT.
[d] Homogenised tissue that was positive by RT-PCR was applied to LV-susceptible Vero-B4 cells.
Abbreviations: WAG: Wistar Albino Glaxo, SD: Sprague Dawley, n.d.: not done

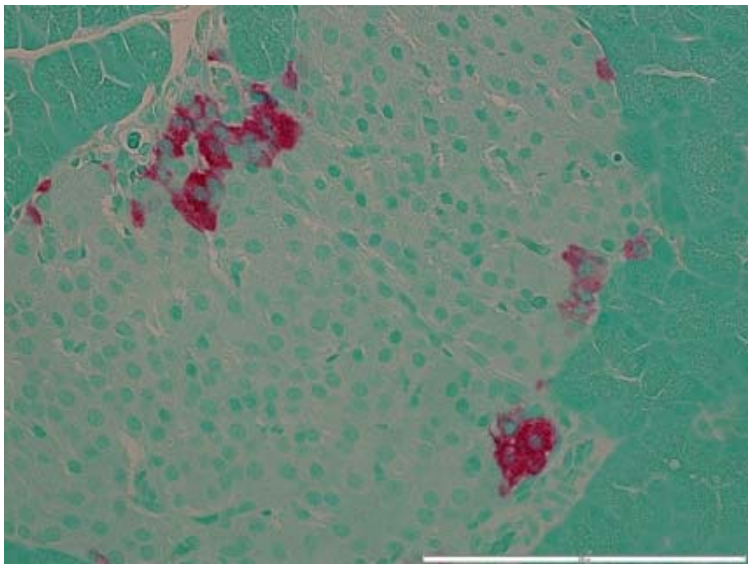

Figure 3.9 Rat pancreatic islet cell staining by immunohistochemistry. LV is stained (red) with an LV-specific polyclonal anti-VP1 antiserum and background is stained in green.

All attempts to isolate LV from tissues of RT-PCR-positive animals on Vero-B4 cells were unsuccessful. The inoculated cells did not show signs of CPE. No LV antigen could be detected by IFA and no LV genome could be detected by RT-PCR.

3.4 Ljungan virus prevalence in wild rodents trapped in Germany and Thailand

LV was found in different species of voles and mice in Scandinavia, USA, and Northern Italy (Niklasson *et al.*, 1999; Johansson *et al.*, 2003; Niklasson *et al.*, 2006b; Tolf *et al.*, 2009a; Hauffe *et al.*, 2010). Nothing is known about LV presence in Germany. Therefore, different rodent and insectivora species were screened for LV by RT-PCR.

In total, 454 animals were analysed, belonging to 15 different species. Animals were trapped in 28 urban and sylvatic areas in Germany. A pilot study on bank voles from Sweden revealed the highest LV copy numbers in the brain of LV infected animals positive for LV (see figure 3.17). The brain was therefore chosen as the target organ for screening by RT-PCR analysis.

A total of 44 (9.7 %) animals were found positive for LV, belonging to the following species: voles (*Arvicolidae*): field vole (M*icrotus agrestis*) (8/47 [17 %]), common vole (*Microtus arvalis*) (5/26 [19.2 %]), bank vole (*Myodes glareolus*) (8/95 [8.4 %]); mice (*Muridae*): striped field mouse (*Apodemus agrarius*) (4/48 [8.3 %]), yellow-necked mouse (*Apodemus flavicollis*) (12/93 [12.9 %]), long-tailed field mouse (*Apodemus sylvaticus*) (1/18 [5.5 %]), harvest mouse (*Micromys minutus*) (1/5), house mouse (*Mus musculus*) (1/4) and brown rat (*Rattus norvegicus*) (2/7 [22.2 %]). No insectivore was positive for LV (table 3.5).

Statistical data analysis showed that LV infection is species dependent (Chi square test: α=0.031, p=0.003). Infection rate among animals is 12.1 % (only including the nine species with LV positive individuals [N=348]). No species is significantly more or less frequently infected with LV (Chi square test).

A possible correlation between LV infection with gender and also weight (used as criterion for animal age because no respective data were available) was investigated. Females tend to be more often LV infected than males (N=416; chi square test: α=0.101; fisher's exact: p=0.051). Correlation of LV infection with animal weight was tested at the species level. LV-infected male *Microtus agrestis* voles have a significantly higher body weight than animals negative for LV (N=34; Student's T-test: α=0.0007). No correlation was found between LV infection and body weight with animals of the *Myodes glareolus* and *Apodemus flavicollis* species, respectively.

Table 3.5 Species investigated for LV presence (Germany).

Species	No. LV positive / No. total (%)		
	female	male	total
Apodemus agrarius	2/21 (9.5 %)	2/27 (7.4 %)	4/48 (8.3 %)
Apodemus flavicollis	6/39 (15.4 %)	6/54 (11.1 %)	12/93 (12.9 %)
Apodemus sylvaticus	1/8 (12.5 %)	0/10	1/18 (5.5 %)
Apodemus spec.	1/4 (25 %)	0/3	1/7 (14.3 %)
Crocidura russula	0/1	0/1	0/2
Crocidura spec.	0/2	0/12	0/14
Micromys minutus	0/1	1/4 (25 %)	1/5 (20%)
Microtus agrestis	2/13 (15.4 %)	6/34 (17.5 %)	8/47 (17 %)
Microtus arvalis	0/4	5/22 (22.7 %)	5/26 (19.2 %)
Microtus spec.	0/15	1/38 (2.3 %)	1/53 (1.9 %)
Mus domesticus	0/1	0/3	0/4
Mus musculus	1/1	0/3	1/4 (25 %)
Myodes glareolus	5/34 (14.7 %)	3/61 (4.9 %)	8/95 (8.4 %)
Octodon degus	0	0/1	0/1
Rattus norvegicus	2/7 (28.6 %)	0/2	2/9 (22.2 %)
Rattus spec.	0/1	0/1	0/2
Sorex araneus	0/6	0	0/6
Sorex minutus	0/5	0/2	0/7
Sorex spec.	0/1	0/2	0/3
Talpea europaea	0	0/3	0/3
unknown	0/2	0/5	0/7
total	20/166 (12.1 %)	24/288 (8.3 %)	44/454 (9.7 %)

LV-positive animals were found in areas of Brandenburg, Mecklenburg-Western Pomerania, Saxony-Anhalt, Lower Saxony, Baden-Württemberg and in the city of Cologne representing a wide geographic range within Germany in both rural and urban areas, respectively (table 3.6, figure 3.10).

Table 3.6 Trapping locations itemised by numbers of LV positives and rodent species.

No.[a]	location	species[b]	LV pos[c]	No.[a]	location	species[b]	LV pos[c]
1	Altdöbern	M.arv	0/1	18	Mesekenhagen	T.eur	0/1
2	Bernitt	M.dom	0/2	19	Mücke-Merlau	C.rus	0/2
		S.ara	0/2			C.sp	0/1
		S.min	0/3			S.ara	0/1
		total	0/7			S.min	0/1
3	Bosenbach	S.ara	0/1			total	0/5
4	Britz	A.fla	0/4	20	Niemegk	A.fla	1/1
		M.gla	3/10			M.agr	0/1
		M.agr	4/11			total	1/2
		M.arv	0/1	21	Penzin	A.agr	1/33
		total	7/26			A.fla	8/76
5	Calvörde	M.gla	2/10			A.syl	0/17
		M.agr	0/5			M.gla	1/13
		M.arv	0/2			M.min	1/4
		M.sp	1/15			M.agr	0/1
		total	3/32			M.arv	0/4
6	Colmitz	S.ara	0/1			M.sp	0/1
7	Dinslaken	R.sp	0/2			M.dom	0/1
8	Dreetz	S.min	0/2			S.ara	0/1
9	Freiburg	M.dom.	0/1			S.sp	0/1
10	Golmenglin	M.gla	0/11			n.d.	0/5
11	Groß Schönebeck	A.fla	0/1			total	11/157
		M.agr	0/1	22	Raben/Marzehns	M.agr	1/6
		M.arv	5/14	23	Schwenow	M.gla	0/1
		total	5/16			M.agr	1/1
12	Hohenfels	A.fla	0/4			total	1/2
		A.syl	1/1	24	Tornow	A.agr	3/9
		M.mus	0/2			M.mus	1/2
		O.deg	0/1			total	4/11
		total	1/8	25	Walbeck	M.gla	2/41
13	Horst	A.agr	0/6			M.agr	2/22
		S.min	0/1			M.arv	0/3
		total	0/7			M.sp	0/39
14	Riems	M.min	0/1			n.d.	0/2
		M.arv	0/1			total	4/107
		total	0/2	26	Warburg	C.sp	07
15	Kirchdorf	T.eur	0/1			R.nor	2/9
16	Ködnitz	S.sp	0/1			total	2/16
17	Köln	A.fla	2/6	27	Westergellersen	C.sp	0/3
		A.sp	1/7	28	Wiek	S.min	0/1
		M.gla	0/14				
		C.sp	0/3				
		S.sp	0/2				
		total	3/32				

[a] Numbers corresponding to position on distribution map (figure 3.10).
[b] abbreviations: A.agr: *Apodemus agrarius*, A.fla: *Apodemus flavicollis*, A.syl: *Apodemus sylvaticus*, A.sp: *Apodemus spec.*, C.rus: *Crocidura russula*, C.sp: *Crocidura spec.*, M.min: *Micromys minutus*, M.agr: *Microtus agrestis*, M.arv: *Microtis arvalis*, M.sp: *Microtus spec.*, M.dom: *Mus domesticus*, M.mus: *Mus musculus*, M.gla: *Myodes glareolus*, O.deg: *Octodon degus*, R.nor: *Rattus norvegicus*, R.sp: *Rattus spec.*, S.ara: *Sorex araneus*, S.min.: *Sorex minutus*, S.sp.: *Sorex spec.*, T.eur.: *Talpea europaea*, n.d.: species not determined.
[c] Number LV positive / number total analysed.

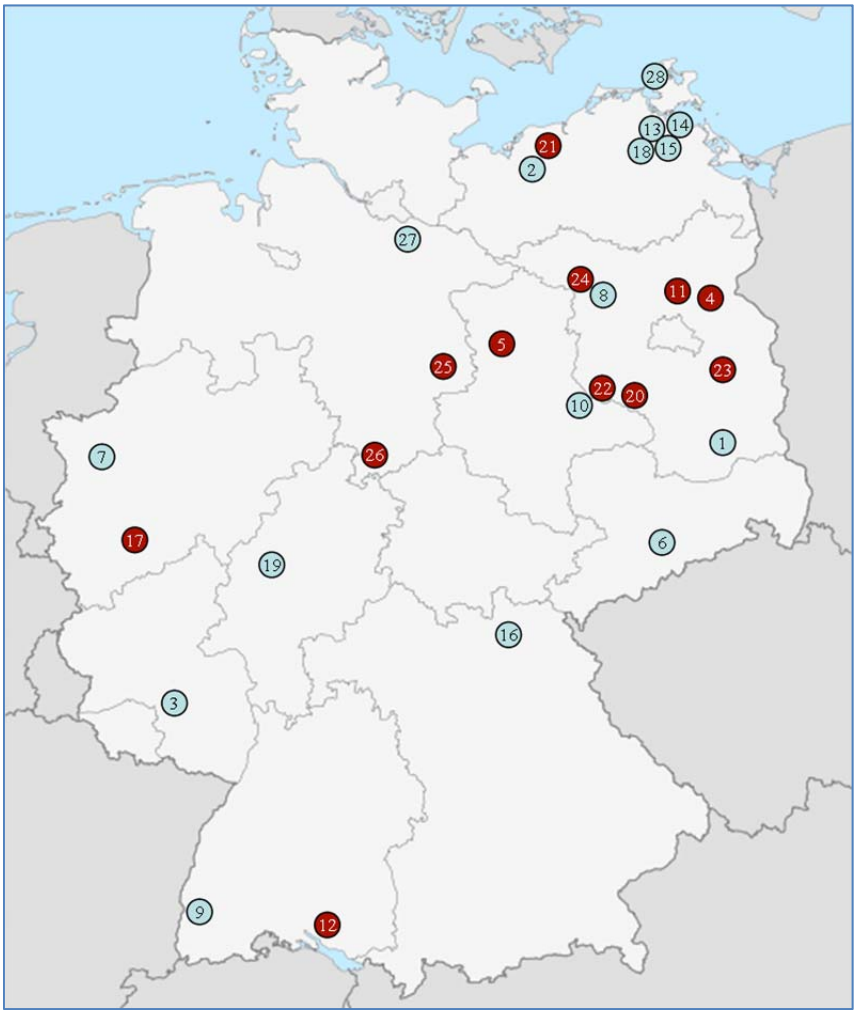

Figure 3.10 Trapping locations for wild rodents in Germany. Red dots: LV-positive animals were found by RT-PCR. Blue dots: all investigated animals were negative for LV by RT-PCR. Locations with positives/total number investigated are shown: 1st Altdöbern (BB) 0/1; 2nd Bernitt (MWP) 0/7; 3rd Bosenbach (RP) 0/1; 4th Britz (BB) 7/26; 5th Calvörde (SA) 3/32; 6th Colmnitz (S) 0/1; 7th Dinslaken (NRW) 0/2; 8th Dreetz (BB) 0/2; 9th Freiburg (BW) 0/1; 10th Golmenglin (SA) 0/11; 11th Groß Schönebeck (BB) 5/16; 12th Hohenfels (BW) 1/8;

continued from figure 3.10: 13th Horst (MWP) 0/7; 14th Insel Riems (MWP) 0/2; 15th Kirchdorf (MWP) 0/1; 16th Ködnitz (B) 0/1; 17th Köln (NRW) 3/32; 18th Mesekenhagen (MWP) 0/1; 19th Mücke-Merlau (H) 0/5; 20th Niemegk (BB) 1/2; 21st Penzin (MWP) 11/157; 22nd Raben/Marzehns (BB) 1/6; 23rd Schwenow (BB) 1/2; 24th Tornow (BB) 4/11; 25th Walbeck (LS) 4/107; 26th Warburg (LS) 2/16; 27th Westergellersen (LS) 0/3; 28th Wiek (MWP) 0/1. Abbreviations: BB: Brandenburg, MWP: Mecklenburg-Western Pomerania, RP: Rhineland-Palatinate, SA: Saxony-Anhalt, S: Saxony, NRW: North Rhine-Westphalia, BW: Baden Württemberg, B: Bavaria, H: Hesse, LS: Lower Saxony

PCR results were confirmed by sequencing. Sequences similar to LV 87-012 were most abundant (27 of 44 positives) and were found in all species positive for LV. Due to high sequence similarity in 5'UTR between strains 87-012 and 174F, a differentiation in either the one or the other strain was not possible for some samples. However, vole species had only sequences similar to 87-012 and/or 174F (first LV genotype). In contrast, some sequences from mouse species also showed similarity to strains 145SL and M1146 (table 3.7).

The picornavirus 5'UTR is highly conserved and is therefore used for screening, but such an assay is not sufficient for genotyping. The genotype can be determined by sequencing of the VP1 region (Oberste *et al.*, 1999a; b). For this purpose, an LV-specific VP1 semi-nested RT-PCR assay was established (3.1.4). All samples positive by 5'UTR RT-PCR were also analysed by VP1 RT-PCR. Only one sample was positive (07/0019). A 500 nt fragment was obtained with closest similarity to both LV strains M1146 and 64-7855 (nt level: 70 %, aa level:72.3 %) (table 3.8). This putative new LV strain was designated as LV Marianne.

Table 3.7 LV 5'UTR sequences obtained from LV-positive rodent samples

Sample	Species[a]	strain[b]	Sample	Species[a]	strain[b]
04/0173	A.agr	M1146	04/0042	M.agr	87-012
04/0176	A.agr	87-012/174F	04/0116	M.agr	87-012
04/0346	A.agr	M1146	04/0136	M.agr	87-012
07/0305	A.agr	87-012	07/0088	M.agr	87-012
04/ 0062	A.fla	M1146	07/0186	M.agr	87-012
07/0049	A.fla	145SL	07/0132	M.sp	87-012
07/0193	A.fla	87-012	04/0067	M.arv	87-012
07/0203	A.fla	87-012	04/0093	M.arv	87-012
07/0209	A.fla	87-012	04/0094	M.arv	87-012/174F
07/0218	A.fla	87-012	04/0099	M.arv	87-012/174F
07/0233	A.fla	87-012	04/0095	M.arv	87-012/174F
07/0255	A.fla	87-012	04/0055	M.gla	87-012/174F
07/0316	A.fla	87-012	04/0037	M.gla	87-012/174F
07/0317	A.fla	87-012	04/0050	M.gla	87-012/174F
59/60Mu/04	A.fla	87-012	07/0019	M.gla	174F
07/0047	A.fla	145SL	07/0036	M.gla	87-012
04/0022	A.syl	87-012	07/0130	M.gla	87-012/174F
07/0051	A.sp	145SL	07/0187	M.gla	87-012
07/0225	M.min	87-012	07/0206	M.gla	87-012
04 /0030	M.agr	87-012	04/0399	M.mus	87-012
04 /0058	M.agr	87-012	08/0280	R.nor	n.d.
04/0041	M.agr	87-012	08/0290	R.nor	n.d.

[a] Abbreviations: A.agr: *Apodemus agrarius*, A.fla: *Apodemus flavicollis*, A.syl: *Apodemus sylvaticus*, A.sp: *Apodemus spec.*, M.min: *Micromys minutus*, M.agr: *Microtus agrestis*, M.arv: *Microtus arvalis*, M.sp: *Microtus spec.*, M.mus: *Mus musculus*, M.gla: *Myodes glareolus*, R.nor: *Rattus norvegicus*

[b] Similarity to known LV strain in partial 5'UTR

n.d.: not determined

Phylogenetic analysis of the 500 nt VP1 segment showed clustering between first and second genotype on the one hand and between third and fourth genotype on the other hand (figure 3.11). Interestingly, the sequenced 5'UTR PCR product of sample 07/0019 shared high similarity with LV 174F.

Table 3.8 Amino acid identities between LV strains (and HPeV) and LV Marianne based on the sequenced 500 nt VP1 segment.

aa identities	Mar	87-012	87-012G	174F	145SL	145SLG	M1146	64-7855
Mar								
87-012	64.5							
87-012G	64.5	99.4						
174F	64.5	100	99.4					
145SL	65.1	78.4	78.4	78.4				
145SLG	64.5	77.8	77.8	77.8	99.4			
M1146	72.3	72.3	72.3	72.3	68.1	67.5		
64-7855	72.3	68.7	68.1	68.7	68.7	68.1	77.1	
HPeV	33.8	34.4	34.4	34.4	37.4	36.6	34.6	34.6

GenBank accession number for each virus strain is shown in figure 3.11. Abbreviations: aa: amino acid, Mar: LV Marianne

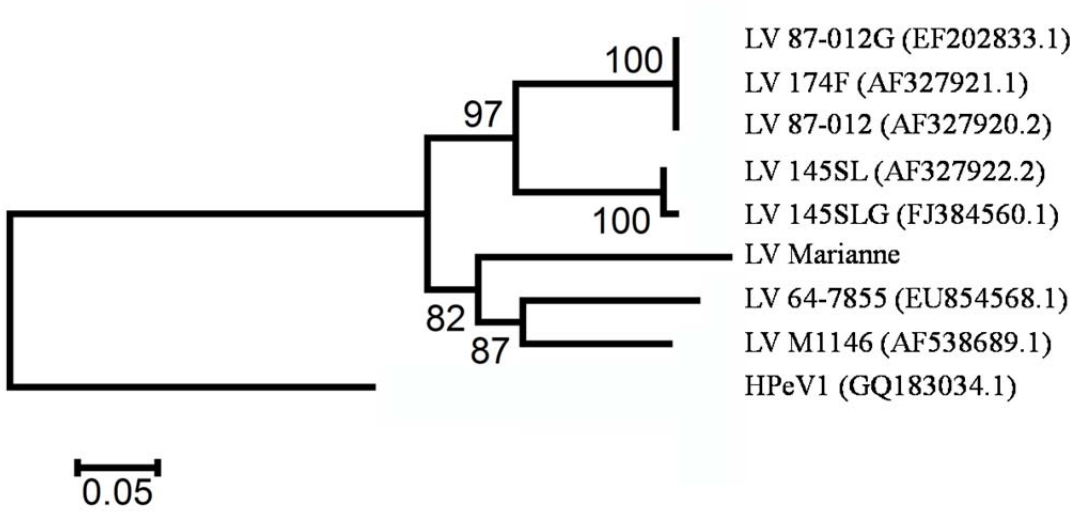

Figure 3.11 Phylogenetic analysis of LV Marianne based on the sequenced 500 nt segment. LV strains available at GenBank were used for analysis (accession numbers are shown in parantheses). HPeV1 was used as outgroup. The evolutionary history was inferred using the Neighbor-Joining method (Saitou and Nei, 1987). The optimal tree with the sum of branch length = 1.15865385 is shown. The percentage of replicate trees in which the associated taxa clustered together in the bootstrap test (1000 replicates) are shown next to the branches (Felsenstein, 1985). The tree is drawn to scale, with branch lengths in the same units as those of the evolutionary distances used to infer the phylogenetic tree. All positions containing gaps and missing data were eliminated from the dataset (complete deletion option). There were a total of 130 positions in the final dataset. Phylogenetic analyses were conducted in MEGA4 (Tamura *et al.*, 2007).

There are also no data about LV prevalence in rodents from Asia. Therefore, brain samples from 87 animals belonging to 8 different rodent species from Thailand were also investigated.

A total of 14 (16.1 %) animals were positive for LV by RT-PCR, belonging to the following species: bandicoot rat (*Bandicota indica*) (7/36 [19.4 %]), Savile's bandicoot rat (*Bandicota savilei*) (1/8 [12.5 %]), ryukyu mouse (*Mus caroli*) (2/6), black rat (*Rattus rattus*) (3/22 [13.6 %]) and common treeshrew (*Tupaia glis*) (1/4). (table 3.9).

Table 3.9 Species investigated for LV presence (Thailand)

Species	No. LV positive / No. total (%)		
	Female	Male	total
Bandicota indica	4/15 (26.7 %)	3/21 (14.3 %)	7/36 (19.4 %)
Bandicota savilei	0/5	1/3 (33.3 %)	1/8 (12.5 %)
Mus caroli	0/1	2/5 (20 %)	2/6 (33.3 %)
Rattus argentiventer	0	0/3	0/3
Rattus exulans	0/2	0/1	0/3
Rattus rattus	1/9 (11.1 %)	2/13 (15.4 %)	3/22 (13.6 %)
Rattus tiomanicus	0/2	0/3	0/5
Tupaia glis	0/2	1/2	1/4 (25 %)
total	5/36 (13.9 %)	9/51 (17.7 %)	14/87 (16.1 %)

Animals were trapped in 5 different provinces in Thailand. LV-positive animals were found in the regions of Bangkok, Buri Nam and Prachuap Khiri Khan (table 3.10, figure 3.12).

No correlation was found between LV infection and gender and LV infection and age, respectively.

Table 3.10 Wild rodent trapping locations in Thailand itemised by LV positives and rodent species

Province	Species	LV pos[a]	Province	Species	LV pos[a]
Bangkok	*B. indica*	1/2	Chumpon	*R. tiomanicus*	0/4
	R. exulans	0/1	Nakhon P	*B.indica*	0/11
	R. rattus	1/5		*M.caroli*	0/1
	R. tiomanicus	0/1		*R.rattus*	0/2
	total	2/9		total	0/14
Buri Ram	*B. indica*	0/4	Prachuap	*B. indica*	6/19
	B. salivei	1/8		*R. argentiventer*	0/3
	M. caroli	2/5		*R. rattus*	2/8
	R. exulans	0/2		*T. glis*	1/4
	R. rattus	0/7		total	9/34
	total	3/26			

[a] Number LV positive / number total analysed

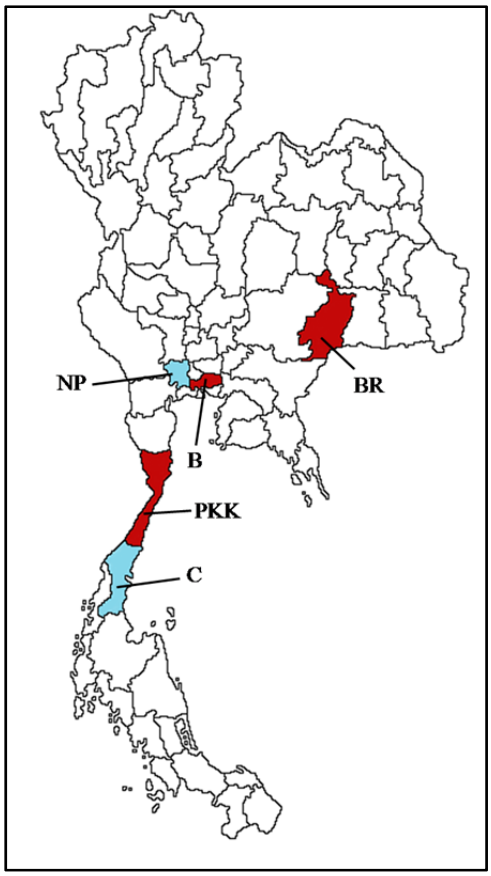

Figure 3.12 Wild rodent trapping locations in Thailand. Red areas: LV-positive animals as detected by RT-PCR. Blue areas: all animals tested negative for LV by RT-PCR. Abbreviations: B: Bangkok, BR: Buri Ram, C: Chumpon, NP: Nakhon Pathom, PKK: Prachuap Khiri Khan.

III

3.5 Ljungan virus RNA persists in tissues of infected laboratory mice

Several viruses have been associated with diabetes. It has been suggested that one potential mechanism for virus-induced autoimmune disease is persistent virus infections (Fujinami *et al.*, 2006). The parvovirus B19 is an example of a virus persisting in various human tissues and subsequently responsible for disease during pregnancy (Soderlund-Venermo *et al.*, 2002).

This thesis investigates the concentration and persistence of LV in several organs of infected CD-1 mice over the course of several months to clarify the continuity of LV infection over the life course. It is postulated that LV persistence might account for the onset of diabetes in bank voles and in LV-infected CD-1 laboratory mice. LV-infected male CD-1 laboratory mice were investigated for the presence of LV-specific RNA by RT-PCR over the course of several months.

LV infection of suckling mice resulted in signs of acute encephalitis, myocarditis and pancreatitis a few dpi. Approximately 70 % of the mice recovered from acute signs of disease. Clinical signs of diabetes followed 15 weeks later. The clinical picture of LV-infected laboratory mice was recently described (Niklasson *et al.*, 2006a; b).

All organs investigated for LV-specific RNA were found positive by real-time RT-PCR. In the acute infection, the highest levels of virus genome equivalents were found in the brain (7.39e+10 LV RNA copy equivalents per g tissue) followed by pancreas (1.07e+9 LV RNA copy equivalents per g tissue) and heart (8.09e+8 LV RNA copy equivalents per g tissue). Virus loads of other organs range from 3.86e+8 (large intestine) to 1.53e+7 LV RNA copy equivalents per g tissue (kidney) (Figure 1). In all organs, levels of LV genome equivalents decreased and reached a minimum at day 56

pi. By day 56 pi, LV RNA levels began to increase in all organs and remained at a constant level from day 98 pi until day 174 pi when the experiment was terminated (Figure 3.12). Thymus and bladder were obtained from some animals. Both organ types were found to be LV positive (thymus: 6.07e+5 [13 dpi, n=1], 3.02e+6 [17 dpi, n=1], 1.25e+4 [27 dpi, n=2] and 5.54e+4 [56 dpi, n=2] LV RNA copy equivalents per g tissue; bladder: 2.15e+6 [98 dpi, n=1] and 7.19e+5 [130 dpi, n=1] LV RNA copy equivalents per g tissue).

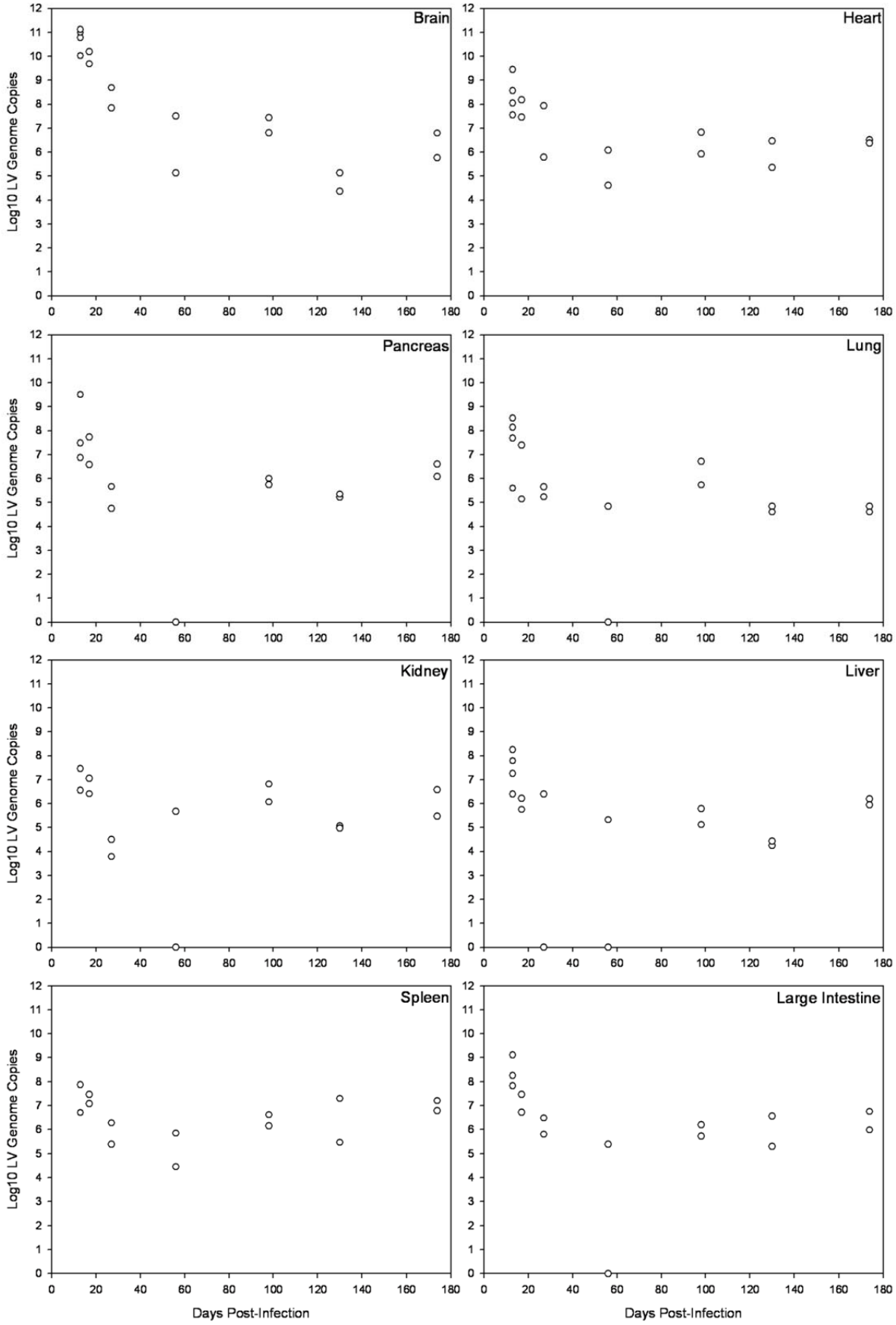
Brain
Heart
Pancreas
Lung
Kidney
Liver
Spleen
Large Intestine
Log10 LV Genome Copies
Days Post-Infection

Figure 3.12 LV genome copies in laboratory mouse organs detected by real-time RT-PCR. Data are plotted as LV genome equivalents per g of tissue. Each circle represents one LV-infected laboratory mouse. Circles on the x-axis mean LV-negative organs.

To highlight the acute phase of infection, an additional study was performed. Suckling mice were infected as described above and the same organs were collected, but a shorter time frame was chosen reflecting the first 10 dpi (table 3.11). Most animals developed clinical symptoms of encephalitis 7 dpi with trembling, irritability and paralysis. On day 10 (when the experiment was terminated), 75 % of infected animals had clinical symptoms, 25 % were symptomless, and 25 % were dead. Body weight was measured during the whole study time. LV infection had an effect on body weight. Infected animals weighed less than non-infected animals until 5 dpi. After 5 dpi, the weight of symptomless animals reached approx. the same level as non-infected animals. In contrast, encephalitis was associated with body weight loss compared to both non-infected counterparts and symptomless animals (figure 3.13).

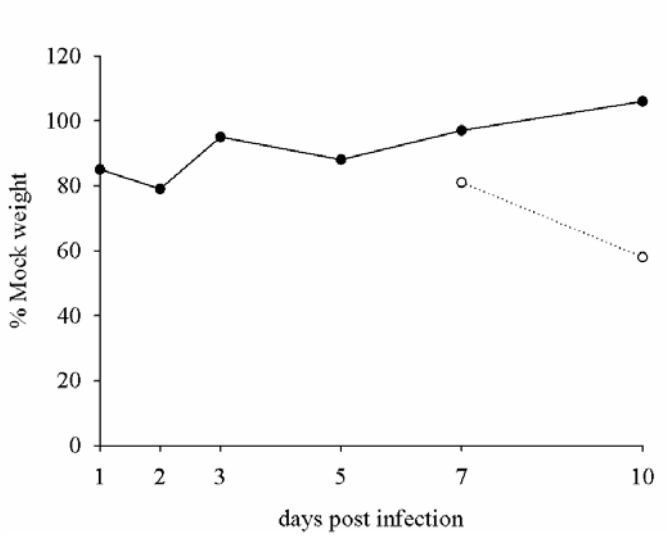

Figure 3.13 Influence of LV infection to body weight during the first 10 dpi. One-day-old CD-1 laboratory mice were intraperitoneally infected with LV 145SL. Changes in weight from Mock-infected counterparts were calculated over time. First symptoms of encephalitis were observed 7 dpi. Animals with encephalitis are shown as dotted line. Symptomless (but infected) animals are shown as solid line. Data are presented for at least three animals per date.

Since the previous study included only male mice, only male mice were also considered for analysis of the acute infection. For 2 dpi, only 1 male was available, whereas 2 males could be included for all other time points (table 3.11).

Table 3.11. Animal designation used for LV infection study with acutely infected laboratory mice.

dpi	1	2	3	5	7	10
Animal designation	A1 B2	B3	A4 C4	B5 C5	A6 B7	A8 B8

All organs were again analysed for LV presence by RT-PCR. One dpi, 1 animal (2B2) was LV positive in all organs, while A1 was negative in all organs. B3 (2 dpi) was LV positive only in spleen ($3.63x10^5$) and bladder (including urine) ($5.2x10^4$). Three dpi, A4 was positive only in intestine (including faeces) ($1.95x10^4$) and C4 was positive in all organs (brain was not available). From 5 dpi on, all organs of all animals were positive for LV, except for brain of A6 that was negative. Interestingly, the highest mean copy numbers were found in intestine until 3 dpi, and lung, brain and heart had the lowest mean copy numbers. However, an increasing mean copy number within time was detected only in brain, heart and slightly in the lung, whereas mean copy numbers in all other organs remained at a constant level until 10 dpi (figure 3.14).

Copy numbers were considered separately for each animal, varied a lot between animals sacrificed at the same time point, and also organ distribution was different among animals, reflecting individual differences of this outbred strain. However, with the exception of A6, the brain was the organ with the highest copy numbers from day 7 on, consistent with signs of acute encephalitis (figure 3.15).

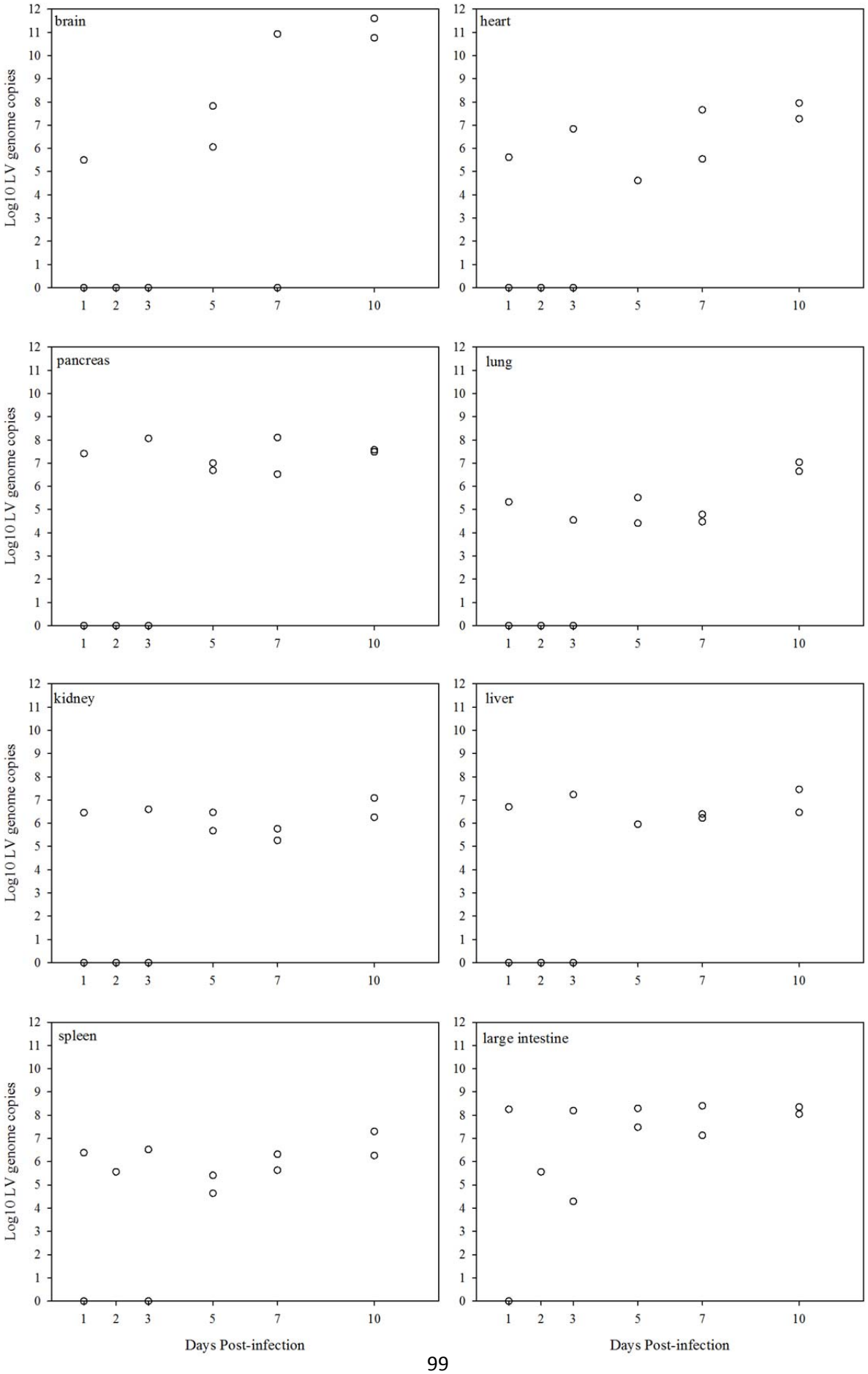
brain
heart
pancreas
lung
kidney
liver
spleen
large intestine
Log10 LV genome copies
Days Post-infection
0 1 2 3 4 5 6 7 8 9 10 11 12
1 2 3 5 7 10

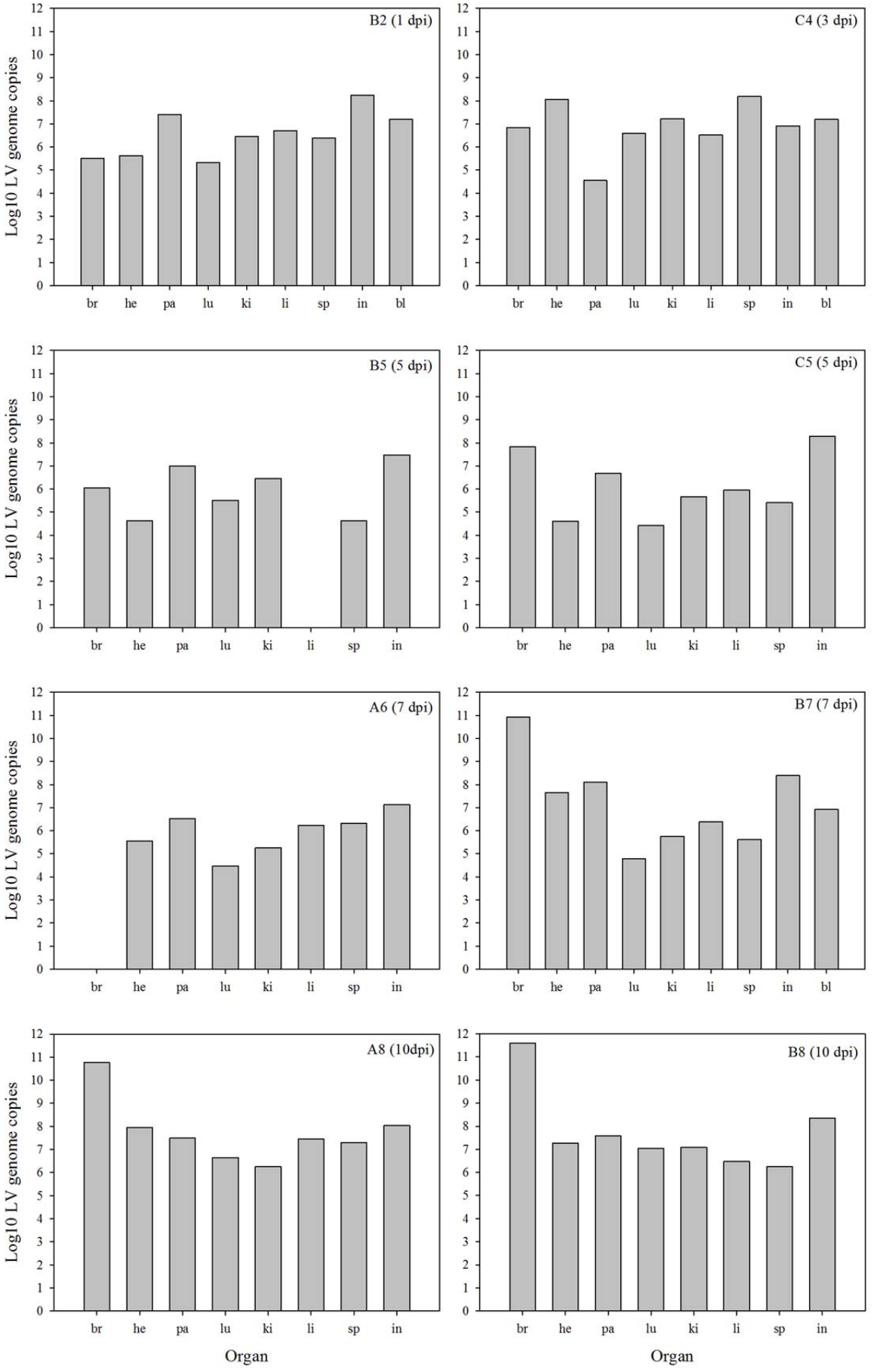
B2 (1 dpi)
C4 (3 dpi)
B5 (5 dpi)
C5 (5 dpi)
A6 (7 dpi)
B7 (7 dpi)
A8 (10dpi)
B8 (10 dpi)
Log10 LV genome copies
Organ
br
he
pa
lu
ki
li
sp
in
bl

Figure 3.14 LV genome copies in laboratory mouse organs detected by real-time RT-PCR. Data are plotted as LV genome equivalents per g of tissue. Each circle represents one LV-infected laboratory mouse. Circles on the x-axis mean LV-negative organs.

Figure 3.15 LV genome copies in laboratory mouse organs detected by real-time RT-PCR. Shown are copy number organ distributions for each animal with more than two LV-positive organs. Data are plotted as LV genome equivalents per g of tissue.

For each animal, virus isolation was attempted from brain and liver. The size of other organs of suckling mice was too small for both RNA extraction and virus isolation. Infectious LV particles could be isolated from both tissue types. An increasing titre was found only in brain, while titre in liver decreased over time (figure 3.16).

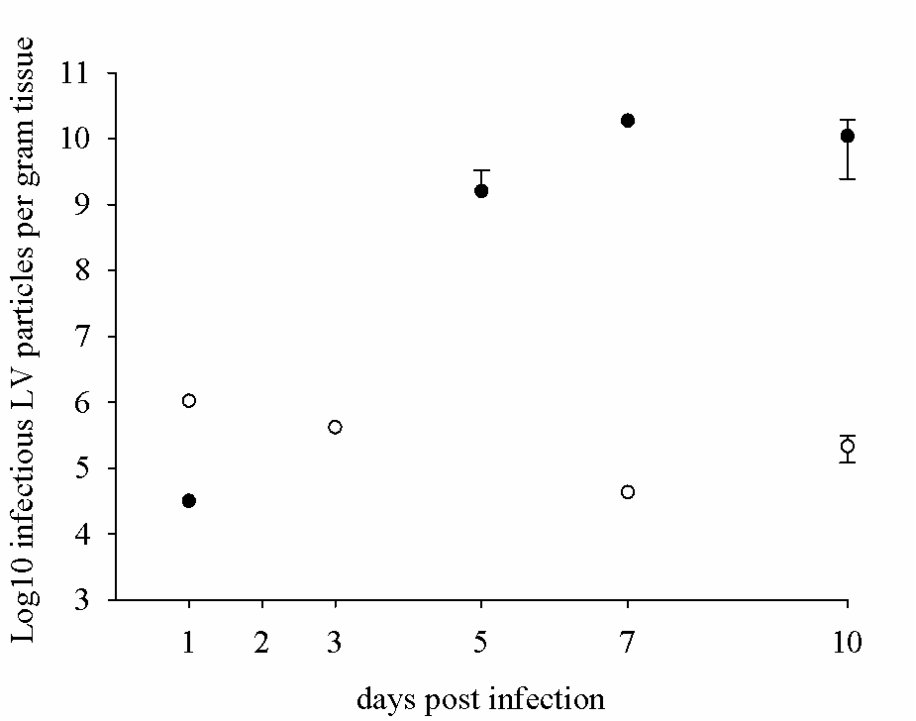

Figure 3.16 LV titre in brain and liver of acutely infected laboratory mice. Titres are shown as per g of tissue. Black circles: brain, white circles: liver.

To extend the findings from laboratory mice to wild rodents, organs obtained from 13 wild-caught bank voles were investigated for the presence of LV. In total, nine animals were found to be positive for LV by real-time RT-PCR (figure 3.17). All voles tested positive in at least two organs, while one was positive in all investigated organs. The highest mean LV genome copy number was found in the brain (figure 3.17).

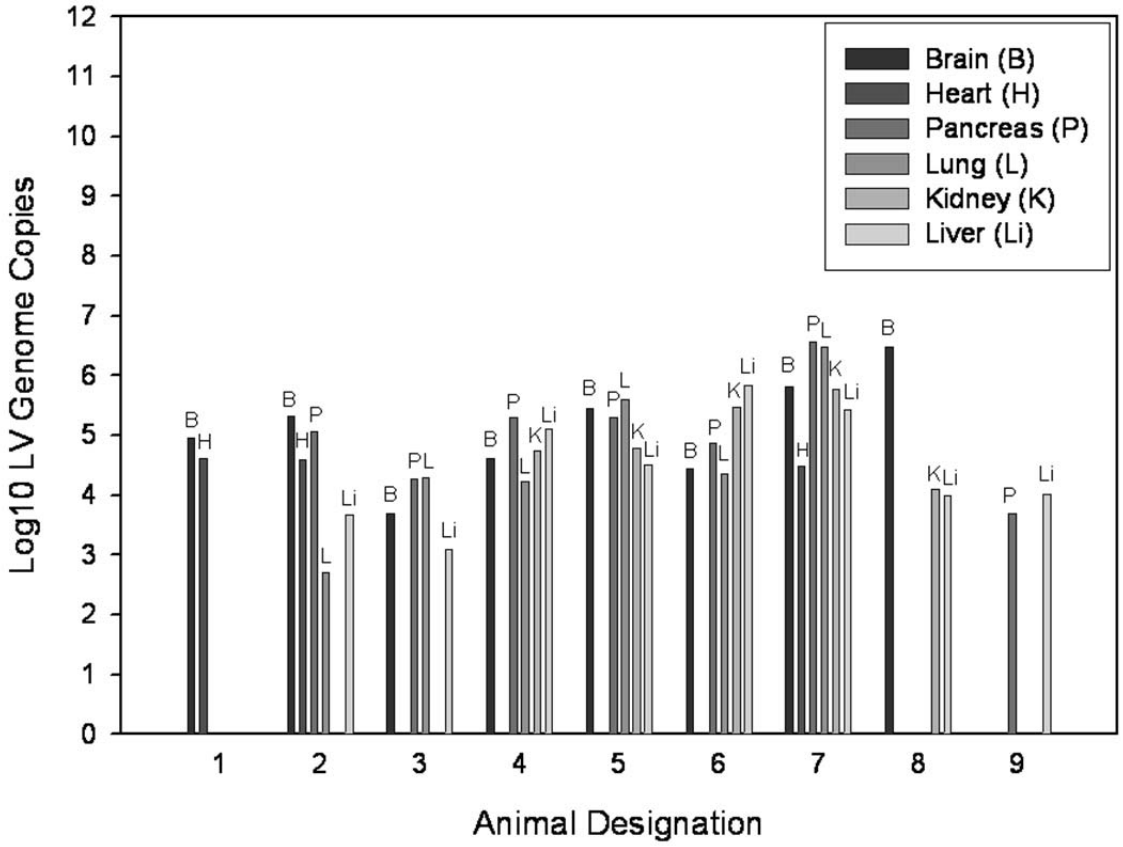

Figure 3.17 LV genome copies in wild bank vole organs detected by real-time RT-PCR. Data representing nine individuals are plotted as LV genome equivalents per g of tissue. Means in LV genome copies in different organs are: 5.45e+5 (brain); 3.68e+4 (heart); 6.21e+5 (pancreas); 5.79e+5 (lung); 2.02e+5 (kidney); 1.41e+5 (liver).

3.6 Ljungan virus infection in lytic versus non-lytic cell culture

3.6.1 Morphological changes of Vero-B4 and BHK21 cells post LV infection

LV-infected Vero-B4 cells showed first signs of CPE 4 dpi. Distinct groups of cells rounded up and became detached from the surface. The number of cells showing CPE increased over time. A full destruction of the cell monolayer could be observed 10 dpi. No CPE was seen in Mock-infected cells (figure 3.18). In contrast, BHK-21 cells showed no CPE post LV infection (data not shown).

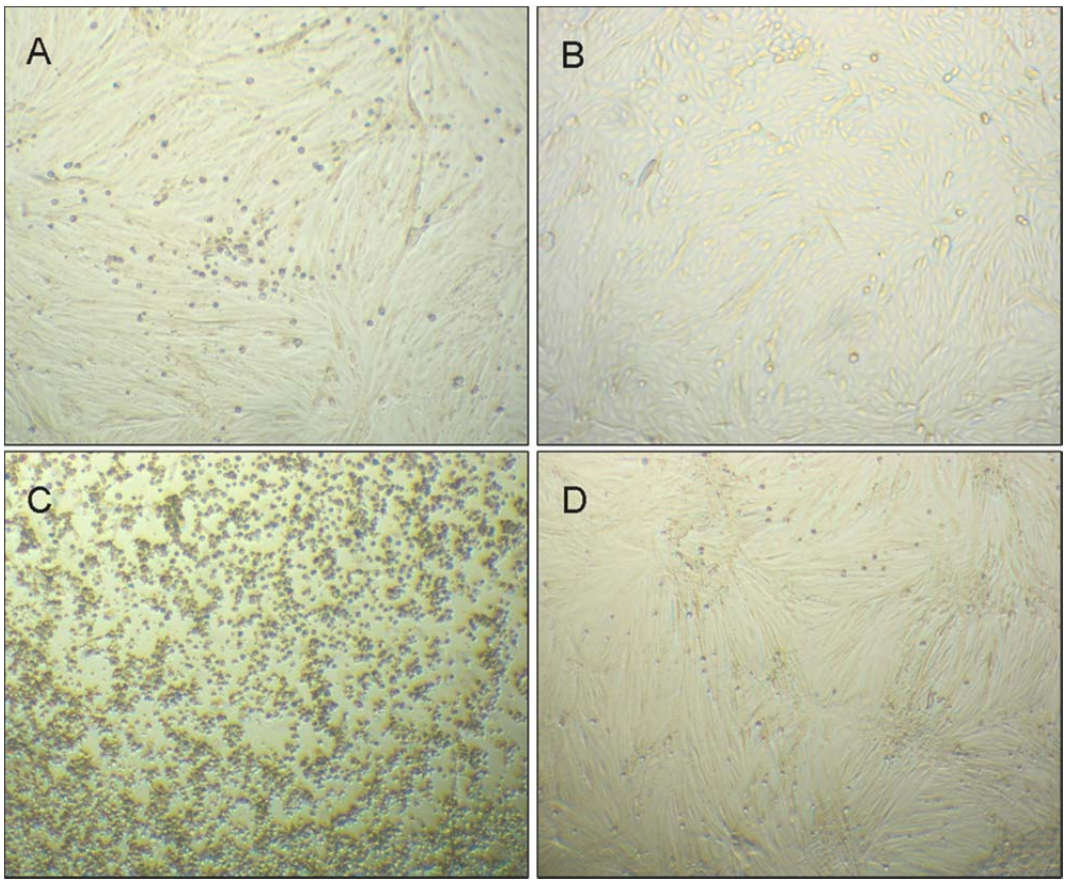

Figure 3.18 Cytopathic changes on Vero-B4 cells post LV infection (A, C) and Mock-infected cells (B, D). A, B: 4 dpi. C, D: 10 dpi.

LV-infected cells were stained with DAPI to visualize the DNA in the nucleus. LV-infected Vero-B4 cells contained condensed chromatin and apoptotic bodies (figure

3.19), features characteristic of apoptosis. These nuclear changes could not be observed in Mock-infected Vero-B4 cells and in LV-infected BHK-21 cells, respectively (data not shown).

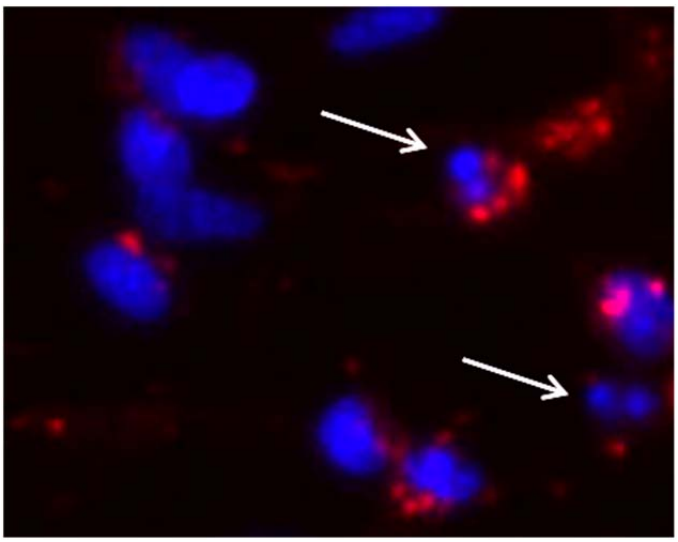

Figure 3.19 Chromatin condensation in LV-infected Vero-B4 cells 7 dpi. Nucleus DNA was stained with DAPI (blue). LV protein was stained with mAb LV-05sA4-H (red). Prominent examples are indicated by arrows. Magnification: 40x.

3.6.2 LV propagation in Vero-B4 and BHK-21 cells

Both Vero-B4 and BHK-21 cells were infected with LV 87-012. Cells were acetone fixed, and presence of LV antigen was detected by IIFT using a polyclonal anti-VP1 rabbit antiserum (Tolf *et al.*, 2008). First fluorescence was observed 3 dpi in both cell lines with staining in the cell cytoplasm, indicating that both cell lines were susceptible to LV. No fluorescence was seen in Mock-infected cells (figure 3.20). Groups of neighbouring fluorescent cells were observed for both, Vero-B4 and BHK-21 cells, respectively (compare also to figure 3.6).

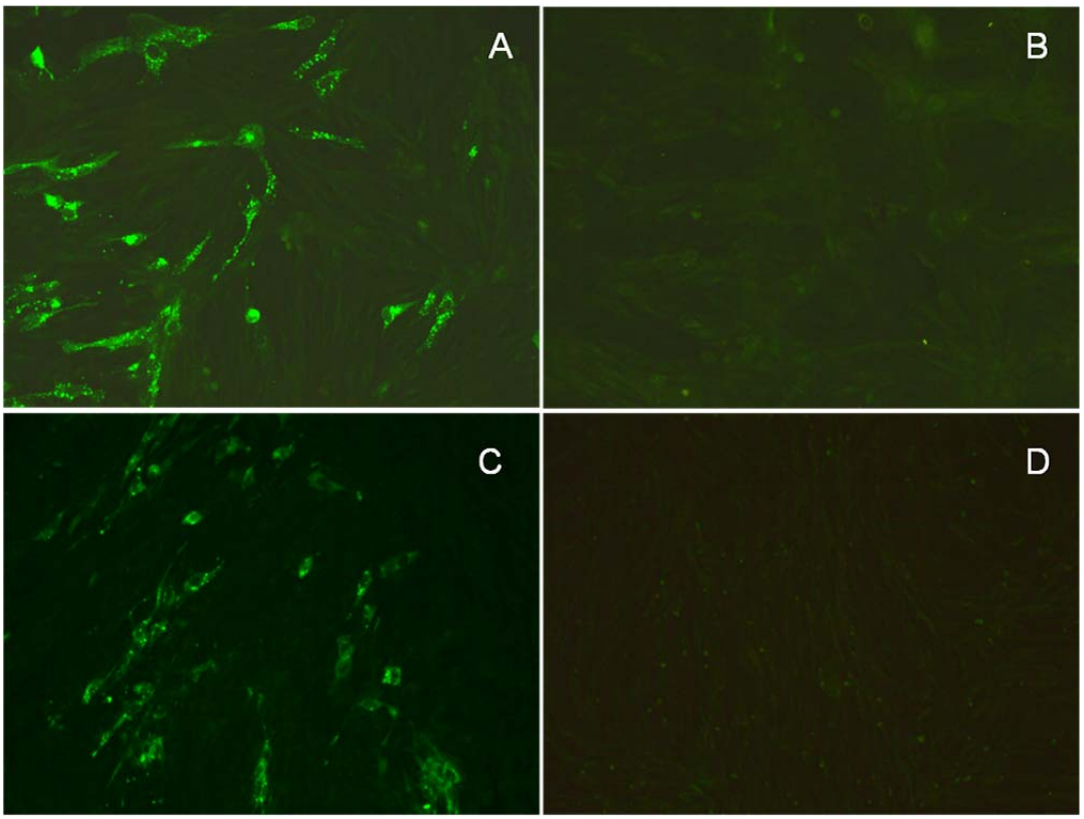

Figure 3.20 IIFT on Vero-B4 (A, B) and BHK-21 (C, D) cells. Cells were infected with LV 87-012 (MOI1) (A, C) (B, D: Mock-infected) acetone fixed 3 dpi and analysed for presence of LV antigen by use of a polyclonal rabbit anti-VP1 antiserum. Magnification: x20.

LV production over time was measured by determining the $CCID_{50}$ of cell culture supernatants of LV infected cells. LV RNA replication in cells was measured by real-time RT-PCR assay.

LV titre in Vero-B4 cells increased logarithmically over time by six log-levels until 8 dpi. After day 8 pi, the titre increased only slightly in these cells (approx. 0.5 log-levels), consistent with the observed complete CPE at this time. In contrast, only a minor increase in virus titre was determined for BHK-21 cells, indicating no or low release of virus particles in the cell culture supernatant (figure 3.21 A).

Detected by real-time RT-PCR, the amount of LV RNA increased in both cell lines with a similar rate of increase (figure 3.21 B). Thus, LV replicates in Vero-B4 as well as in BHK-21 cells with similar growth characteristics. In addition, the number of LV-infected BHK-21 cells positive by IIFT increased until 6 dpi with approx. 90 % of

cells positive (data not shown). These data indicate both, LV RNA production and (at least) LV protein production, but inhibition of virus release or virus assembly in BHK-21 cells.

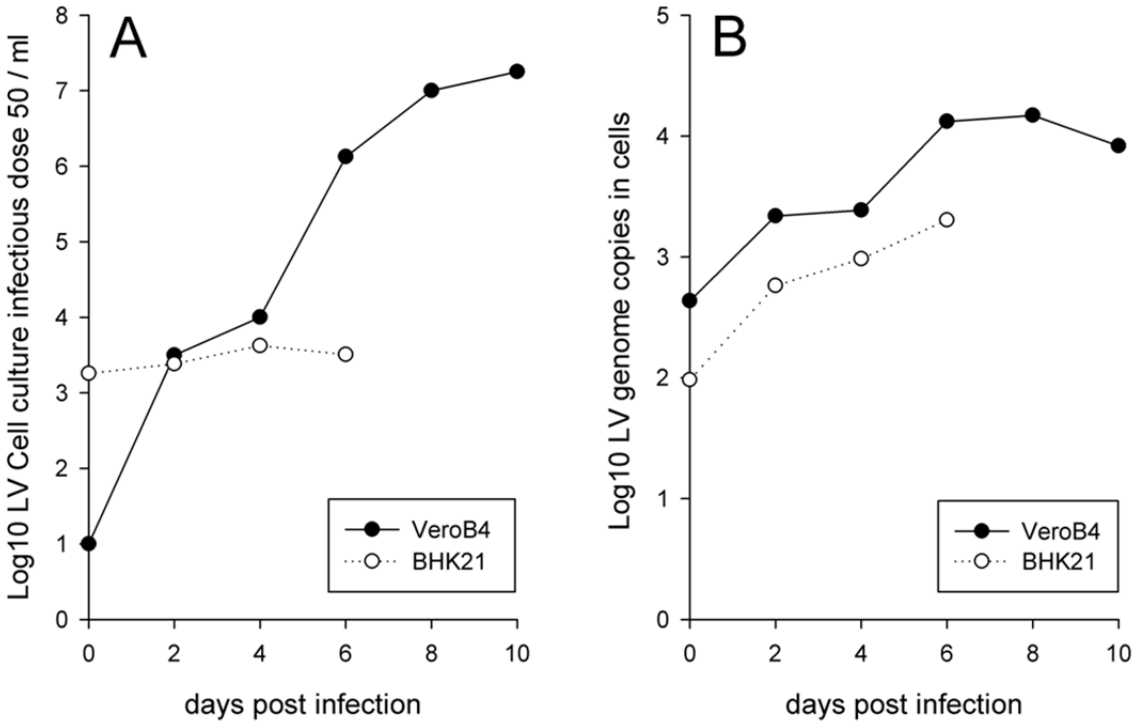

Figure 3.21 Growth kinetics of LV in Vero-B4 and BHK-21 cells. (A) Virus titres as determined by cell culture infectious dose 50 assay. Mean titres of octuple samples are shown for each time point. Note that BHK-21 cells can not be maintained longer than six days. (B) LV RNA replication was determined by real-time RT-PCR assay. Means of duplicate samples are shown for each time point.

3.6.3 DNA fragmentation in LV-infected Vero-B4 and BHK-21 cells

Internucleosomal DNA degradation is a hallmark of apoptosis. DNA extracted from LV-infected Vero-B4 cells showed the typical laddering with DNA degradation. This DNA ladder was not observed in Mock-infected Vero-B4 cells. The topoisomerase I-inhibiting alkaloid camptothecin was used as a positive control for induction of apoptosis (figure 3.22). No DNA fragmentation was observed when detected with

BHK-21 cells. In contrast, DNA extracted from BHK-21 cells treated with camptothecin was indeed fragmented (data not shown).

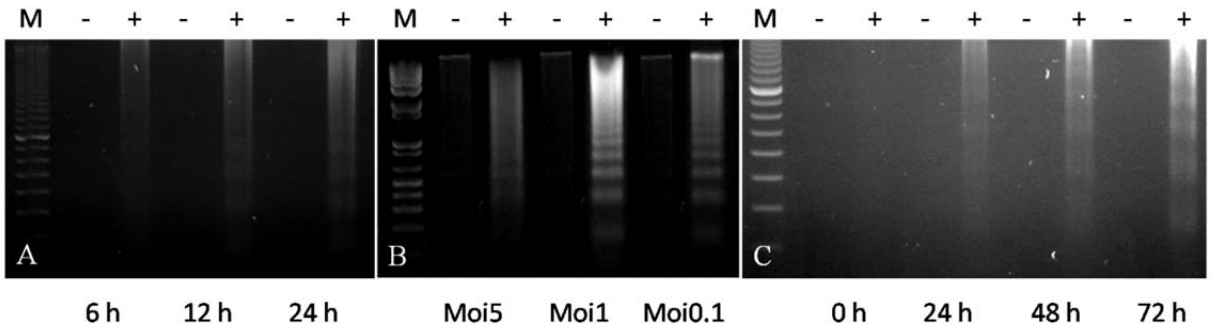

Figure 3.22 DNA fragmentation in Vero-B4 cells treated with camptothecin (A) and infected with LV (B, C). B: Effects of different MOI on DNA laddering. C: MOI1; increasing DNA fragmentation over time. M: marker, - Mock, + camptothecin treated (A) and LV infected, respectively (B, C).

Terminal deoxynucleotidyl transferase-mediated dUTP-biotin nick end labelling (TUNEL) is a more sensitive method for detection of DNA strand breaks. The TUNEL assay was used to confirm these results at the single cell level. Again, DNA fragmentation was observed only in LV-infected Vero-B4 cells, but not in BHK-21 cells while Mock-infected cells were negative for both cell lines. Cells treated with camptothecin were again positive for both cell lines.

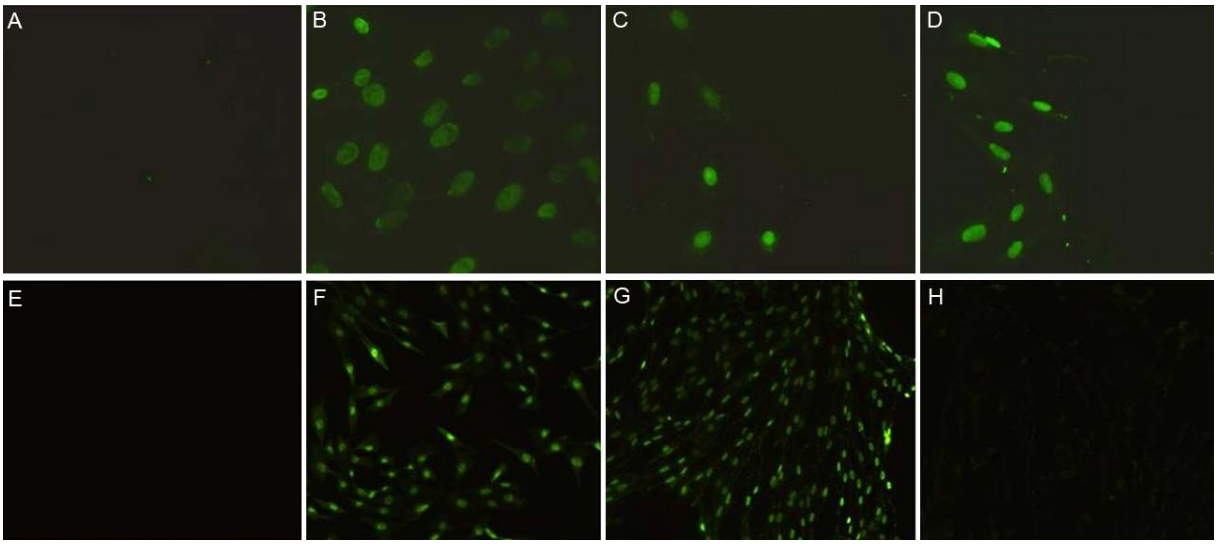

Figure 3.23 TUNEL staining of Vero-B4 (A-D) and BHK-21 (E-F) cells. LV was adsorbed at an MOI1 for 1 h at 37 °C, and DNA fragmentation was determined by dUTP nick end labelling 8 dpi (Vero-B4) and 4 dpi (BHK-21), respectively. Fluorescence was only observed in LV-infected Vero-B4 cells (D) whereas LV-infected BHK-21 (H) and Mock-infected cells (A, E) did not show fluorescence. Treatment with 5 µM Camptothecin was used as a positive control for apoptosis induction (B, F). In order to prove the method, cells were treated with DNase I for 10 min prior to staining (C, G).

3.6.4 Detection of active Caspase-3 in LV-infected Vero-B4 cells

Caspase-3 is a key enzyme in the initiation of apoptotic cell death. This enzyme exists as uncleaved precursor in the cell. Once the apoptotic pathway is initiated, the enzyme is cleaved into its active form (Nicholson *et al.*, 1995).

LV-infected Vero-B4 cells were investigated for presence of active Caspase-3 by IIFT and western immunoblotting. Active caspase-3 was detected in LV-infected cells with co-staining of LV antigen by IIFT. Furthermore, fluorescence was also observed in cells without visible LV antigen (figure 3.24) possibly through bystander apoptosis. Western blotting showed a very weak reaction to active caspase-3, while presence of uncleaved caspase-3, actin and LV proteins VP0, VP3 and VP1 could clearly be detected (data not shown).

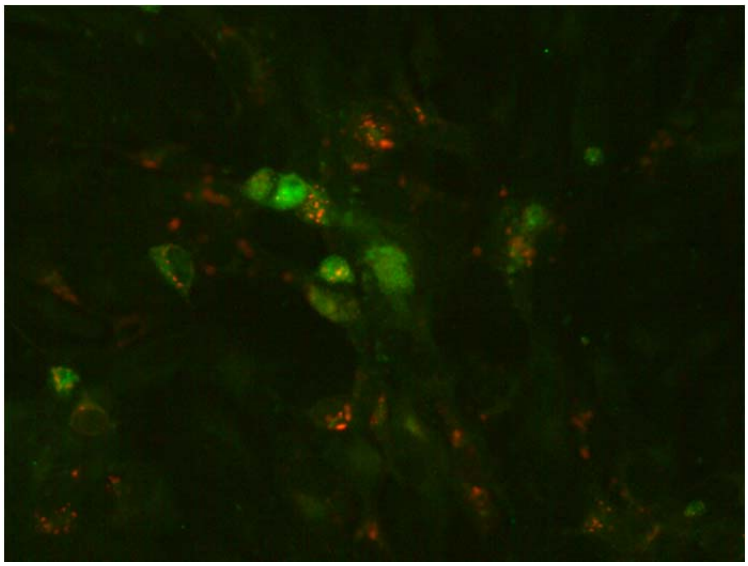

Figure 3.24 Detection of active caspase-3 and LV antigen in Vero-B4 cells 5 dpi. An active caspase-3 specific polyclonal rabbit antibody (green fluorescence) and mAb LV-05sA4-H (red fluorescence) were used for staining.

4 Discussion

4.1 Development and evaluation of methods for detection and characterisation of Ljungan virus

4.1.1 RT-PCR based assays

Real-time PCR has become a "gold standard" for detection and quantitation of viruses and viral load, respectively. Advantages over conventional PCR assays are for instance the higher sensitivity, higher speed, lower inter-assay and intra-assay variability, and the possibility to quantitate viral load allows to adjust antiviral therapies and to monitor patient's therapeutic response (Mackay *et al.*, 2002).

These benefits were enhanced by developing a novel real-time RT-PCR assay for detection and quantitation of LV genomes. A highly conserved genome region targeting the LV 5'UTR was chosen for primer and probe design. The assay specifically detects all known LV strains, but not the related parecho- and cardioviruses (Niklasson *et al.*, 1999), showing, high assay specificity. The ratio between viral RNA copies and infectious virus particles differs between various virus stocks of the same virus. For determination of assay sensitivity it is therefore not recommended to use RNA extracted from virus stocks whose titre was determined by cell culture-based assays (Drosten *et al.*, 2002). This problem was circumvented by using *in vitro* transcribed RNA to determine the assay sensitivity. Detection limit of both one-step and two-step RT-PCR assay is ≤ 10 copies per reaction. This detection limit is close to other PCR assays for detection of parechoviruses (Nix *et al.*, 2008). The real-time assay was linear over the tested range of either virus RNA or *in vitro*-transcribed RNA. Assay reproducibility was determined by intra- intervariability tests with ≤ 1 C_T value for both assays, showing the high reproducibility for this RT-PCR. LV real-time RT-PCR was established as both one-step and two-step assay. Mean C_T values of the two-step assay were below mean C_T values of the one-step assay for all *in vitro*-transcribed RNA concentrations tested, indicating a higher sensitivity of the two-step assay. However, the use of one-step RT-PCR is less time consuming and also reduces the risk of contamination which makes it more suitable for diagnostic approaches. Picornaviruses replicate by using an intermediate of positive- and

negative-strand RNA. Determination of the ratio of positive- and negative strands gives information about the kind of virus infection, i.e. acute or persistent (Girard *et al.*, 2002). Such conclusions are also possible for LV by using the two-step assay with either the forward primer (for detection of negative strands) or the reverse primer (for detection of positive strands) in reverse transcription reaction. The assay was evaluated using RNA extracted from LV-infected laboratory mouse tissues. LV RNA from different LV strains used for infection was specifically detected and quantitated with different viral loads in all types of organs tested. This approach was extended to "field" conditions with organs taken from rodents trapped in the wild. Again, LV RNA could be detected, and viral load in different organs reflected that obtained for laboratory mice, showing that this assay can be applied in fast and reliable detection of LV RNA in different sample types.

Melting curve analysis was established to confirm RT-PCR results and also to obtain strain information of samples positive by RT-PCR. Sequences identical to the targeted 5'UTR region of LV strains 87-012, 174F and 145SL could be detected, and these strains could clearly be distinguished within a few minutes. This assay offers an alternative to sequence analysis of PCR products. However, probes could only be designed for these three strains because of too high sequence variation to M1146 and 64-7588. A positive RT-PCR but negative melting curve result should therefore be analysed further. To overcome this problem, pyrosequencing was developed. This assay enables the detection of sequences from all known LV strains. Furthermore, it should be possible to obtain short sequences not similar to known LVs. However, pyrosequencing lacks sensitivity. High copy numbers are necessary for positive results.

Picornaviruses are known to recombine within species (Simmonds, 2006). Several recombination breakpoints were identified for HPeVs (Zoll *et al.*, 2009b). There are also few data for LV, indicating recombination events also in this species (Tolf *et al.*, 2009a). Genotyping of picornaviruses has been established by use of VP1 sequences (Oberste *et al.*, 1999b; Al-Sunaidi *et al.*, 2007). The 5'UTR targeting real-time PCR is highly sensitive and suitable for screening purposes, but not for genotyping and further

characterisation of LV-positive samples. Two further RT-PCR assays were established to address this challenge. Primers were designed based on all available LV sequences to amplify RT-PCR products from the LV 2A/2B and VP1 regions, respectively. RNA from all available LV strains could be amplified, and these assays could also be successfully applied to wild rodent samples. Using VP1 RT-PCR, only 1 out of 44 samples that was LV positive by 5'UTR RT-PCR was also positive by VP1 RT-PCR, indicating a higher sensitivity of 5'UTR RT-PCR.

RT-PCR assays described here widely expand the spectrum available for LV detection and characterisation. However, for a full characterisation of LV-positive specimens, further tests are needed, such as virus isolation and a broad spectrum of serological assays.

4.1.2 Development and characterisation of murine monoclonal antibodies to LV

MAbs provide a powerful tool for detection and characterisation of viruses. The production and characterisation of murine mAbs specific to LV is described here. A number of 22 mAbs were found to be specific to LV. These mAbs were expanded and further characterised by IIFT, IHC, western immunoblotting and immune precipitation. The potential to inhibit the infection of cell culture with LV was also determined.

Evaluated by IIFT, all 22 mAbs were reactive to LV strains 87-012 and 174F, that constitute the first LV genotype. These data indicate a high antigen cross reactivity among both strains. Such a result is not surprising because of the high amino acid similarity of 99 % in the P1 region between both strains (Johansson *et al.*, 2002). In contrast, only three mAbs (LV-05sA1-D, LV-05sA4-G and LV-05sA4-H) showed also reactivity to LV 145SL (84 % amino acid similarity to 87-012 in P1 region), the only member of the second LV genotype, suggesting the occurrence of common epitopes among the three LV strains recognised by these three mAbs.

Immunohistochemistry is used to stain antigen(s) in tissue sections. Fixation of tissue material is necessary for e.g. preservation of cell structures, but there is also the

difficulty that fixative solutions may change antigenic epitopes (Shi *et al.*, 1997; Ramos-Vara, 2005) making it a higher challenge for mAbs to recognise these epitopes. However, 5 mAbs were identified with positive binding to LV antigen in IHC. All of these 5 mAbs belong to the IgM subclass. A possible reason might be that IgM antibodies have higher avidity but less specificity to the antigen than do IgG antibodies.

Using IIFT and IHC, a potential cross reactivity of the mAbs to other closely related members of the picornaviridae was tested, i.e. the LV strain M1146 (third LV genotype) and the closely HPeV type 1 and 2, respectively. No cross reactivity of mAbs to these viruses was detected. The specificity of mAbs to LV genotypes 1 and 2 without cross reactivity to closely related picornaviruses is important for testing diagnostic samples by immuno assays.

All mAbs failed to react with denatured protein tested by western immunoblotting suggesting the conformational nature of epitopes required for binding to the LV capsid. To determine the target capsid protein(s) of each mAb, an immunoprecipitation of capsid proteins was attempted with mAbs bound to Protein G conjugated magnetic beads. The protein target(s) of 20 mAbs were successfully identified except for subclass IgM mAbs LV-05fB2-Q and LV-06s05b-33 which might be due to the low affinity of IgM antibodies to Protein G. Attempts using Protein L-conjugated beads were not successful either (data not shown). Eight mAbs precipitated VP1 as target protein, two mAbs recognised VP0 and no mAb was specific to VP3. The major antigenic sites in other picornaviruses, e.g. poliovirus and coxsackievirus A9, are located in VP1 (Minor *et al.*, 1986; Pulli *et al.*, 1998). Using the peptide scanning technique and an enzyme immunoassay, respectively, Joki-Korpela *et al.* (2000) identified two antigenic sites in HPeV1, one in VP1 and one in VP0. The latter was shown to be highly conserved among HPeV1 isolates and also closely related to LV (Joki-Korpela *et al.*, 2000). Another study by Tolf *et al.* (2008) describes the characterisation of rabbit polyclonal antibodies to LV capsid proteins. Antibodies against VP1 and VP0 could detect native LV proteins but no native protein was detected by use of an anti-VP3 antibody, suggesting the presence of immunodominant

epitopes in capsid proteins VP1 and VP0, but not in VP3 (Tolf *et al.*, 2008). Immunoprecipitation with 10 mAbs resulted in more than one band after visualising. Four mAbs recognised VP0 and VP3, two mAbs VP0 and VP1 and four mAbs showed reactivity to all three capsid proteins. B-cell epitopes are thought to be conformational (Alho *et al.*, 2003). Considering the three-dimensional structure of picornaviruses, it might be possible that antibodies bind to epitopes that are part of more than one capsid protein. Furthermore, in a study determining the putative common epitope of enteroviruses by sequence-independent single-primer amplification mediated immunoscreening analyses, several clones were identified that were concentrated at the capsid protein junctions covering two proteins (Shin *et al.*, 2003). However, a possible co-precipitation of capsid proteins during immunoprecipitation can not be excluded. Further studies should be undertaken to determine immunogenic epitopes of LV, e.g. by peptide scanning technique or by studying virus neutralisation escape mutants.

Seven mAbs inhibited LV infection to cell culture. Three neutralising mAbs were class IgG and four neutralising mAbs were class IgM antibodies. All three class IgG and one class IgM mAbs had VP1 as target protein. In addition, for two neutralising class IgM mAbs VP0 is involved in binding to the virion. Rabbit antisera were raised against synthetic peptides covering immunodominant sites of HPeV1 in VP1 and VP0, respectively. Both peptides neutralised infectivity of HPeV1 in cell culture (Joki-Korpela *et al.*, 2000). Furthermore, the VP1 protein of poliovirus induces a neutralising antibody response in mice and rabbits (Fiore *et al.*, 1997). Our results are in line with these data.

In conclusion, murine mAbs specific to LV but not to other picornaviruses were produced. These mAbs should prove useful for the development of assays for the specific detection of LV, e.g. in human tissue by IHC. Furthermore, for epidemiological studies an easy-to-perform but specific assay is needed. The cELISA assay described here could be adapted for human sera to elucidate the role of LV in humans since a possible association of LV and human disease has been reported (Niklasson *et al.*, 2007a, 2009a, 2009b; Samsioe *et al.*, 2009). MAbs can also be used

for investigation of LV pathogenesis *in vitro* and *in vivo*. For instance, the mAb treatment of LV infected animal models developing diabetes (Niklasson *et al.*, 2007b; Holmberg *et al.*, 2009) is encouraged. MAbs described here will also help analyse immunodominant regions of the LV capsid and will hence contribute to understand characteristics of parechoviruses that are distinct from other picornaviruses.

4.2 LV presence in rodent species

This thesis demonstrates that three strains of laboratory rats widely used as animal models are infected with Ljungan virus. These strains, along with the previous observation of LV in the BB rat (Niklasson *et al.*, 2007), present a previously unrecognized picture of widespread presence of a pathogenic agent in laboratory rats. The four strains positive for LV encompass a broad range of genetic variation within laboratory rats as a whole (Thomas *et al.*, 2003; Sudo *et al.*, 2007).

Both wild rats and laboratory rats are naturally infected with a number of pathogens. During the period of domestication, many of the original rat stocks harboured different pathogens whose elimination from the host was more and more successful when improvements in sanitation, nutrition and husbandry were made, together with procedures which enable the elimination of pathogens not transmitted in utero (Baker, 1998). Active surveillance of pathogens in breeding facilities led to a decline of microbiological contamination in laboratory animals (Hankenson *et al.*, 2003).

There are several possible explanations as to why a new pathogen, apparently widespread among laboratory rat strains, might only be detected at this time. If the laboratory animal is the natural reservoir for a pathogen it often causes no or minimal disease in the animal. Such a pathogen causing only minor disease will be difficult to diagnose clinically, and will typically also be difficult to cultivate by common isolation techniques, making the chance of detecting such a pathogen low. Additional characteristics of LV biology add to this picture. Data from wild rodents and laboratory mice suggest that Ljungan virus disease outcome is dependent on the stress level of the infected host (Niklasson *et al.*, 2006a; Niklasson *et al.*, 2006b; Samsioe *et*

al., 2006). LV is also difficult to cultivate, making it characteristically difficult to trace and identify. In the present study evidence of Ljungan virus infection in laboratory rats is presented by three independent methods. LV was found in by RT-PCR (LV-specific viral RNA), IHC (LV-specific protein) and IIFT (LV-specific antibody reaction). The low titre of antibodies detected by IIFT found in the present study is consistent with the findings in LV infected wild rodents (personal communication Bo Niklasson).

It has recently been suggested that LV is involved in the pathogenesis of diabetes in the BB rat type 1 diabetes model (Niklasson *et al.*, 2007b). LV causes malformation and perinatal deaths in laboratory mice infected during controlled conditions (Samsioe *et al.*, 2006), and it has also been suggested that LV is a zoonotic pathogen responsible for intrauterine deaths in pregnant women (Niklasson *et al.*, 2007a; Samsioe *et al.*, 2009) and central nervous system malformation in humans (Niklasson *et al.*, 2009).

Additional studies are needed to elucidate the potential role of LV as a pathogen in the BB rat and other rat strains and what impact this pathogen might have on their use as a range of animal models of human disease. The potential role as a human pathogen should also be investigated to reduce the risk of pregnant women working in an animal facility.

LV was first isolated from bank voles in Northern Europe and has later been identified in species from voles and mice in North America and South Europe (Niklasson *et al.*, 1999; Johansson *et al.*, 2003; Tolf *et al.*, 2009a; Hauffe *et al.*, 2010). It was not known whether LV circulated in Germany, and therefore the natural reservoirs of LV and the geographical distribution of LV remained unknown. Rodents and insectivores were trapped at 28 different sites in Germany and analysed for LV presence by RT-PCR.

LV was found in several species of voles and mice, i.e. *Microtus agrestis*, *Microtus arvalis, Myodes glareolus, Apodemus agrarius, Apodemus flavicollis, Apodemus sylvaticus, Micromys minutus, Mus musculus*, *Rattus norvegicus*. These results considerably extend the known host range of LV, including the commensal house mouse and brown rat. No species was significantly more or less LV positive. In addition, no insectivore carried LV. These data suggest that LV is prevalent in many

rodent species to a similar extent, and that the host range is limited to rodents. However, additional studies on other mammals (and possibly also on invertebrates like insects and ticks) are necessary to determine the whole host range of LV. All species found positive for LV are extremely common in Europe and Asia (Mitchell-Jones *et al.*, 1999; IUCN red list of threatened species). Therefore, a wide geographical distribution of LV in these rodent species seems likely. LV has been suggested to play a role in the origin of cyclic rodent population density in northern latitudes (Niklasson *et al.*, 2006b). Such cycles in rodent populations have also been observed in Germany (personal communication Dr. Jens Jacob, Julius Kühn-Institut, Münster, Germany). The influence of LV as a pathogen (apparently abundant in many rodent species) on rodent population dynamics should therefore be elucidated.

In this study, LV was found at different sites of Germany, encompassing the North, South, East, and the West showing that this virus is widely distributed within Germany. The reason for LV-negative sites might be due to the small sample size of these areas.

Although not significant, a trend was found that females are more often LV infected than males. Niklasson *et al.* (2006a) found that LV-infected male laboratory mice develop disease to a higher extent than females. If this is also true for wild rodents, one explanation might be that diseased male rodents are more difficult to catch because of a higher susceptibility to morbidity and mortality, and also to predation. For many viruses, animal infection shows sex differences in disease pathogenesis. One example is coxsackievirus B3 (CVB3). Male mice are more susceptible to CVB3 infection than females accompanied with a strong cytotoxic T-cell response in male mice, but not in female mice (Wong *et al.*, 1977). In addition, coxsackievirus is associated with the development of diabetes mellitus post infection of pancreas Langerhans islet cells. This virus-associated disease occurs predominantly in males (Yoon *et al.*, 1978). In contrast, in lymphocytic choriomeningitis virus (LCMV) infections female mice are more susceptible to morbidity and mortality (Quinn *et al.*, 1993). It has been suggested that female mice more likely develop T_H1 lymphocytes and are more resistant to pathology when T_H1 response is beneficial (CVB3), whereas females develop disease

in infections where T_H1 response is deleterious (LCMV) (Whitacre *et al.*, 1999). Immune response post LV infection should be investigated in future studies. Ecological and/or behavioural rodent biology may be another reason for a sex difference in LV infection.

Sequences from LV 5'UTR were created for LV-positive samples. Sequences close to 4 of the 5 known LV strains were found. A virus-host coevolution, as discussed for hantavirus (Plyusnin and Morzunov, 2001), seems unlikely, since no LV strain corresponded to one rodent species exclusively. Indeed, *Microtus* species and *Myodes glareolus* were only positive for LV 87-012 and/or 174F, but LV 145SL was originally isolated from a bank vole, supporting this idea. Interestingly, LV M1146 sequences were also found in German mice, revealing that the term "American LV" is not correct. LVs should rather be designated by strain or genotype.

Using VP1 RT-PCR one bank vole sample was positive and a 500 nt fragment could be achieved. The best matching sequence were LV M1146 and 65-7855 with 72.3 % aa identity each. Lowest aa identity was 64.5 % between the new sequence and LV strains 87-012 and 174F, respectively. Genetic identity to HPeV1 was only 33.8 % compared to all previously described LVs. In enteroviruses, serotype correlates with genotype and molecular analysis has been established for genotype determination. Strains with no less than 75 % nt and 88 % aa identity of VP1 are considered as one genotype (Oberste *et al.*, 1999b). These criteria were also established for LV (Tolf *et al.*, 2009a). Based on these data, a putative new LV genotype was found extending the information available on LVs. This sequence data should be further analysed to obtain complete sequence information on this strain. This will help to gain insight into LV phylogeny and evolution.

LV was also found in animals from Thailand. This is the first report extending the known geographical distribution of LV also to Asia. These findings support the assumption of a worldwide LV distribution. Three rat species were analysed positive for LV, i.e. *Rattus rattus*, *Bandicota indica* and *Bandicota savilei*, the latter two only distributed in South-East Asia, while the house rat is a commensal animal that is found

worldwide (IUCN red list of threatened species). In addition, the *Mus caroli* species (that is also only present in East Asia) was identified to be a host for LV. The finding of three LV positive species endemic in Asia raises interesting questions about LV evolution. Is there an ancestral rodent species from which LV originated or was LV transmitted from migrating rodents, such as the house rat that originates from Asia? More sequence information from additional LV strains are necessary to address this question as well as the extension of studies on LV prevalence in other continents including more rodent species. Interestingly, one tree shrew species (*Tupaia glis*) was positive for LV. Again, additional studies should clarify whether species from the order *Scandentia* are reservoir hosts for LV or if this finding is a result of a possible spill-over infection.

In this study, rats were found to be LV carriers from both the laboratory and the wild and also from different areas in the world. Rats are live close to the human environment with several millions of individuals. LV is suggested to be transmitted by the faecal-oral route (Niklasson *et al.*, 1999). Is the rat one major reservoir for LV, and is it responsible for transmission to humans?

4.3 LV pathogenesis

It has been reported previously that LV infection is associated with diabetes in LV-infected laboratory mice and in wild rodents (Niklasson *et al.*, 2006a, b). This led to the hypothesis that LV persistence might contribute to the outcome of diabetes. Thus, the abundance of LV genome in several organs obtained from LV-infected CD-1 laboratory mice was investigated in the course of time post infection. All investigated organs were found positive for LV throughout the tested period, indicating a persistent systemic infection. One possible explanation as to why all organs were found to be LV positive is that viruses often persist in immune cells, i.e. lymphocytes and/or monocytes (Oldstone, 1991). The highest LV genome copy numbers during the acute infection were present in the brain. In addition, the amount of LV genome copy numbers and infectious virus particles increased over the first 10 dpi. This is

concordant with the clinical picture of encephalitis. Thus, LV might have a tropism for the nervous system immediately post infection. In addition, LV genome copy numbers also increased in heart tissue during acute infection. This indicates a replicating LV infection also in this organ which might lead to clinical signs of myocarditis as described by Niklasson *et al.* (2006a, b). The transition from the acute to the persistent infection occurs between day 17 pi and day 56 pi because mice surviving acute clinical signs of disease recovered. In addition, a decline in the viral load could be detected in all organs until day 56 pi. By day 56 pi the virus load rose slightly and remained at a more or less constant level by day 98, with slight variation among individuals. Because CD-1 mice are an outbred strain, variation in LV susceptibility among several individuals could be due to genetic variability. The increase in the LV load after day 56 pi might be the result of behavioural stress (post puberty of mice). It has recently been demonstrated that a combination of LV infection and environmental stress may cause diabetes in CD-1 laboratory mice (Niklasson *et al.*, 2006b).

Furthermore, 13 wild bank voles were investigated for the presence of LV and nine of them were found positive for LV in different organs. These results indicate a systemic LV infection of wild bank voles, too. While there is indeed no direct proof of a persistent LV infection in wild bank voles, the detected LV genome copy numbers are only somewhat below the detected LV genome copies of LV-infected laboratory mice during persistent infection. All investigated wild bank voles were freeranging, independent individuals at the time of trapping and there is no evidence of the timepoint in life when these animals became infected with LV. It was recently shown that adult laboratory mice are less susceptible for LV infection than suckling mice or adolescents (Niklasson *et al.*, 2006a). Furthermore, the voles were trapped during a peak of population densities which occurs every three to four years in Northern Scandinavian latitudes (Hörnfeldt *et al.*, 1986; Hörnfeldt, 1994, 2004; Stenseth, 1999). A large fraction of bank voles trapped during a peak density have diabetes (Niklasson *et al.*, 2006a). High population densities in bank voles are thought to contribute to stress directly or indirectly, by increasing predator numbers and predation pressure, resource shortage or prevalence of other pathogens (Niklasson *et al.*, 2006a). LV

infection in combination with stress could be shown to be essential for the outcome of diabetes in the laboratory (Niklasson *et al.*, 2006b). Due to the fact that the vole samples were obtained from a frozen sample bank it could not be investigated whether the analysed animals had diabetes. However, part of the reason for the high number of animals positive for LV might be the time of trapping because the rate of animals positive for LV at non-peaks is lower than that found in this study (preliminary unpublished results).

In summary, LV RNA persists in infected CD-1 laboratory mice. LV causes a systemic infection that leads to diabetes later in life. This leads to the suggestion that LV persistence might contribute to disease onset because the findings match the previous results that LV, in combination with environmental factors, is the causative agent of disease in both wild bank voles and laboratory mice.

Furthermore, this study provides an animal model to study the mechanism(s) of LV persistence *in vivo*. Moreover, RT-PCR data from LV-infected bank voles will aid future investigations on the prevalence of LV in wild rodents in combination with signs of disease, temporal variations and LV genotype circulation in various rodent species.

Green monkey kidney cells (GMK) and BHK-21 cells, respectively, were found to be susceptible for LV infection (Niklasson *et al.*, 1999; Johansson *et al.*, 2004). To compare LV infection in Vero-B4 cells (that also originate from green monkey kidney) and BHK-21 cells, LV-infected cells were analysed for production of infectious particles, LV protein and LV RNA. In both cell lines, LV protein and LV RNA were produced to a similar extent. There was an increase of LV titre in Vero-B4 cells, correlating with the increase in LV RNA and protein, respectively. In contrast, only low levels of virus titres were produced by BHK-21 cells, suggesting that Vero-B4 cells are permissive for LV infection, while LV infection in BHK-21 cells is restricted. The high increase of virus titre correlated well with increasing CPE of Vero-B4 cells over time, whereas no CPE was visible for LV-infected BHK-21 cells. A number of RNA viruses including influenza virus (Hinshaw *et al.*, 1994), sindbis virus (Levine *et*

al., 1993), and Theiler's murine encephalomyelitis virus (Jelachich and Lipton, 1996) trigger apoptosis as a result of productive infection. These viruses use the cellular apoptotic pathway for cell egress resulting in CPE. Other viruses such as poxviruses (Ink *et al.*, 1995) and Epstein-Barr virus (Gregory *et al.*, 1991) have established mechanisms inhibiting apoptosis to maintain their infection.

It was recently shown that lytic LV variants may evolve during continuing cell culture passages with mutations over the whole virus genome of the cell culture-adapted LV variant (Ekström *et al.*, 2007a). Own observations are in line with these findings. Original virus stocks isolated from rodents in SMB showed no or minor CPE 14 dpi. In contrast, when LV was passaged more than 30 times in Vero-B4 cells a CPE was observed a few hours post infection resulting in high virus titres (data not shown). A study by Tolf *et al.* (2009b) showed that lytic LV infection of GMK cells is associated with three significant aa substitutions in the capsid proteins VP0 and VP1 and that lytic replication is associated with an apoptotic response in GMK cells.

To determine whether lytic LV production in Vero-B4 cells is a result of apoptosis, characteristic features of apoptosis were analysed for both Vero-B4 and BHK-21 cells. Internucleosomal DNA degradation, chromatin condensation, and active caspase-3 were only detected in lytic Vero-B4 cells post LV infection. LV was passaged six times in either Vero-B4 or BHK-21 cells before infection of Vero-B4 and BHK-21 cells, respectively. Although passaged in the respective cell line before infection, cell lysis was only observed in Vero-B4 cells indicating that LV adaptation to the host cell is only one of the events contributing to cell lysis. It is suggested that tissue type or host species are other important determinants for lytic versus non-lytic infection. The observations presented here may reflect events during LV life cycle *in vivo*. Acutely infected laboratory mice show signs of encephalitis and myocarditis (Niklasson *et al.*, 2006b; this thesis). The infected animals have pathological lesions in the brain and heart (data not shown). Increasing LV RNA copy numbers were also found in both organs during acute infection, in addition to increasing LV titres in the brain. Furthermore, LV infection leads to a full destruction of pancreas beta cells in both wild bank voles and laboratory mice infected with LV (Niklasson *et al.*, 2003a, b).

These pathological findings could be a result of apoptosis, such as in coxsackievirus-infected heart and CNS, respectively (Gebhard *et al.*, 1998; Feuer *et al.*, 2003). Non-lytic LV infection, however, could be the result of apoptosis-inhibiting effects, that are varying in different hosts or tissues and are induced by either virus or cell.

Further studies should clarify the mechanisms of both LV persistence and LV apoptosis. This knowledge would help understand LV pathogenesis and could then be applied as a model system for investigation of human disease. Furthermore, to know the pathogenetic mechanisms of a very abundant pathogen will be helpful to learn how this pathogen is maintained in its reservoirs.

5 References

Abed, Y., and G. Boivin. 2006. Human parechovirus types 1, 2 and 3 infections in Canada. Emerg Infect Dis **12:**969-75.

Adachi, K., A. Muraishi, Y. Seki, K. Yamaki, and M. Yoshizuka. 1996. Coxsackievirus B3 genomes detected by polymerase chain reaction: evidence of latent persistency in the myocardium in experimental murine myocarditis. Histol Histopathol **11:**587-96.

Agirre, A., A. Barco, L. Carrasco, and J. L. Nieva. 2002. Viroporin-mediated membrane permeabilization. Pore formation by nonstructural poliovirus 2B protein. J Biol Chem **277:**40434-41.

Agol, V. I., G. A. Belov, K. Bienz, D. Egger, M. S. Kolesnikova, L. I. Romanova, L. V. Sladkova, and E. A. Tolskaya. 2000. Competing death programs in poliovirus-infected cells: commitment switch in the middle of the infectious cycle. J Virol **74:**5534-41.

Aldabe, R., and L. Carrasco. 1995. Induction of membrane proliferation by poliovirus proteins 2C and 2BC. Biochem Biophys Res Commun **206:**64-76.

Aldabe, R., A. Barco, and L. Carrasco. 1996. Membrane permeabilization by poliovirus proteins 2B and 2BC. J Biol Chem **271:**23134-7.

Alho, A., J. Marttila, J. Ilonen, and T. Hyypiä. 2003. Diagnostic potential of parechovirus capsid proteins. J Clin Microbiol **41:**2294-9.

Al-Sunaidi, M., C. H. Williams, P. J. Hughes, D. P. Schnurr, and G. Stanway. 2007. Analysis of a new human parechovirus allows the definition of parechovirus types and the identification of RNA structural domains. J Virol **81:**1013-21.

Bachrach, H. L. 1968. Foot-and-mouth disease. Annu Rev Microbiol **22:**201-44.

Baker, D. G. 1998. Natural pathogens of laboratory mice, rats, and rabbits and their effects on research. Clin Microbiol Rev **11:**231-66.

Banerjee, R., and A. Dasgupta. 2001. Interaction of picornavirus 2C polypeptide with the viral negative-strand RNA. J Gen Virol **82:**2621-7.

Banerjee, R., A. Echeverri, and A. Dasgupta. 1997. Poliovirus-encoded 2C polypeptide specifically binds to the 3'-terminal sequences of viral negative-strand RNA. J Virol **71:**9570-8.

Banerjee, R., W. Tsai, W. Kim, and A. Dasgupta. 2001. Interaction of poliovirus-encoded 2C/2BC polypeptides with the 3' terminus negative-strand cloverleaf requires an intact stem-loop b. Virology **280:**41-51.

Baumgarte, S., L. K. de Souza Luna, K. Grywna, M. Panning, J. F. Drexler, C. Karsten, H. I. Huppertz, and C. Drosten. 2008. Prevalence, types, and RNA concentrations of human parechoviruses, including a sixth parechovirus type, in stool samples from patients with acute enteritis. J Clin Microbiol **46:**242-8.

Beard, C. W., and P. W. Mason. 2000. Genetic determinants of altered virulence of Taiwanese foot-and-mouth disease virus. J Virol **74:**987-91.

Belnap, D. M., D. J. Filman, B. L. Trus, N. Cheng, F. P. Booy, J. F. Conway, S. Curry, C. N. Hiremath, S. K. Tsang, A. C. Steven, and J. M. Hogle. 2000. Molecular tectonic model of virus structural transitions: the putative cell entry states of poliovirus. J Virol **74:**1342-54.

Benschop, K. S., J. Schinkel, M. E. Luken, P. J. van den Broek, M. F. Beersma, N. Menelik, H. W. van Eijk, H. L. Zaaijer, C. M. VandenBroucke-Grauls, M. G. Beld, and K. C. Wolthers. 2006. Fourth human parechovirus serotype. Emerg Infect Dis **12:**1572-5.

Benschop, K., X. Thomas, C. Serpenti, R. Molenkamp, and K. Wolthers. 2008. High prevalence of human Parechovirus (HPeV) genotypes in the Amsterdam region and identification of specific HPeV variants by direct genotyping of stool samples. J Clin Microbiol **46:**3965-70.

Benschop, K. S., M. de Vries, R. P. Minnaar, G. Stanway, L. van der Hoek, K. C. Wolthers, and P. Simmonds. 2010. Comprehensive full-length sequence analyses of human parechoviruses: diversity and recombination. J Gen Virol **91:**145-54.

Berkovich, S., and J. Pangan. 1968. Recoveries of virus from premature infants during outbreaks of respiratory disease: the relation of ECHO virus type 22 to disease of the upper and lower respiratory tract in the premature infant. Bull N Y Acad Med **44:**377-87.

Bernstein, H. D., N. Sonenberg, and D. Baltimore. 1985. Poliovirus mutant that does not selectively inhibit host cell protein synthesis. Mol Cell Biol **5:**2913-23.

Bernstein, H. D., P. Sarnow, and D. Baltimore. 1986. Genetic complementation among poliovirus mutants derived from an infectious cDNA clone. J Virol **60:**1040-9.

Bienz, K., D. Egger, and L. Pasamontes. 1987. Association of polioviral proteins of the P2 genomic region with the viral replication complex and virus-induced membrane synthesis as visualized by electron microscopic immunocytochemistry and autoradiography. Virology **160:**220-6.

Blixt, M., B. Niklasson, and S. Sandler. 2007. Characterization of beta-cell function of pancreatic islets isolated from bank voles developing glucose intolerance/diabetes: an animal model showing features of both type 1 and type 2 diabetes mellitus, and a possible role of the Ljungan virus. Gen Comp Endocrinol **154:**41-7.

Boivin, G., Y. Abed, and F. D. Boucher. 2005. Human parechovirus 3 and neonatal infections. Emerg Infect Dis **11:**103-5.

Boonyakiat, Y., P. J. Hughes, F. Ghazi, and G. Stanway. 2001. Arginine-glycine-aspartic acid motif is critical for human parechovirus 1 entry. J Virol **75:**10000-4.

Calvert, J., T. Chieochansin, K. S. Benschop, E. C. McWilliam Leitch, J. F. Drexler, K. Grywna, H. da Costa Ribeiro, Jr., C. Drosten, H. Harvala, Y. Poovorawan, K. C. Wolthers, and P. Simmonds. 2010. Recombination dynamics of human parechoviruses: investigation of type-specific differences in frequency and epidemiological correlates. J Gen Virol **91:**1229-38.

Campanella, M., A. S. de Jong, K. W. Lanke, W. J. Melchers, P. H. Willems, P. Pinton, R. Rizzuto, and F. J. van Kuppeveld. 2004. The coxsackievirus 2B protein suppresses apoptotic host cell responses by manipulating intracellular Ca2+ homeostasis. J Biol Chem **279:**18440-50.

Carrillo, E. C., C. Giachetti, and R. H. Campos. 1984. Effect of lysosomotropic agents on the foot-and-mouth disease virus replication. Virology **135:**542-5.

Cavanagh, R. D., X. Lambin, T. Ergon, M. Bennett, I. M. Graham, D. van Soolingen, and M. Begon. 2004. Disease dynamics in cyclic populations of field voles (Microtus agrestis): cowpox virus and vole tuberculosis (Mycobacterium microti). Proc Biol Sci **271:**859-67.

Chang, K. H., C. Day, J. Walker, T. Hyypiä, and G. Stanway. 1992. The nucleotide sequences of wild-type coxsackievirus A9 strains imply that an RGD motif in VP1 is functionally significant. J Gen Virol **73 (Pt 3):**621-6.

Chen, B. C., M. F. Cheng, T. S. Huang, Y. C. Liu, C. W. Tang, C. S. Chen, and Y. S. Chen. 2009. Detection and identification of human parechoviruses from clinical specimens. Diagn Microbiol Infect Dis **65:**254-60.

Chomczynski, P., and N. Sacchi. 1987. Single-step method of RNA isolation by acid guanidinium thiocyanate-phenol-chloroform extraction. Anal Biochem **162:**156-9.

Colbere-Garapin, F., G. Duncan, N. Pavio, I. Pelletier, and I. Petit. 1998. An approach to understanding the mechanisms of poliovirus persistence in infected cells of neural or non-neural origin. Clin Diagn Virol **9:**107-13.

Coller, B. A., N. M. Chapman, M. A. Beck, M. A. Pallansch, C. J. Gauntt, and S. M. Tracy. 1990. Echovirus 22 is an atypical enterovirus. J Virol **64:**2692-701.

de Jong, A. S., E. Wessels, H. B. Dijkman, J. M. Galama, W. J. Melchers, P. H. Willems, and F. J. van Kuppeveld. 2003. Determinants for membrane association and permeabilization of the coxsackievirus 2B protein and the identification of the Golgi complex as the target organelle. J Biol Chem **278:**1012-21.

de Jong, A. S., W. J. Melchers, D. H. Glaudemans, P. H. Willems, and F. J. van Kuppeveld. 2004. Mutational analysis of different regions in the coxsackievirus 2B protein: requirements for homo-multimerization, membrane permeabilization, subcellular localization, and virus replication. J Biol Chem **279:**19924-35.

de Jong, A. S., H. J. Visch, F. de Mattia, M. M. van Dommelen, H. G. Swarts, T. Luyten, G. Callewaert, W. J. Melchers, P. H. Willems, and F. J. van Kuppeveld. 2006. The coxsackievirus 2B protein increases efflux of ions from the endoplasmic reticulum and Golgi, thereby inhibiting protein trafficking through the Golgi. J Biol Chem **281:**14144-50.

de Jong, A. S., F. de Mattia, M. M. Van Dommelen, K. Lanke, W. J. Melchers, P. H. Willems, and F. J. van Kuppeveld. 2008. Functional analysis of picornavirus 2B proteins: effects on calcium homeostasis and intracellular protein trafficking. J Virol **82:**3782-90.

Deitz, S. B., D. A. Dodd, S. Cooper, P. Parham, and K. Kirkegaard. 2000. MHC I-dependent antigen presentation is inhibited by poliovirus protein 3A. Proc Natl Acad Sci U S A **97:**13790-5.

Dodd, D. A., T. H. Giddings, Jr., and K. Kirkegaard. 2001. Poliovirus 3A protein limits interleukin-6 (IL-6), IL-8, and beta interferon secretion during viral infection. J Virol **75:**8158-65.

Doedens, J. R., and K. Kirkegaard. 1995. Inhibition of cellular protein secretion by poliovirus proteins 2B and 3A. Embo J **14:**894-907.

Doherty, M., D. Todd, N. McFerran, and E. M. Hoey. 1999. Sequence analysis of a porcine enterovirus serotype 1 isolate: relationships with other picornaviruses. J Gen Virol **80 (Pt 8):**1929-41.

Donnelly, M. L., D. Gani, M. Flint, S. Monaghan, and M. D. Ryan. 1997. The cleavage activities of aphthovirus and cardiovirus 2A proteins. J Gen Virol **78 (Pt 1):**13-21.

Donoso Mantke, O., R. Kallies, B. Niklasson, A. Nitsche, and M. Niedrig. 2007. A new quantitative real-time reverse transcriptase PCR assay and melting curve analysis for detection and genotyping of Ljungan virus strains. J Virol Methods **141:**71-7.

Dorn-Beineke, A., S. Nittka, and M. Neumaier. 2007. Technology and Production of Murine Monoclonal and Recombinant Antibodies and Antibody Fragments p. 93-121. *In* R. Pörtner (ed.), Animal Cell Biotechnology, Methods and Protocols, vol. 24. Humana Press, Totowa.

Drexler, J. F., K. Grywna, A. Stocker, P. S. Almeida, T. C. Medrado-Ribeiro, M. Eschbach-Bludau, N. Petersen, H. da Costa-Ribeiro-Jr, and C. Drosten. 2009. Novel human parechovirus from Brazil. Emerg Infect Dis **15:**310-3.

Drosten, C., S. Gottig, S. Schilling, M. Asper, M. Panning, H. Schmitz, and S. Gunther. 2002. Rapid detection and quantification of RNA of Ebola and Marburg viruses, Lassa virus, Crimean-Congo hemorrhagic fever virus, Rift Valley fever

virus, dengue virus, and yellow fever virus by real-time reverse transcription-PCR. J Clin Microbiol **40:**2323-30.

Echeverri, A. C., and A. Dasgupta. 1995. Amino terminal regions of poliovirus 2C protein mediate membrane binding. Virology **208:**540-53.

Ekström, J. O., C. Tolf, C. Fahlgren, E. S. Johansson, G. Arbrandt, B. Niklasson, K. A. Edman, and A. M. Lindberg. 2007a. Replication of Ljungan virus in cell culture: the genomic 5'-end, infectious cDNA clones and host cell response to viral infections. Virus Res **130:**129-39.

Ekström, J. O., C. Tolf, K. A. Edman, and A. M. Lindberg. 2007b. Physicochemical properties of the Ljungan virus prototype virion in different environments: inactivated by heat but resistant to acidic pH, detergents and non-physiological environments such as Virkon-containing solutions. Microbiol Immunol **51:**841-50.

Evans, D. J., and J. W. Almond. 1998. Cell receptors for picornaviruses as determinants of cell tropism and pathogenesis. Trends Microbiol **6:**198-202.

Evans, D. M., G. Dunn, P. D. Minor, G. C. Schild, A. J. Cann, G. Stanway, J. W. Almond, K. Currey, and J. V. Maizel, Jr. 1985. Increased neurovirulence associated with a single nucleotide change in a noncoding region of the Sabin type 3 poliovaccine genome. Nature **314:**548-50.

Faria, N. R., M. de Vries, F. J. van Hemert, K. Benschop, and L. van der Hoek. 2009. Rooting human parechovirus evolution in time. BMC Evol Biol **9:**164.

Felsenstein, J. 1985. Confidence limits on phylogenies: An approach using the bootstrap. Evolution **39:**783-791.

Feuer, R., I. Mena, R. Pagarigan, M. K. Slifka, and J. L. Whitton. 2002. Cell cycle status affects coxsackievirus replication, persistence, and reactivation in vitro. J Virol **76:**4430-40.

Feuer, R., I. Mena, R. R. Pagarigan, S. Harkins, D. E. Hassett, and J. L. Whitton. 2003. Coxsackievirus B3 and the neonatal CNS: the roles of stem cells, developing neurons, and apoptosis in infection, viral dissemination, and disease. Am J Pathol **163:**1379-93.

Figueroa, J. P., D. Ashley, D. King, and B. Hull. 1989. An outbreak of acute flaccid paralysis in Jamaica associated with echovirus type 22. J Med Virol **29:**315-9.

Finney, D. J. 1978. Statistical methods in biological assay, vol. 3rd edition, London.

Fiore, L., B. Ridolfi, D. Genovese, G. Buttinelli, S. Lucioli, A. Lahm, and F. M. Ruggeri. 1997. Poliovirus Sabin type 1 neutralization epitopes recognized by immunoglobulin A monoclonal antibodies. J Virol **71:**6905-12.

Flint, J. S., L. W. Enquist, V. R. Racaniello, and A. M. Skalka. 2004. Principles of Virology: Molecular Biology, Pathogenesis, and Control of Animal Viruses. ASM Press, Washingto, DC.

Fox, G., N. R. Parry, P. V. Barnett, B. McGinn, D. J. Rowlands, and F. Brown. 1989. The cell attachment site on foot-and-mouth disease virus includes the amino acid sequence RGD (arginine-glycine-aspartic acid). J Gen Virol **70 (Pt 3):**625-37.

Freimanis, T., K. E. Heller, B. Schonecker, and M. Bildsoe. 2003. Effects of postnatal stress on the development of type 1 diabetes in bank voles (Clethrionomys glareolus). Int J Exp Diabesity Res **4:**21-5.

Fricks, C. E., and J. M. Hogle. 1990. Cell-induced conformational change in poliovirus: externalization of the amino terminus of VP1 is responsible for liposome binding. J Virol **64:**1934-45.

Fujinami, R. S., M. G. von Herrath, U. Christen, and J. L. Whitton. 2006. Molecular mimicry, bystander activation, or viral persistence: infections and autoimmune disease. Clin Microbiol Rev **19:**80-94.

Fujita, K., S. S. Krishnakumar, D. Franco, A. V. Paul, E. London, and E. Wimmer. 2007. Membrane topography of the hydrophobic anchor sequence of poliovirus 3A and 3AB proteins and the functional effect of 3A/3AB membrane association upon RNA replication. Biochemistry **46:**5185-99.

Gamarnik, A. V., and R. Andino. 2000. Interactions of viral protein 3CD and poly(rC) binding protein with the 5' untranslated region of the poliovirus genome. J Virol **74:**2219-26.

Gebhard, J. R., C. M. Perry, S. Harkins, T. Lane, I. Mena, V. C. Asensio, I. L. Campbell, and J. L. Whitton. 1998. Coxsackievirus B3-induced myocarditis: perforin exacerbates disease, but plays no detectable role in virus clearance. Am J Pathol **153:**417-28.

Gern, J. E. 2010. The ABCs of rhinoviruses, wheezing, and asthma. J Virol **84:**7418-26.

Ghazi, F., P. J. Hughes, T. Hyypiä, and G. Stanway. 1998. Molecular analysis of human parechovirus type 2 (formerly echovirus 23). J Gen Virol **79 (Pt 11):**2641-50.

Giachetti, C., S. S. Hwang, and B. L. Semler. 1992. cis-acting lesions targeted to the hydrophobic domain of a poliovirus membrane protein involved in RNA replication. J Virol **66:**6045-57.

Gilg, O., I. Hanski, and B. Sittler. 2003. Cyclic dynamics in a simple vertebrate predator-prey community. Science **302:**866-8.

Girard, S., T. Couderc, J. Destombes, D. Thiesson, F. Delpeyroux, and B. Blondel. 1999. Poliovirus induces apoptosis in the mouse central nervous system. J Virol **73:**6066-72.

Girard, S., A. S. Gosselin, I. Pelletier, F. Colbere-Garapin, T. Couderc, and B. Blondel. 2002. Restriction of poliovirus RNA replication in persistently infected nerve cells. J Gen Virol **83:**1087-93.

Gorbalenya, A. E., V. M. Blinov, A. P. Donchenko, and E. V. Koonin. 1989. An NTP-binding motif is the most conserved sequence in a highly diverged monophyletic group of proteins involved in positive strand RNA viral replication. J Mol Evol **28:**256-68.

Gregory, C. D., C. Dive, S. Henderson, C. A. Smith, G. T. Williams, J. Gordon, and A. B. Rickinson. 1991. Activation of Epstein-Barr virus latent genes protects human B cells from death by apoptosis. Nature **349:**612-4.

Hall, T. A. 1999. BioEdit: a user-friendly biological sequence alignment editor and analysis program for Windows 95/98/NT. Oxford University Press Nucleic Acids Symposium Series **41:**95-98.

Hankenson, F. C., N. A. Johnston, B. J. Weigler, and R. F. Di Giacomo. 2003. Zoonoses of occupational health importance in contemporary laboratory animal research. Comp Med **53:**579-601.

Hanski, I., and H. Henttonen. 1996. Predation on competing rodent species: a simple explanation of complex patterns. J. Anim. Ecol. **65:**220–232.

Hanski, I., H. Henttonen, E. Korpimäki, L. Oksanen, and P. Turchin. 2001. Small-rodent dynamics and predation. Ecology **82:**1505–1520.

Hansson, L., and H. Henttonen. 1985. Gradients in density variations of small rodents: the importance of latitude and snow cover. Oecologia **67:**394–402.

Harris, J. R., and V. R. Racaniello. 2005. Amino acid changes in proteins 2B and 3A mediate rhinovirus type 39 growth in mouse cells. J Virol **79:**5363-73.

Harris, K. S., S. R. Reddigari, M. J. Nicklin, T. Hammerle, and E. Wimmer. 1992. Purification and characterization of poliovirus polypeptide 3CD, a proteinase and a precursor for RNA polymerase. J Virol **66:**7481-9.

Harris, K. S., W. Xiang, L. Alexander, W. S. Lane, A. V. Paul, and E. Wimmer. 1994. Interaction of poliovirus polypeptide 3CDpro with the 5' and 3' termini of the poliovirus genome. Identification of viral and cellular cofactors needed for efficient binding. J Biol Chem **269:**27004-27014.

Harvala, H., I. Robertson, T. Chieochansin, E. C. McWilliam Leitch, K. Templeton, and P. Simmonds. 2009. Specific association of human parechovirus type 3 with

sepsis and fever in young infants, as identified by direct typing of cerebrospinal fluid samples. J Infect Dis **199:**1753-60.

Hauffe, H. C., B. Niklasson, T. Olsson, A. Bianchi, A. Rizzoli, and W. Klitz. 2010. Ljungan virus detected in bank voles (Myodes glareolus) and yellow-necked mice (Apodemus flavicollis) from Northern Italy. J Wildl Dis **46:**262-6.

Hay, S., and G. Kannourakis. 2002. A time to kill: viral manipulation of the cell death program. J Gen Virol **83:**1547-64.

Hinshaw, V. S., C. W. Olsen, N. Dybdahl-Sissoko, and D. Evans. 1994. Apoptosis: a mechanism of cell killing by influenza A and B viruses. J Virol **68:**3667-73.

Holmberg, R., W. Klitz, M. Blixt, P. O. Berggren, L. Juntti-Berggren, and B. Niklasson. 2009. Antiviral treatments reduce severity of diabetes in Ljungan virus-infected CD-1 mice and delay onset in diabetes-prone BB rats. Microbiol Immunol **53:**567-72.

Hope, D. A., S. E. Diamond, and K. Kirkegaard. 1997. Genetic dissection of interaction between poliovirus 3D polymerase and viral protein 3AB. J Virol **71:**9490-8.

Hörnfeldt, B., O. Löfgren, and B.-G. Carlsson. 1986. Cycles in voles and small game in relation to variations in plant production indices in northern Sweden. Oecologia **68**.

Hörnfeldt, B. 1994. Delayed density dependence as a determinat of vole cycles. Ecology **75:**791-806.

Hörnfeldt, B. 2004. Long-term decline in numbers of cyclic voles in boreal Sweden: analysis and presentation of hypothesis. Oikos **107:**376-392.

Hughes, P. J., and G. Stanway. 2000. The 2A proteins of three diverse picornaviruses are related to each other and to the H-rev107 family of proteins involved in the control of cell proliferation. J Gen Virol **81:**201-7.

Hyypiä, T., C. Horsnell, M. Maaronen, M. Khan, N. Kalkkinen, P. Auvinen, L. Kinnunen, and G. Stanway. 1992. A distinct picornavirus group identified by sequence analysis. Proc Natl Acad Sci U S A **89:**8847-51.

Ink, B. S., C. S. Gilbert, and G. I. Evan. 1995. Delay of vaccinia virus-induced apoptosis in nonpermissive Chinese hamster ovary cells by the cowpox virus CHOhr and adenovirus E1B 19K genes. J Virol **69:**661-8.

Ito, M., T. Yamashita, H. Tsuzuki, N. Takeda, and K. Sakae. 2004. Isolation and identification of a novel human parechovirus. J Gen Virol **85:**391-8.

Jamison, R. M. 1974. An electron microscopic study of the intracellular development of echovirus 22. Arch Gesamte Virusforsch **44:**184-94.

Jaspert, R., T. Geske, A. Teichmann, Y. M. Kassner, K. Kretzschmar, and J. L'Age-Stehr. 1995. Laboratory scale production of monoclonal antibodies in a tumbling chamber. J Immunol Methods **178:**77-87.

Jelachich, M. L., and H. L. Lipton. 1996. Theiler's murine encephalomyelitis virus kills restrictive but not permissive cells by apoptosis. J Virol **70:**6856-61.

Jia, X. Y., D. F. Summers, and E. Ehrenfeld. 1993. Primary cleavage of the HAV capsid protein precursor in the middle of the proposed 2A coding region. Virology **193:**515-9.

Johansson, S., B. Niklasson, J. Maizel, A. E. Gorbalenya, and A. M. Lindberg. 2002. Molecular analysis of three Ljungan virus isolates reveals a new, close-to-root lineage of the Picornaviridae with a cluster of two unrelated 2A proteins. J Virol **76:**8920-30.

Johansson, E. S., B. Niklasson, R. B. Tesh, D. R. Shafren, A. P. Travassos da Rosa, and A. M. Lindberg. 2003. Molecular characterization of M1146, an American isolate of Ljungan virus (LV) reveals the presence of a new LV genotype. J Gen Virol **84:**837-44.

Johansson, E. S., J. O. Ekström, D. R. Shafren, G. Frisk, T. Hyypiä, K. Edman, and A. M. Lindberg. 2004. Cell culture propagation and biochemical analysis of the Ljungan virus prototype strain. Biochem Biophys Res Commun **317:**1023-9.

Johnson, H. N. 1965. Diseases derived from wildlife. Calif Health **23:**35-39.

Joki-Korpela, P., and T. Hyypiä. 1998. Diagnosis and epidemiology of echovirus 22 infections. Clin Infect Dis **27:**129-36.

Joki-Korpela, P., M. Roivainen, H. Lankinen, T. Poyry, and T. Hyypiä. 2000. Antigenic properties of human parechovirus 1. J Gen Virol **81:**1709-18.

Joki-Korpela, P., V. Marjomaki, C. Krogerus, J. Heino, and T. Hyypiä. 2001. Entry of human parechovirus 1. J Virol **75:**1958-67.

Jore, J., B. De Geus, R. J. Jackson, P. H. Pouwels, and B. E. Enger-Valk. 1988. Poliovirus protein 3CD is the active protease for processing of the precursor protein P1 in vitro. J Gen Virol **69 (Pt 7):**1627-36.

Kim, M. C., Y. K. Kwon, S. J. Joh, A. M. Lindberg, J. H. Kwon, J. H. Kim, and S. J. Kim. 2006. Molecular analysis of duck hepatitis virus type 1 reveals a novel lineage close to the genus Parechovirus in the family Picornaviridae. J Gen Virol **87:**3307-16.

Klingel, K., C. Hohenadl, A. Canu, M. Albrecht, M. Seemann, G. Mall, and R. Kandolf. 1992. Ongoing enterovirus-induced myocarditis is associated with persistent heart muscle infection: quantitative analysis of virus replication, tissue damage, and inflammation. Proc Natl Acad Sci U S A **89:**314-8.

Kohler, G., and C. Milstein. 1975. Continuous cultures of fused cells secreting antibody of predefined specificity. Nature **256:**495-7.

Koskiniemi, M., R. Paetau, and K. Linnavuori. 1989. Severe encephalitis associated with disseminated echovirus 22 infection. Scand J Infect Dis **21:**463-6.

Krogerus, C., D. Egger, O. Samuilova, T. Hyypiä, and K. Bienz. 2003. Replication complex of human parechovirus 1. J Virol **77:**8512-23.

Kusov, Y. Y., C. Probst, M. Jecht, P. D. Jost, and V. Gauss-Muller. 1998. Membrane association and RNA binding of recombinant hepatitis A virus protein 2C. Arch Virol **143:**931-44.

Lama, J., M. A. Sanz, and L. Carrasco. 1998. Genetic analysis of poliovirus protein 3A: characterization of a non-cytopathic mutant virus defective in killing Vero cells. J Gen Virol **79 (Pt 8):**1911-21.

Lambert, J. F., B. O. Benoit, G. A. Colvin, J. Carlson, Y. Delville, and P. J. Quesenberry. 2000. Quick sex determination of mouse fetuses. J Neurosci Methods **95:**127-32.

Le Gall, O., P. Christian, C. M. Fauquet, A. M. King, N. J. Knowles, N. Nakashima, G. Stanway, and A. E. Gorbalenya. 2008. Picornavirales, a proposed order of positive-sense single-stranded RNA viruses with a pseudo-T = 3 virion architecture. Arch Virol **153:**715-27.

Lee, E. S., J. Jiang, G. C. Sund, W. T. Simonson, J. Graham, G. Dietsch, B. Schimpf, S. Bieg, G. Peterman, and A. Lernmark. 1999. Recombinant human platelet-activating factor acetylhydrolase reduces the frequency of diabetes in the diabetes-prone BB rat. Diabetes **48:**43-9.

Legay, V., J. J. Chomel, E. Fernandez, B. Lina, M. Aymard, and S. Khalfan. 2002. Encephalomyelitis due to human parechovirus type 1. J Clin Virol **25:**193-5.

Levine, B., Q. Huang, J. T. Isaacs, J. C. Reed, D. E. Griffin, and J. M. Hardwick. 1993. Conversion of lytic to persistent alphavirus infection by the bcl-2 cellular oncogene. Nature **361:**739-42.

Levorson, R. E., B. A. Jantausch, B. L. Wiedermann, H. M. Spiegel, and J. M. Campos. 2009. Human parechovirus-3 infection: emerging pathogen in neonatal sepsis. Pediatr Infect Dis J **28:**545-7.

Li, L., J. Victoria, A. Kapoor, A. Naeem, S. Shaukat, S. Sharif, M. M. Alam, M. Angez, S. Z. Zaidi, and E. Delwart. 2009. Genomic characterization of novel human parechovirus type. Emerg Infect Dis **15:**288-91.

Lindberg, A. M., and S. Johansson. 2002. Phylogenetic analysis of Ljungan virus and A-2 plaque virus, new members of the Picornaviridae. Virus Res **85:**61-70.

Lipman, N. S., L. R. Jackson, L. J. Trudel, and F. Weis-Garcia. 2005. Monoclonal versus polyclonal antibodies: distinguishing characteristics, applications, and information resources. Ilar J **46:**258-68.

Mackay, I. M., K. E. Arden, and A. Nitsche. 2002. Real-time PCR in virology. Nucleic Acids Res **30:**1292-305.

Main, A. J., R. E. Shope, and R. C. Wallis. 1976. Characterization of Whitney's Clethrionomy gapperi virus isolates from Massachusetts. J Wildl Dis **12:**154-64.

Mason, P. W., E. Rieder, and B. Baxt. 1994. RGD sequence of foot-and-mouth disease virus is essential for infecting cells via the natural receptor but can be bypassed by an antibody-dependent enhancement pathway. Proc Natl Acad Sci U S A **91:**1932-6.

Mayo, M. A., and C. R. Pringle. 1998. Virus taxonomy--1997. J Gen Virol **79 (Pt 4):**649-57.

McBride, A. E., A. Schlegel, and K. Kirkegaard. 1996. Human protein Sam68 relocalization and interaction with poliovirus RNA polymerase in infected cells. Proc Natl Acad Sci U S A **93:**2296-301.

Minor, P. D., M. Ferguson, D. M. Evans, J. W. Almond, and J. P. Icenogle. 1986. Antigenic structure of polioviruses of serotypes 1, 2 and 3. J Gen Virol **67 (Pt 7):**1283-91.

Mirzayan, C., and E. Wimmer. 1994. Biochemical studies on poliovirus polypeptide 2C: evidence for ATPase activity. Virology **199:**176-87.

Mitchell-Jones, A. J., G. Amori, W. Bogdanowicz, B. Krystufek, P. J. H. Reijnders, F. Spitzenberger, M. Stubbe, J. B. M. Thissen, V. Vohralik, and J. Zima. 1999. The Atlas of European Mammals. Poyser, London.

Nateri, A. S., P. J. Hughes, and G. Stanway. 2000. In vivo and in vitro identification of structural and sequence elements of the human parechovirus 5' untranslated region required for internal initiation. J Virol **74:**6269-77.

Neznanov, N., A. Kondratova, K. M. Chumakov, B. Angres, B. Zhumabayeva, V. I. Agol, and A. V. Gudkov. 2001. Poliovirus protein 3A inhibits tumor necrosis factor (TNF)-induced apoptosis by eliminating the TNF receptor from the cell surface. J Virol **75:**10409-20.

Nicholson, D. W., A. Ali, N. A. Thornberry, J. P. Vaillancourt, C. K. Ding, M. Gallant, Y. Gareau, P. R. Griffin, M. Labelle, Y. A. Lazebnik, and et al. 1995. Identification and inhibition of the ICE/CED-3 protease necessary for mammalian apoptosis. Nature **376:**37-43.

Niklasson, B., B. Hörnfeldt, and B. Lundman. 1998. Could myocarditis, insulin-dependent diabetes mellitus, and Guillain-Barre syndrome be caused by one or more infectious agents carried by rodents? Emerg Infect Dis **4:**187-93.

Niklasson, B., L. Kinnunen, B. Hörnfeldt, J. Horling, C. Benemar, K. O. Hedlund, L. Matskova, T. Hyypiä, and G. Winberg. 1999. A new picornavirus isolated from bank voles (Clethrionomys glareolus). Virology **255:**86-93.

Niklasson, B., K. E. Heller, B. Schonecker, M. Bildsoe, T. Daniels, C. S. Hampe, P. Widlund, W. T. Simonson, J. B. Schaefer, E. Rutledge, L. Bekris, A. M. Lindberg, S. Johansson, E. Ortqvist, B. Persson, and A. Lernmark. 2003a. Development of type 1 diabetes in wild bank voles associated with islet autoantibodies and the novel ljungan virus. Int J Exp Diabesity Res **4:**35-44.

Niklasson, B., B. Hörnfeldt, E. Nyholm, M. Niedrig, O. Donoso-Mantke, H. R. Gelderblom, and A. Lernmark. 2003b. Type 1 diabetes in Swedish bank voles (Clethrionomys glareolus): signs of disease in both colonized and wild cyclic populations at peak density. Ann N Y Acad Sci **1005:**170-5.

Niklasson, B., A. Samsioe, M. Blixt, S. Sandler, A. Sjoholm, E. Lagerquist, A. Lernmark, and W. Klitz. 2006a. Prenatal viral exposure followed by adult stress produces glucose intolerance in a mouse model. Diabetologia **49:**2192-9.

Niklasson, B., E. Nyholm, R. E. Feinstein, A. Samsioe, and B. Hörnfeldt. 2006b. Diabetes and myocarditis in voles and lemmings at cyclic peak densities--induced by Ljungan virus? Oecologia **150:**1-7.

Niklasson, B., A. Samsioe, N. Papadogiannakis, A. Kawecki, B. Hörnfeldt, G. R. Saade, and W. Klitz. 2007a. Association of zoonotic Ljungan virus with intrauterine fetal deaths. Birth Defects Res A Clin Mol Teratol **79:**488-93.

Niklasson, B., T. Hultman, R. Kallies, M. Niedrig, R. Nilsson, P. O. Berggren, L. Juntti-Berggren, S. Efendic, A. Lernmark, and W. Klitz. 2007b. The BioBreeding rat diabetes model is infected with Ljungan virus. Diabetologia **50:**1559-60.

Niklasson, B., A. Samsioe, N. Papadogiannakis, S. Gustafsson, and W. Klitz. 2009a. Zoonotic Ljungan virus associated with central nervous system malformations in terminated pregnancy. Birth Defects Res A Clin Mol Teratol **85:**542-5.

Niklasson, B., P. R. Almqvist, B. Hörnfeldt, and W. Klitz. 2009b. Sudden infant death syndrome and Ljungan virus. Forensic Sci Med Pathol **5:**274-9.

Nix, W. A., K. Maher, E. S. Johansson, B. Niklasson, A. M. Lindberg, M. A. Pallansch, and M. S. Oberste. 2008. Detection of all known parechoviruses by real-time PCR. J Clin Microbiol **46:**2519-24.

Nunez, J. I., E. Baranowski, N. Molina, C. M. Ruiz-Jarabo, C. Sanchez, E. Domingo, and F. Sobrino. 2001. A single amino acid substitution in nonstructural protein 3A can mediate adaptation of foot-and-mouth disease virus to the guinea pig. J Virol **75:**3977-83.

Oberste, M. S., K. Maher, and M. A. Pallansch. 1998. Complete sequence of echovirus 23 and its relationship to echovirus 22 and other human enteroviruses. Virus Res **56:**217-23.

Oberste, M. S., K. Maher, D. R. Kilpatrick, and M. A. Pallansch. 1999a. Molecular evolution of the human enteroviruses: correlation of serotype with VP1 sequence and application to picornavirus classification. J Virol **73:**1941-8.

Oberste, M. S., K. Maher, D. R. Kilpatrick, M. R. Flemister, B. A. Brown, and M. A. Pallansch. 1999b. Typing of human enteroviruses by partial sequencing of VP1. J Clin Microbiol **37:**1288-93.

Oldstone, M. B. 1991. Molecular anatomy of viral persistence. J Virol **65:**6381-6.

Paul, A. V., J. H. van Boom, D. Filippov, and E. Wimmer. 1998a. Protein-primed RNA synthesis by purified poliovirus RNA polymerase. Nature **393:**280-4.

Paul, A. V., J. Mugavero, A. Molla, and E. Wimmer. 1998b. Internal ribosomal entry site scanning of the poliovirus polyprotein: implications for proteolytic processing. Virology **250:**241-53.

Paul, A. V., J. Peters, J. Mugavero, J. Yin, J. H. van Boom, and E. Wimmer. 2003. Biochemical and genetic studies of the VPg uridylylation reaction catalyzed by the RNA polymerase of poliovirus. J Virol **77:**891-904.

Peltola, V., M. Waris, R. Osterback, P. Susi, T. Hyypiä, and O. Ruuskanen. 2008. Clinical effects of rhinovirus infections. J Clin Virol **43:**411-4.

Pernas-Alonso, R., F. Morelli, U. di Porzio, and C. Perrone-Capano. 1999. Multiplex semi-quantitative reverse transcriptase-polymerase chain reaction of low abundance neuronal mRNAs. Brain Res Brain Res Protoc **4:**395-406.

Pettersson, R. F., V. Ambros, and D. Baltimore. 1978. Identification of a protein linked to nascent poliovirus RNA and to the polyuridylic acid of negative-strand RNA. J Virol **27:**357-65.

Plyusnin, A., and S. P. Morzunov. 2001. Virus evolution and genetic diversity of hantaviruses and their rodent hosts. Curr Top Microbiol Immunol **256:**47-75.

Pulli, T., H. Lankinen, M. Roivainen, and T. Hyypiä. 1998. Antigenic sites of coxsackievirus A9. Virology **240:**202-12.

Quinn, D. G., A. J. Zajac, J. A. Frelinger, and D. Muller. 1993. Transfer of lymphocytic choriomeningitis disease in beta 2-microglobulin-deficient mice by CD4+ T cells. Int Immunol **5:**1193-8.

Racaniello, V. R. 2007. Picornaviridae: The Viruses and their Replication. *In* D. M. Knipe and P. M. Howley (ed.), Fields Virology 5th edition. Lippincott Williams and Wilkins, Hagerstown.

Ramos-Vara, J. A. 2005. Technical aspects of immunohistochemistry. Vet Pathol **42:**405-26.

Reagan, K. J., B. Goldberg, and R. L. Crowell. 1984. Altered receptor specificity of coxsackievirus B3 after growth in rhabdomyosarcoma cells. J Virol **49:**635-40.

Richards, O. C., J. F. Spagnolo, J. M. Lyle, S. E. Vleck, R. D. Kuchta, and K. Kirkegaard. 2006. Intramolecular and intermolecular uridylylation by poliovirus RNA-dependent RNA polymerase. J Virol **80:**7405-15.

Rodriguez, P. L., and L. Carrasco. 1993. Poliovirus protein 2C has ATPase and GTPase activities. J Biol Chem **268:**8105-10.

Rodriguez, P. L., and L. Carrasco. 1995. Poliovirus protein 2C contains two regions involved in RNA binding activity. J Biol Chem **270:**10105-12.

Rossmann, M. G., E. Arnold, J. W. Erickson, E. A. Frankenberger, J. P. Griffith, H. J. Hecht, J. E. Johnson, G. Kamer, M. Luo, A. G. Mosser, et al. 1985. Structure of a human common cold virus and functional relationship to other picornaviruses. Nature **317:**145-53.

Ruoslahti, E., and M. D. Pierschbacher. 1987. New perspectives in cell adhesion: RGD and integrins. Science **238:**491-7.

Ryan, M. D., and M. Flint. 1997. Virus-encoded proteinases of the picornavirus super-group. J Gen Virol **78 (Pt 4):**699-723.

Saitou, N., and M. Nei. 1987. The neighbor-joining method: A new method for reconstructing phylogenetic trees. Molecular Biology and Evolution **4:**406-425.

Samsioe, A., R. Feinstein, G. Saade, A. Sjoholm, B. Hörnfeldt, R. Fundele, W. Klitz, and B. Niklasson. 2006. Intrauterine death, fetal malformation, and delayed pregnancy in Ljungan virus-infected mice. Birth Defects Res B Dev Reprod Toxicol **77:**251-6.

Samsioe, A., A. Sjoholm, B. Niklasson, and W. Klitz. 2008. Fetal death persists through recurrent pregnancies in mice following Ljungan virus infection. Birth Defects Res B Dev Reprod Toxicol **83:**507-10.

Samsioe, A., N. Papadogiannakis, T. Hultman, A. Sjoholm, W. Klitz, and B. Niklasson. 2009. Ljungan virus present in intrauterine fetal death diagnosed by both immunohistochemistry and PCR. Birth Defects Res A Clin Mol Teratol **85:**227-9.

Samuilova, O., C. Krogerus, T. Poyry, and T. Hyypiä. 2004. Specific interaction between human parechovirus nonstructural 2A protein and viral RNA. J Biol Chem **279:**37822-31.

Samuilova, O., C. Krogerus, I. Fabrichniy, and T. Hyypiä. 2006. ATP hydrolysis and AMP kinase activities of nonstructural protein 2C of human parechovirus 1. J Virol **80:**1053-8.

Sandoval, I. V., and L. Carrasco. 1997. Poliovirus infection and expression of the poliovirus protein 2B provoke the disassembly of the Golgi complex, the organelle target for the antipoliovirus drug Ro-090179. J Virol **71:**4679-93.

Schoenecker, B., K. E. Heller, and T. Freimanis. 2000. Development of stereotypies and polydipsia in wild caught bank voles (Clethrionomys glareolus) and their laboratory-bred offspring. Is polydipsia a symptom of diabetes mellitus? Appl Anim Behav Sci **68:**349-357.

Schultheiss, T., S. U. Emerson, R. H. Purcell, and V. Gauss-Muller. 1995. Polyprotein processing in echovirus 22: a first assessment. Biochem Biophys Res Commun **217:**1120-7.

Shaver, D. N., A. L. Barron, and D. T. Karzon. 1961. Distinctive cytopathology of ECHO viruses types 22 and 23. Proc Soc Exp Biol Med **106:**648-652.

Shi, S. R., M. E. Key, and K. L. Kalra. 1991. Antigen retrieval in formalin-fixed, paraffin-embedded tissues: an enhancement method for immunohistochemical staining based on microwave oven heating of tissue sections. J Histochem Cytochem **39:**741-8.

Shi, S. R., R. J. Cote, and C. R. Taylor. 1997. Antigen retrieval immunohistochemistry: past, present, and future. J Histochem Cytochem **45:**327-43.

Shin, S. Y., K. S. Kim, Y. S. Lee, Y. S. Chung, K. S. Park, D. S. Cheon, B. K. Na, Y. Kang, H. M. Cheong, Y. Moon, J. H. Choi, H. E. Cho, N. Y. Min, J. S. Son, Y. H. Park, Y. Jee, J. D. Yoon, C. Y. Song, and K. H. Lee. 2003. Identification of enteroviruses by using monoclonal antibodies against a putative common epitope. J Clin Microbiol **41:**3028-34.

Shiroki, K., T. Ishii, T. Aoki, Y. Ota, W. X. Yang, T. Komatsu, Y. Ami, M. Arita, S. Abe, S. Hashizume, and A. Nomoto. 1997. Host range phenotype induced by mutations in the internal ribosomal entry site of poliovirus RNA. J Virol **71:**1-8.

Simmonds, P. 2006. Recombination and selection in the evolution of picornaviruses and other Mammalian positive-stranded RNA viruses. J Virol **80:**11124-40.

Simmonds, P., and J. Welch. 2006. Frequency and dynamics of recombination within different species of human enteroviruses. J Virol **80:**483-93.

Soderlund-Venermo, M., K. Hokynar, J. Nieminen, H. Rautakorpi, and K. Hedman. 2002. Persistence of human parvovirus B19 in human tissues. Pathol Biol (Paris) **50:**307-16.

Stanway, G. 1990. Structure, function and evolution of picornaviruses. J Gen Virol **71 (Pt 11):**2483-501.

Stanway, G., N. Kalkkinen, M. Roivainen, F. Ghazi, M. Khan, M. Smyth, O. Meurman, and T. Hyypiä. 1994. Molecular and biological characteristics of echovirus 22, a representative of a new picornavirus group. J Virol **68:**8232-8.

Stanway, G., and T. Hyypiä. 1999. Parechoviruses. J Virol **73:**5249-54.

Stanway, G., F. Brown, P. Christian, T. Hovi, T. Hyypiä, A. M. King, N. J. Knowles, S. M. Lemon, P. D. Minor, M. A. Pallansch, A. C. Palmenberg, and T. Skern. 2000. Taxonomy of the Picornaviridae: Species Designations and Three New Genera, Europic.

Stanway, G., F. Brown, P. Christian, T. Hovi, T. Hyypiä, A. M. Q. King, N. J. Knowles, S. M. Lemon, P. D. Minor, M. A. Pallansch, A. C. Palmenberg, and T. Skern. 2005. Family Picornaviridae., p. 757-778. *In* C. M. Fauquet, M. A. Mayo, J. Maniloff, U. Desselberger, and L. A. Ball (ed.), Virus Taxonomy. Eighth Report of the International Committee on Taxonomy of Viruses. Elsevier/Academic Press, London.

Stenseth, N. C. 1999. Population cycles in voles and lemmings: density dependence and phase dependence in a stochastic world. Oikos **87:**427-461.

Sudo, T., H. Ito, H. Hayashi, Y. Nagamura, K. Toga, and Y. Yamada. 2007. Genetic strain differences in platelet aggregation and thrombus formation of laboratory rats. Thromb Haemost **97:**665-72.

Tam, P. E., and R. P. Messner. 1999. Molecular mechanisms of coxsackievirus persistence in chronic inflammatory myopathy: viral RNA persists through formation of a double-stranded complex without associated genomic mutations or evolution. J Virol **73:**10113-21.

Tamura, K., J. Dudley, M. Nei, and S. Kumar. 2007. MEGA4: Molecular Evolutionary Genetics Analysis (MEGA) software version 4.0. Mol Biol Evol **24:**1596-9.

Tauriainen, S., M. Martiskainen, S. Oikarinen, M. Lonnrot, H. Viskari, J. Ilonen, O. Simell, M. Knip, and H. Hyoty. 2007. Human parechovirus 1 infections in young children--no association with type 1 diabetes. J Med Virol **79:**457-62.

Tauriainen, S., S. Oikarinen, K. Taimen, J. Laranne, M. Sipila, M. Lonnrot, J. Ilonen, O. Simell, M. Knip, and H. Hyoty. 2008. Temporal relationship between

human parechovirus 1 infection and otitis media in young children. J Infect Dis **198:**35-40.

Teterina, N. L., M. S. Rinaudo, and E. Ehrenfeld. 2003. Strand-specific RNA synthesis defects in a poliovirus with a mutation in protein 3A. J Virol **77:**12679-91.

Thomas, M. A., C. F. Chen, M. I. Jensen-Seaman, P. J. Tonellato, and S. N. Twigger. 2003. Phylogenetics of rat inbred strains. Mamm Genome **14:**61-4.

Tolf, C., J. O. Ekström, M. Gullberg, G. Arbrandt, B. Niklasson, G. Frisk, J. A. Liljeqvist, K. Edman, and A. M. Lindberg. 2008. Characterization of polyclonal antibodies against the capsid proteins of Ljungan virus. J Virol Methods **150:**34-40.

Tolf, C., M. Gullberg, E. S. Johansson, R. B. Tesh, B. Andersson, and A. M. Lindberg. 2009a. Molecular characterization of a novel Ljungan virus (Parechovirus; Picornaviridae) reveals a fourth genotype and indicates ancestral recombination. J Gen Virol **90:**843-53.

Tolf, C., M. Gullberg, J. O. Ekström, N. Jonsson, and A. Michael Lindberg. 2009b. Identification of amino acid residues of Ljungan virus VP0 and VP1 associated with cytolytic replication in cultured cells. Arch Virol **154:**1271-84.

Tosteson, M. T., and M. Chow. 1997. Characterization of the ion channels formed by poliovirus in planar lipid membranes. J Virol **71:**507-11.

Towner, J. S., T. V. Ho, and B. L. Semler. 1996. Determinants of membrane association for poliovirus protein 3AB. J Biol Chem **271:**26810-8.

Triantafilou, K., M. Triantafilou, Y. Takada, and N. Fernandez. 2000. Human parechovirus 1 utilizes integrins alphavbeta3 and alphavbeta1 as receptors. J Virol **74:**5856-62.

Ulrich, R. G., J. Schmidt-Chanasit, M. Schlegel, J. Jacob, H. J. Pelz, M. Mertens, M. Wenk, T. Buchner, D. Masur, K. Sevke, M. H. Groschup, F. W. Gerstengarbe, M. Pfeffer, R. Oehme, W. Wegener, M. Bemmann, L. Ohlmeyer, R. Wolf, H. Zoller, J. Koch, S. Brockmann, G. Heckel, and S. S. Essbauer. 2008. Network "Rodent-borne pathogens" in Germany: longitudinal studies on the geographical distribution and prevalence of hantavirus infections. Parasitol Res **103 Suppl 1:**S121-9.

Ulrich, R. G., G. Heckel, H. J. Pelz, L. H. Wieler, M. Nordhoff, G. Dobler, J. Freise, F. R. Matuschka, J. Jacob, J. Schmidt-Chanasit, F. W. Gerstengarbe, T. Jakel, J. Suss, B. Ehlers, A. Nitsche, R. Kallies, R. Johne, S. Gunther, K. Henning, R. Grunow, M. Wenk, L. C. Maul, K. P. Hunfeld, R. Wolfel, G. Schares, H. C. Scholz, S. O. Brockmann, M. Pfeffer, and S. S. Essbauer. 2009.

[Rodents and rodent associated disease vectors: the network of "rodent carrying pathogens" introduces itself]. Bundesgesundheitsblatt Gesundheitsforschung Gesundheitsschutz **52:**352-69.

van der Sanden, S., E. de Bruin, H. Vennema, C. Swanink, M. Koopmans, and H. van der Avoort. 2008. Prevalence of human parechovirus in the Netherlands in 2000 to 2007. J Clin Microbiol **46:**2884-9.

Van Dyke, T. A., and J. B. Flanegan. 1980. Identification of poliovirus polypeptide P63 as a soluble RNA-dependent RNA polymerase. J Virol **35:**732-40.

van Kuppeveld, F. J., J. T. van der Logt, A. F. Angulo, M. J. van Zoest, W. G. Quint, H. G. Niesters, J. M. Galama, and W. J. Melchers. 1993. Genus- and species-specific identification of mycoplasmas by 16S rRNA amplification. Appl Environ Microbiol **59:**655.

van Kuppeveld, F. J., J. G. Hoenderop, R. L. Smeets, P. H. Willems, H. B. Dijkman, J. M. Galama, and W. J. Melchers. 1997. Coxsackievirus protein 2B modifies endoplasmic reticulum membrane and plasma membrane permeability and facilitates virus release. Embo J **16:**3519-32.

Verboon-Maciolek, M. A., F. G. Utrecht, F. Cowan, P. Govaert, A. M. van Loon, and L. S. de Vries. 2008a. White matter damage in neonatal enterovirus meningoencephalitis. Neurology **71:**536.

Verboon-Maciolek, M. A., F. Groenendaal, C. D. Hahn, J. Hellmann, A. M. van Loon, G. Boivin, and L. S. de Vries. 2008b. Human parechovirus causes encephalitis with white matter injury in neonates. Ann Neurol **64:**266-73.

Wakatsuki, K., D. Kawamoto, H. Hiwaki, K. Watanabe, and H. Yoshida. 2008. Identification and characterization of two strains of human parechovirus 4 isolated from two clinical cases in Fukuoka City, Japan. J Clin Microbiol **46:**3144-6.

Ward, C. D., M. A. Stokes, and J. B. Flanegan. 1988. Direct measurement of the poliovirus RNA polymerase error frequency in vitro. J Virol **62:**558-62.

Watanabe, K., M. Oie, M. Higuchi, M. Nishikawa, and M. Fujii. 2007. Isolation and characterization of novel human parechovirus from clinical samples. Emerg Infect Dis **13:**889-95.

Wessels, E., D. Duijsings, R. A. Notebaart, W. J. Melchers, and F. J. van Kuppeveld. 2005. A proline-rich region in the coxsackievirus 3A protein is required for the protein to inhibit endoplasmic reticulum-to-golgi transport. J Virol **79:**5163-73.

Wessely, R., A. Henke, R. Zell, R. Kandolf, and K. U. Knowlton. 1998a. Low-level expression of a mutant coxsackieviral cDNA induces a myocytopathic effect in culture: an approach to the study of enteroviral persistence in cardiac myocytes. Circulation **98:**450-7.

Wessely, R., K. Klingel, L. F. Santana, N. Dalton, M. Hongo, W. Jonathan Lederer, R. Kandolf, and K. U. Knowlton. 1998b. Transgenic expression of replication-restricted enteroviral genomes in heart muscle induces defective excitation-contraction coupling and dilated cardiomyopathy. J Clin Invest **102:**1444-53.

Wesslen, L., C. Pahlson, G. Friman, J. Fohlman, O. Lindquist, and C. Johansson. 1992. Myocarditis caused by Chlamydia pneumoniae (TWAR) and sudden unexpected death in a Swedish elite orienteer. Lancet **340:**427-8.

Whitacre, C. C., S. C. Reingold, and P. A. O'Looney. 1999. A gender gap in autoimmunity. Science **283:**1277-8.

Whitney, E., A. P. Roz, and G. A. Rayner. 1970. Two viruses isolated from rodents (Clethrionomys gapperi and Microtus pennsvlvanicus) trapped in St. Lawrence County, New York. J Wildl Dis **6:**48-55.

Whitton, J. L., C. T. Cornell, and R. Feuer. 2005. Host and virus determinants of picornavirus pathogenesis and tropism. Nat Rev Microbiol **3**(10):765-76.

Wigand, R., and A. B. Sabin. 1961. Properties of ECHO types 22, 23 and 24 viruses. Arch Gesamte Virusforsch **11:**224-47.

Williams, C. H., M. Panayiotou, G. D. Girling, C. I. Peard, S. Oikarinen, H. Hyoty, and G. Stanway. 2009. Evolution and conservation in human parechovirus genomes. J Gen Virol **90:**1702-12.

Wolthers, K. C., K. S. Benschop, J. Schinkel, R. Molenkamp, R. M. Bergevoet, I. J. Spijkerman, H. C. Kraakman, and D. Pajkrt. 2008. Human parechoviruses as an important viral cause of sepsislike illness and meningitis in young children. Clin Infect Dis **47:**358-63.

Wong, C. Y., J. J. Woodruff, and J. F. Woodruff. 1977. Generation of cytotoxic T lymphocytes during coxsackievirus B-3 infection. III. Role of sex. J Immunol **119:**591-7.

Xiang, W., K. S. Harris, L. Alexander, and E. Wimmer. 1995a. Interaction between the 5'-terminal cloverleaf and 3AB/3CDpro of poliovirus is essential for RNA replication. J Virol **69:**3658-67.

Xiang, W., A. Cuconati, A. V. Paul, X. Cao, and E. Wimmer. 1995b. Molecular dissection of the multifunctional poliovirus RNA-binding protein 3AB. Rna **1:**892-904.

Yamashita, T., K. Sakae, H. Tsuzuki, Y. Suzuki, N. Ishikawa, N. Takeda, T. Miyamura, and S. Yamazaki. 1998. Complete nucleotide sequence and genetic organization of Aichi virus, a distinct member of the Picornaviridae associated with acute gastroenteritis in humans. J Virol **72:**8408-12.

Yoon, J. W., T. Onodera, and A. L. Notkins. 1978. Virus-induced diabetes mellitus. XV. Beta cell damage and insulin-dependent hyperglycemia in mice infected with coxsackie virus B4. J Exp Med **148:**1068-80.

Zhirnov, O. P., T. E. Konakova, T. Wolff, and H. D. Klenk. 2002. NS1 protein of influenza A virus down-regulates apoptosis. J Virol **76:**1617-25.

Zoll, J., H. A. Heus, F. J. van Kuppeveld, and W. J. Melchers. 2009a. The structure-function relationship of the enterovirus 3'-UTR. Virus Res **139:**209-16.

Zoll, J., J. M. Galama, and F. J. van Kuppeveld. 2009b. Identification of potential recombination breakpoints in human parechoviruses. J Virol **83:**3379-83.

6 Abbreviations

A	Adenine
aa	Amino acid
AdV	Adenovirus
AMP	Adenosine monophosphate
approx.	Approximately
APS	Ammoniumperoxodisulfate
Aqua dest.	Water (distilled by Millipore)
ATCC	American Tissue and Cell Culture Collection
ATP	Adenosine triphosphate
BB	BioBreeding
bp	Base pair
BSA	Bovine serum albumin
C	Cytosine
$CCID_{50}$	Cell culture infectious dose 50
cDNA	Complementary (copy) DNA
cm	Centimetre
CNS	Central nervous system
CPE	Cytopathogenic effect
cre	Cis-acting replication element
CT	Threshold cycle
C-terminus	Carboxyl-terminus
CVB	Coxsackievirus B
°C	Degree Celsius
d	Day
DAPI	4′,6-Diamidino-2-phenylindol
ddNTP	Didesoxynucleoside triphosphate
dNTP	Desoxynucleoside triphosphate
DMEM	Dulbecco´s Modified Eagles Medium
DMSO	Dimethylsulfoxid
DNA	Desoxyribonucleicacid
Dnase	Deoxyribonuclease
dpi	Days post infection
ds	Double strand
DTT	Dithiothreitol
dUTP	Deoxyuridine Triphosphate
ECHO	Entero cytopathogenic human orphan

ECACC	European Collection of Cell Cultures
E. coli	*Escherichia coli*
EDTA	Ethylendiamine tetraacetic acid
e.g.	*Exempli gratia* (for example)
EIA	Enzyme immunoassay
eIF4	Eukaryotic initiation factor-4A
ELISA	Enzyme-linked immunosorbent assay
EMCV	Encephalomyocarditis virus
ER	Endoplasmic reticulum
et al.	*Et alii (and others)*
FCS	Fetal calf serum
FITC	Fluorescein isothiocyanate
FMDV	Foot-and-mouth disease virus
6-FAM	6-FAM-phosphoramidite
g	Gram
G	Guanine
(x) g	Centrifugal force (9.81 m/s2)
GMK	Green monkey kidney
GTP	Guanosine-5'-triphosphate
h	Hour
HAV	Hepatitis-A virus
HPeV	Human Parechovirus
HPRT	Hypoxanthine-guanine Phosphoribosyl Transferase
HRP	Horseradish peroxidase
i.e.	*Id est* (that is)
IFA	Immunofluorescence assay
i.p.	Intraperitoneal
IgG	Immunoglobulin subclass G
IgM	Immunoglobulin subclass M
IHC	Immunohistochemistry
IIFT	Indirect Immunofluorescence test
IRES	Internal ribosomal entry site
IPTG	Isopropyl β-D-1 thiogalactopyranoside
IUFD	Intra uterine fetal death
iv	*In vitro*
LB	Lysogeny broth
L-Gln	L-glutamine
LV	Ljungan virus
M	Molar or nucleotide code for A or C
mAb	Monoclonal antibody

MCA	Melting curve analysis
mg	Milligram
MGB	Minor groove binder
min	Minute
ml	Milliliter
mM	Millimolar
MMLV	Moloney murine leukemia virus
MOI	Multiplicity of infection
MOPS	(3-[N-Morpholino] propane-sulfonic acid)
mRNA	Messenger RNA
µg	Microgram
µl	Microliter
N	Amount
NCBI	National Center for Biotechnology Information
n.d.	Not done
NEAA	Non essential amino acids
nm	Nanometer
nmol	Nanomol
no.	Number
nt	Nucleotide
N-terminus	Amino-terminus
OD	Optical density
ORF	Open reading frame
PAA	Polyacrylamide
PBS	Phophate buffered saline
PBS-T	PBS containing 0.1 % TWEEN® 20
PCR	Polymerase chain reaction
pH	*Potentia hydrogenii*
pi	Post infection
pmol	Picomol
R	Nucleotide code: A or G
RGD	Amino acid motif: Arginyl-glycyl-aspartic acid
RKI	Robert Koch-Institute
RNA	Ribonucleic acid
RNase	Ribonuclease
ROX	6-Carboxy-X-Rhodamine
rpm	Rounds per minute
RT	Reverse transcriptase
sec	Second
S	Svedberg

SARS	severe acute respiratory syndrome
SD	Sprague Dawley® or standard deviation
SDS	Sodium dodecylsulfate
SDS-PAGE	SDS-polyacrylamide gelelectrophoresis
SMB	Suckling mouse brain
SOC	Super optimal broth with catabolite repression (medium)
ss	Single strand
T	Thymine
TBE	Tick-borne encephalitis or Tris-borate-EDTA
TEMED	N,N,N´,N´-tetramethyl ethylendiamine
Tm	Melting temperature
TMB	Tetramethylbenzidine
TOPO	Topoisomerase
Tris	Tris hydroxymethyl aminomethane
TUNEL	Terminal transferase dUTP nick end labelling
T1D	Type-1 diabetes
U	Uracil or unit
UTR	Untranslated region
UV	Ultraviolet light
V	Volts
VP	Virus protein
VPg	Virus protein genome linked
W	Nucleotide code: A or T
WAG	Wistar Albino Glaxo
X-gal	Bromo-chloro-indolyl-galactopyranoside
Y	Nucleotide code: C or T

Acknowledgements

First of all I wish to thank Matthias Niedrig for giving me the opportunity to do my PhD thesis in his lab. Thanks for giving me your support and for giving me plenty of rope to try things as I wanted. I always found a sympathetic ear, and I felt at home.

Furthermore I would like to thank Prof. Rupert Mutzel for agreeing to be my reviewer without any hesitation.

My deepest gratitude belongs to Bo Niklasson. Without you this thesis would not have been possible. Thank you for all your support and encouragement, for your introduction to Ljungan virus science and for teaching me in taking things easy, even when things did not work. I am grateful for inviting me to Sweden many times. I always had a splendid time there.

This thesis was financially supported by the “Johan Claesson Foundation”. Many thanks Johan. Your interest in science made this thesis possible.

I wish to express my gratitude to all my collaborators: Rainer Ulrich and the network of rodent carrying pathogens for support and helpful discussion regarding rodent-things; Gustav Arbrandt who was a great partner in developing antibodies (let’s have a “good” 1.5 liter bottle of red wine for just EUR 1.50 to celebrate this); the rat men: Jakob Ettinger (a Bier, a Musi, Holadrio) and Sebastian Voigt; Andreas Nitsche and Jan-Felix Drexler for all those sequence things; Oliver Donoso Mantke, Annika Samsioe, Therese Olsson, Thomas Hultman, Birger Hörnfeldt and William Klitz.

I wish to thank all the people who helped in technical things and discussed my experiments: Hi-Gung Bae (I miss your smile and your excellent culinary art), Anette Teichmann, Jung-Won Sim-Brandenburg, Inga Nehlmeier, Klaus Kretzschmar, Sonja Linke, Oliver Bader, Kazimir Madela, Aleksiander Radonic, Christina Domingo-Carrasco (yes…I miss you too), the girls from the sequencing lab and the people from the animal facilities. You all made an excellent job.

Many thanks to my PhD student “fellow sufferers” and all members of Matthias Niedrig’s group. The extraordinary atmosphere in this group contributed to the successful conclusion of my thesis.

I am very grateful to Ursula Erikli and Sandra Junglen for excellent editing and revising the manuscript.

Many, many thanks to Marcel Müller. I could include your name in almost each section mentioned above. You helped me in so many things…impossible to list them all. I am looking forward to work with you again…this time in Bonn.

I am very grateful to “my” diploma students Juliane Paul and Bettina Weber. Thank you for your contribution to this work. You teached me that teaching is a hard job. I wish you all the best for the future.

I also wish to thank all students who crossed my way during an internship for their excellent job: Nicole Börner, Katharina Branz, Sabrina Brückner, Julia Hütter and Anna Woloszyk.

Many thanks to Christian Drosten who gave me the opportunity to finish the thesis in Bonn. I am looking forward to work with you in the future.

My sincere thanks are due to my family and friends for their encouragement and interest in my work. Special thanks to my brother Stephan who introduced me to the lab work in Bonn.

Finally, I wish to give my warmest thanks to my Henriette for all the support and her loving care over the last years. Thank you for beeing not angry with me when the dinner was already cold and I still in the lab. You are the best persistence experiment I have ever started.

Well…the wind sits in the shoulder of my sail and I am pretty sure I forgot somebody. Sorry for that. Please feel also acknowledged.

List of pre-publications of this thesis and other published articles

Different parts of this thesis have been published in advance with the admittance of the “FreieUniversität Berlin” represented by Prof. Dr. Rupert Mutzel. Pre-publications are listed below:

Publications

Kallies R*, Arbrandt G*, Niklasson B, Niedrig M. 2010. Development and characterisation of murine monoclonal antibodies to Ljungan virus genotypes 1 and 2. J Virol Methods, submitted.

Kallies R, Niklasson B, Samsioe A, Hörnfeldt B, Donoso Mantke O, Niedrig M. 2010. Ljungan virus RNA persists in infected laboratory mice. J Gen Virol, submitted.

Ulrich RG, Heckel G, Pelz HJ, Wieler LH, Nordhoff M, Dobler G, Freise J, Matuschka FR, Jacob J, Schmidt-Chanasit J, Gerstengarbe FW, Jäkel T, Süss J, Ehlers B, Nitsche A, **Kallies R**, Johne R, Günther S, Henning K, Grunow R, Wenk M, Maul LC, Hunfeld KP, Wölfel R, Schares G, Scholz HC, Brockmann SO, Pfeffer M, Essbauer SS. 2009. Rodents and rodent associated disease vectors: the network of "rodent carrying pathogens" introduces itself. Bundesgesundheitsblatt Gesundheitsforschung Gesundheitsschutz. 52(3):352-69.

Niklasson B, Hultman T, **Kallies R**, Niedrig M, Nilsson R, Berggren PO, Juntti-Berggren L, Efendic S, Lernmark A, Klitz W. 2007. The BioBreeding rat diabetes model is infected with Ljungan virus. Diabetologia. 50(7):1559-60.

Donoso Mantke O*, **Kallies R***, Niklasson B, Nitsche A, Niedrig M. 2007. A new quantitative real-time reverse transcriptase PCR assay and melting curve analysis for detection and genotyping of Ljungan virus strains. J Virol Methods. 141(1):71-7.

* both authors contributed equally

Other publications

Donoso Mantke O, Meyer R, Prösch S, Nitsche A, Leitmeyer K, **Kallies R**, Niedrig M. 2005. High prevalence of cardiotropic viruses in myocardial tissue from explanted hearts of heart transplant recipients and heart donors: a 3-year retrospective study from a German patients' pool. J Heart Lung Transplant. 24(10):1632-8.

Declaration of authorship

I certify that the work presented here is, to the best of my knowledge and belief, original and the result of my own investigations, except as acknowledged, and has not been submitted, either in part or whole, for a degree at this or any other University.

Berlin,

René Kallies

Curriculum Vitae

For reasons of data protection,
the curriculum vitae is not included in the online version